UNIVERSITY OF SOUTHAMPTON

FACULTY OF ENGINEERING, SCIENCE & MATHEMATICS

School of Chemistry

CHARACTERISATION AND INVESTIGATION OF STRUCTURAL RELATIONSHIPS OF 4,4'-DISUBSTITUTED CHALCONES

by

Graham John Tizzard

Thesis for the degree of Doctor of Philosophy

November 2008

UNIVERSITY OF SOUTHAMPTON

ABSTRACT

FACULTY OF ENGINEERING, SCIENCE & MATHEMATICS

SCHOOL OF CHEMISTRY

Doctor of Philosophy

CHARACTERISATION AND INVESTIGATION OF STRUCTURAL RELATIONSHIPS OF 4,4'-DISUBSTITUTED CHALCONES

By Graham John Tizzard

In this thesis the structural relationships of a family of fifty crystal structures of 4,4'-disubstitituted chalcones, X-C_6H_5-CO-C_2H_2-C_6H_5-Y, where X = CF_3, Br, Cl, F, H, Me, Et, OMe and Y = Br, Cl, F, H, Me, Et, OMe are investigated by comparative study of the molecular packing in each of the structures. The members of this family contain no strong hydrogen bond donor functionalities and thus directionally more diffuse intermolecular interactions dominate in the crystal structures. The concept of supramolecular constructs (*CrystEngComm.*, 2005, **7**, 324) is used to compare this family and common zero- to three-dimensional structure fragments are identified and discussed. It is shown that five fragments of closely-packed chalcone molecules form the basic motifs for 94% of the crystal structures and that these structures can be divided into three groups based on the presence of one or more of these basic motifs. The largest group comprises 68% of the crystal structures which contain a one-dimensional close-packed row of molecules. The majority of these structures are approximately close-packed and may be characterised by combinations of four basic two-dimensional sheet fragments based on the one-dimensional motif. The remaining two groups comprise 26% of the crystal structures and are each based on a combination of two of the five fragments. There is evidence of weak hydrogen bonding in many of the structures of these groups. Only the structures of Y = F, H, OMe substituted chalcones are found in these groups. The results of this thesis highlight the great importance that the molecular shape plays in the assembly of molecules in the solid state especially in such cases where only weak hydrogen bonds are present.

TABLE OF CONTENTS

LIST OF FIGURES

LIST OF TABLES

DECLARATION OF AUTHORSHIP

I, **Graham John Tizzard**, declare that the thesis entitled:

Characterisation and Investigation of Structural Relationships of 4,4'-Disubstituted Chalcones

and the work presented in the thesis are both my own, and have been generated by me as the result of my own original research. I confirm that:

- this work was done wholly or mainly while in candidature for a research degree at this University;
- where any part of this thesis has previously been submitted for a degree or any other qualification at this University or any other institution, this has been clearly stated;
- where I have consulted the published work of others, this is always clearly attributed;
- where I have quoted from the work of others, the source is always given. With the exception of such quotations, this thesis is entirely my own work;
- I have acknowledged all main sources of help;
- where the thesis is based on work done by myself jointly with others, I have made clear exactly what was done by others and what I have contributed myself;
- none of this work has been published before submission.

Signed: ……..

Date:…….

ACKNOWLEDGEMENTS

I would like to thank my supervisor, Professor Mike Hursthouse for allowing me the opportunity to undertake this research. His unwavering support and guidance throughout has been invaluable. I would also like to thank Dr. Terry Threlfall for providing the samples that made this work possible and Dr. Thomas Gelbrich for his help on the workings of XPac. I am also very grateful to all the NCS and Hursthouse research group members both past and present for all their help and advice and finally a very special thanks to Sue, without whose support and patience this would have not been completed.

ABBREVIATIONS

SC, SCs	supramolecular construct, supramolecular constructs
3-D, 2-D, 1-D, 0-D	3, 2, 1, 0 dimensional
COSP	corresponding ordered series of points
OSP	ordered series of points

Chapter 1 Introduction

In this chapter the organic solid state and the forces leading to the formation of molecular crystals will be described and classified. This will lead on to the background and justification for the work described in this thesis.

Crystals of molecular organic compounds consist of discrete molecules held together in a periodic arrangement by a variety of forces which are weak compared with those of the chemical bonds of the molecule. These forces include directional hydrogen bonds and isotropic van der Waals forces and the crystal structure is the result of the complex interplay and subtle balance of these. With the development of 'crystal engineering' of the organic solid state over the last two decades, it is hydrogen bonding that has received the most attention due to the reliable and reproducible nature of this interaction. However, large numbers of structures contain no hydrogen bonding functionalities and the assembly of these relies on the directionally more diffuse intermolecular interactions such as van der Waals forces. These interactions are much more difficult to 'pinpoint', structurally, in the way that bonding with a covalent component can be identified. However, the results of these interactions, in the form assemblies of molecules within a structure, may be identified. This thesis is concerned with the identification and study of such assemblies within the crystal structures of a large family of molecules with no classical hydrogen bond donors and thus no strong hydrogen bonds. It is first relevant, however to consider the variety and nature of the intermolecular forces and interactions in the organic solid state.

Intermolecular Forces and Interactions

Intermolecular forces and the interactions derived from them are responsible for the cohesion of crystal structures and hence their form and bulk properties in the solid state. The potential energy of a structure is the sum of short range repulsive forces and long range attractive forces and the equilibrium between these results in the crystal structure. The long range attractive forces may be conveniently subdivided into electrostatic, induction and dispersion forces.

Repulsion or Exchange Forces

Most stable molecules have closed electron shells; that is all their molecular orbitals are doubly occupied and cannot accept other electrons without violating the Pauli exclusion principle whereby two electrons cannot occupy the same region of space simultaneously. Thus at very short intermolecular distances, when the electron clouds of adjacent molecules overlap, the electrons tend to avoid this overlap region and so no longer shield the nuclear charges on molecules as effectively which results in increased Coulombic repulsion between the nuclei of adjacent molecules. These repulsive forces exert their influence at very short range and have an approximately r^{-12} relationship where r is the interatomic distance. These repulsive forces also occur intramolecularly and are responsible for the shape and conformation of individual molecules.

Electrostatic or Coulomb Forces

Due to the different electronegativities of the component atoms of a molecule, the permanent charge distributions of molecules are often not uniform. This non-uniform charge distribution may be modelled as a series of multipole moments and the electrostatic energy between two molecules expressed in terms of monopole-monopole, monopole-dipole, dipole-dipole, quadrupole-quadrupole etc. components. Each of these terms has different distance dependency, thus for monopole-monopole interactions, the relationship is r^{-1}, for monopole-dipole interactions it is r^{-2}, for dipole-dipole interactions it is r^{-3} and for quadrupole-quadrupole interactions it is r^{-5}. Hence, these interactions are long-range exerting their influence over distances greater than a molecular diameter. Individual electrostatic interactions are pairwise additive and may be either attractive or repulsive. According to Kitaigorodskii[1] these interactions must cancel out in crystals with only translational symmetry (i.e. space group $P1$), but for other space groups the total electrostatic interaction is attractive.

Induction Forces

A permanent dipole can also interact with a polarisable atom or group in an adjacent molecule to create an induced dipole. Induction interactions are always attractive whatever the relative orientations of the adjacent molecules.

The induction energy distance dependency relationship is r^{-6}. Induction energy tends to be small in symmetrical environments such as solids.

Dispersion or London Forces

The forces outlined above are not sufficient to account for the stabilisation energies of crystals of non-polar molecules and thus the most significant of the long range forces in molecular crystals are the dispersion forces. These forces are ubiquitous, occurring between all atoms and molecules and the first explanation of them was provided by Fritz London who considered them to be electrical in nature[2]. The electrons in atoms and molecules are in continual motion, even in their ground state, and thus even in molecules whose electrical multipole moments are equal to zero, at any given instant a temporary multipole moment may occur. These instantaneous multipole moments polarise adjacent molecules, creating induced multipole moments in them. The time-averaged instantaneous multipole moments and the resulting induced counterparts give rise to an attractive force between molecules. The dispersion energy distance dependency relationship is r^{-6} and these forces are additive and approximately proportional to the size of the molecule as each polarisable bond and atom can contribute. Dispersion forces are the major proportion of lattice energy in molecular crystals and are especially important in crystal structures of molecules with highly polarisable moieties such as benzene rings or hetero atoms[3]. Dispersion and repulsion forces are collectively referred to as van der Waals forces.

Hydrogen Bonding

Whilst the concept of hydrogen bonding has been recognised from the beginning of the last century, it is Pauling's work that provides the classical definition of hydrogen bonding[4]. He defines a hydrogen bond as a largely ionic interaction between two electronegative atoms where the hydrogen atom is attracted to both atoms and thus acts as a bond between them. This arises from the large deshielding effect in the forward direction of the H atom by the covalently bonded electronegative 'donor' atom and the corresponding electrostatic attraction to the electronegative 'acceptor' atom. This definition includes interactions of type X–H···A, where both X and A can be any of the

following elements: N, O, F, Cl, Br and I. Hydrogen bonds involving these elements are typically linear (X–H–A angle ~180°) and have interaction energies of 15 – 40 kJ mol^{-1}. These classic strong hydrogen bonds are of immense importance in structural chemistry and biochemistry and indeed much of the development of 'crystal engineering' has relied heavily on the use of such bonding to design and create organic solid-state assemblies. However, whilst this type of interaction is common amongst organic crystal structures, it is not universal and this type of hydrogen bonding does not occur in all structures.

Whilst the strict definition of hydrogen bonding above held sway for many years, further studies revealed evidence of so called weak hydrogen bonding such as C–H···O and O–H···π interactions. The interaction energy of these types of hydrogen bonds ranges from 2 – 15 kJ mol^{-1} and the linear constraints of strong hydrogen bonds are typically more relaxed with X–H–A angles ranging from 90 – 180°. Weak hydrogen bonds are primarily of an electrostatic nature and thus their strength decreases more slowly over distance than that of the van der Waals forces. The longer range of these interactions compared with van der Waals forces means that they are thought to have an orientating effect on molecules prior to nucleation and crystallisation.

The discussion of hydrogen bonding so far has concentrated on interactions involving three atoms, the donor and acceptor atoms and the H atom itself. However more complex arrangements of bifurcated and trifurcated hydrogen bonding involving the donor and H-atoms along with two or three acceptor atoms respectively also exist. Hydrogen bonds are considered composite in the nature of the forces involved with electrostatic, covalent, dispersion-repulsion and polarisation components. It is however widely accepted that the predominant component is electrostatic and thus the energy distance dependence relationship for these interactions is between r^{-1} and r^{-3}. The profound influence of strong hydrogen bond donor and acceptors on the crystal structures of molecules that contain them led Etter to develop general rules for the packing of hydrogen bonded molecules in crystals[5,6,7]. The main rules generally applicable to all systems are:

- All good donors and acceptors are used in hydrogen bonding

- Hydrogen bonds forming six-membered intramolecular rings are formed in preference to intermolecular hydrogen bonds
- The remaining donors and acceptors after intramolecular hydrogen bond formation will form intermolecular hydrogen bonds.

It should be noted that the above rules apply only to molecules with both strong donors and acceptors and do not apply in systems, such as those studied here, where only weak hydrogen bonding may be present.

Other Interactions

The halogens Cl, Br and I participate in short non-bonded interactions in crystal structures; however the nature of these interactions is debated. Nyburg[8] and Price[9] suggest these are due to the elliptically shaped (anisotropic) atoms, whilst Williams[10] and Desiraju[11] maintain there are specific attractive forces between halogen atoms in crystals. The distinctions in geometries between symmetrical halogen interactions, Cl···Cl, Br···Br and I···I and unsymmetrical interactions, I···Cl, Br···F and I···F suggest atomic polarisation is an important factor. Halogen atoms also exhibit interactions with N and O and this type of interaction has become increasingly important in crystal engineering for the assembly of small organic 'building blocks'[12]. It is a charge-transfer interaction of the n→σ* type between an electron rich atom and a halogen atom bonded to an electron-deficient organic fragment or belonging to a dihalogen molecule[13]. It is a directional interaction and similar to hydrogen bonding with respect to its strength being distance and angle dependent.

π···π interactions occur between aromatic moieties of molecules. These arise from the stabilizing dispersion interactions due to polarisable π-electron density. There is also an anisotropic electrostatic component which is influential in determining the geometry of the interaction. This is due to the multipole arising from the polarisation of the C–H bond and leads to greater electron density at the core of the aromatic moiety than at the hydrogen atom 'edge'. This polarisation results on the commonly encountered offset face-to-face and edge-to face packing motifs. It should however be noted, that this phenomenon is not well-understood and recent work by Grimme recommends the term "π–π

interactions" in the discussion of noncovalent binding between neutral closed-shell systems be used with care as there is little theoretical evidence for the special role of π orbitals for systems with ten or less carbons[14].

The basis of our understanding of the form of molecular crystals arising from the interactions of the forces described above is Kitaigorodskii's principle of close packing[1]. Thus, molecules in a crystal tend to assume equilibrium positions whereby the potential energy of the system is minimised. Assuming isotropic attractive and repulsive forces, molecules approach each other so that the number of lowest energy contacts is as large as possible. Hence, the number of intermolecular contacts is maximised and these contacts are around the minima of atom-atom potential curves. To accomplish this, the projections from one molecule must dovetail with the hollows of its neighbour so that they fill space as tightly as possible. This model provides a rationale for observed packing efficiencies, space group distribution and molecular motifs in molecular crystals; however it is a highly simplified model of crystal packing and the packing of many molecular species deviate from the Kitaigorodskii model.

Polymorphism

Polymorphism is the phenomenon whereby a compound may occur in more than one crystalline form. This may result from a difference in the packing arrangements of molecules in the different forms, known as packing polymorphism, or it may arise from the existence of different conformers of the molecule and this is known as conformational polymorphism. Different polymorphs of a substance may display distinct physiochemical properties such as different melting points, solubility rates, stability etc. and as these properties are clearly linked to a particular form; polymorphic compounds allow the effects of different packing modes to be explored.

At a specific temperature and pressure a single polymorph of a polymorphic compound is the thermodynamically stable form and other polymorphs occurring under these conditions are metastable to varying degrees. It was first observed by Wilhelm Ostwald that it is often the least stable polymorph that crystallises first and subsequently transforms into the stable form and he formulated this as Ostwald's step rule[15]. This may be rationalised by

considering that the processes of crystallisation, namely nucleation and crystal growth are governed by both kinetic and thermodynamic factors and thus conditions may favour the nucleation and growth of the metastable form over the stable form.

Desiraju[16] demonstrated that the frequency of occurrence of polymorphic modifications is not necessarily uniform in all categories of substance. His analysis revealed that the phenomenon is probably more common with molecules that have conformational flexibility and/or multiple groups capable of hydrogen bonding or coordination. Coincidentally and importantly, this is inherently the situation for many pharmaceuticals and thus polymorphism is of huge importance in the pharmaceutical industry. The reasons for this are as follows: different physiochemical properties, such as dissolution rates, of different polymorphs can have direct medical implications; it poses challenges for large-scale reproducible preparation of a compound and the discovery of new forms may expose intellectual property rights through patent litigation and thus polymorph screening is an important part of the drug development process. However, whilst Desiraju's analysis reveals general trends, it is not only these types of molecules that give extensive polymorphism. Many pigments, often with rigid planar molecules are polymorphic and this may be ascribed to different packing modes. Despite the clear relevance of polymorphism to any systematic study of crystal structure, this it is still a relatively poorly understood phenomenon as attested by the recent discovery of a new crystal form of maleic acid[17], 124 years after the first crystal was studied.

Crystal Structure Analysis

Going hand-in-hand with the burgeoning scientific interest in the study of polymorphism, crystal engineering and crystal structure prediction has been the need for systematic analysis protocols to enable the comparison of different crystal structures. In 1998 Nangia and Desiraju[18] argued that a full understanding of crystal structure and crystal engineering requires a comparison of the entire molecule and all interactions in the crystalline state. The analysis of crystal structures for similarities and differences is one of the key issues facing structural chemists today and to that end a number of methods have been developed in recent years to compare crystal structures[19,20,21,22,23,24]. Many of

these have concentrated on the comparison of subsets of structures i.e. comparing polymorphs of a single compound, or the analysis of directed interactions such as hydrogen bonding. However as has been indicated previously, crystal structures are assembled by the interplay of a number of forces and thus these methods compare only a subset of the interactions contained within crystal structures.

To be of more general utility, an analysis method should be flexible enough to identify components of a structure that may reflect the influence of the more diffuse interactions and thus be able to identify assemblies that are mainly the result of close-packing as well as networks of directed interactions. It should also be able to compare crystal structures of different molecular species to allow the systematic investigation of related families of structures, thus allowing the investigation of the effects of systematic substituent variation. With these points in mind the XPac[25] procedure has been developed in our laboratory, a summary of which follows (a more detailed explanation of the methodology is given in Chapter 2).

The XPac procedure is based on the concept of the supramolecular construct (SC) which is defined as any *geometrically* similar assembly of molecules occurring in two or more structures. SCs may be 3-D (isostructurality), 2-D (similar sheets, packed differently), 1-D (similar stacks or rows of molecules bundled differently) or 0-D (discrete molecular assemblies such as dimers, arranged differently). The emphasis on geometrical closeness rather than bonding interactions allows the 'capture' of implicit information regarding all interactions within the SC by this methodology and does not rely on identification of explicit anisotropic interactions. To enable comparison of structures and thus identification of potential SCs, the common shape of the molecular components of the crystal structures is defined by the user via a corresponding ordered series of points (COSP). This has several advantages over simply comparing the whole molecule; it allows comparison of similar fragments of non-identical species and thus the crystal structures of these species may be compared; by careful selection of the COSP, the user may select whether conformational similarity is included in the search for SCs e.g. by selection of only two points *para* to represent phenyl moieties of species under investigation, the differences in rotations of these rings in different structures may be excluded from the search for SCs. Comparisons of crystal structures, identifying similar

arrangements of the selected COSP, is accomplished by evaluation of large numbers of internal coordinates of representative clusters comprising a kernel molecule and a 'shell' of nearest neighbours generated by the space group symmetries of the crystal structures under investigation. These processes are completely automated within the XPac procedure.

Aims of Research

The study of single-crystal structures of organic molecules can yield much detail about molecular structure and conformation as well as the nature of the crystal packing. However, other information of interest such as why a molecular conformation or packing arrangement exists or how a particular crystal growth mechanism is favoured is not readily available. By the detailed comparative study of large groups of structures of similar molecules it is believed that some indicators towards answering these questions may be gained. As part of the overall effort to develop this knowledge-based approach, one of the avenues of research our group is engaged in is the study of the crystal structures of families of closely related molecules. Each of these families is examined for patterns that identify similarities or differences between members that may be related to particular features of these structures. For this thesis the family of structures chosen for study were 4,4' di-substituted chalcones or 1,3-diphenyl-2-propen-1-ones (see Figure 1-1 below).

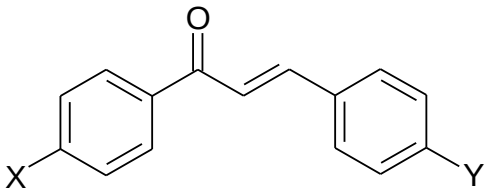

Figure 1-1: *4,4' di-substituted chalcone; X = Br, Cl, F, F_3C, H, Me, Et, MeO; Y = Br, Cl, F, H, Me, Et, OMe*

Chalcones occur in nature from ferns to higher plants[26]. They are highly bioactive and have been reported to show useful medicinal activity[27]. Some derivatives have pesticidal activity[28], and another was reported to be antimutagenic[29]. Moreover, methyl and hydroxyl substituted compounds are known as potent antioxidants[30]. They are known to be polymorphic and are

included in Deffet's *Repertoire des Composes Polymorphs*[31], which summarised the literature sources and the polymorphic behaviour of over 1000 organic compounds. According to this, polymorphism is a fairly common phenomenon amongst these compounds. In 1929 Weygand[32] reported the trimorphic behaviour of *p*-methylchalcone, the first organic compound reported with three polymorphs.

The synthesis of substituted chalcones is relatively straightforward; para-substituted acetophenone and para-substituted benzaldehyde are dissolved in ethanol with aqueous sodium hydroxide. The product crystallises immediately or after a few hours and is recovered by filtration. Additionally the starting materials are readily available commercially. These make them an attractive candidate family for systematic investigation.

The chalcones are a particularly interesting family of compounds to explore due to their lack of hydrogen bonding functionalities. The parent molecule has only one strong H-bond acceptor, the carbonyl O, and no donators and our choice of substituents purposely avoided introducing any strong H-bond donators, thus substituents such as amines or hydroxyl groups were excluded. Hence, uniquely amongst the families of compounds under study by our group, packing arrangements for a large family of related molecules *without* the influence of strong H-bonding will be explored. With the overarching influence of strong H-bonding removed, it may be possible to discern the effects of the more diffuse forces present in crystal structures. Additionally, by comparing crystal structures of differently substituted chalcones, patterns of arrangements may be revealed which are substituent-dependent.

Thus in summary this family of compounds was chosen for the following properties:

- The structures have few degrees of conformational freedom – only the phenyl rings may rotate freely
- Limited H-bonding functionalities – parent compound has single strong acceptor and no strong donors
- Indications of extensive polymorphism
- Simple synthesis and readily available starting materials

To achieve this objective, there were three parts to this project:

1. Synthesis and crystallisation
2. Data collection
3. Data analysis and interpretation

The synthesis and crystallization was kindly undertaken by Dr. T. Threlfall specifically for this work and is only touched on briefly herein. The substituents chosen were Br, Cl, F, F_3C, H, Me, Et and OMe and as noted earlier include no strong H-bond donor groups. These substituents give a potential family of 56 compounds, excluding any polymorphs. Crystals were examined by single crystal x-ray diffraction to give crystal structures for each compound. Additionally the CSD was harvested for suitable candidate structures. The structural relationships between these were then analysed using the XPac algorithm and these results interpreted. A full discussion of these is given in Chapter 3.

[1] A.I. Kitaigorodskii, *Molecular Crystals and Molecules*, Academic Press, New York, 1973

[2] F. London, *Trans. Faraday Soc.*, 1937, **33**, 8-26.

[3] G. R. Desiraju, *Crystal Engineering: The Design of Organic Solids*, Elsevier, Amsterdam, 1989

[4] L. Pauling, *The Nature of the Chemical Bond*, Cornell University Press, Ithica, 1939

[5] M. C. Etter, *J. Am. Chem. Soc.*, 1982, **104**, 1095-1096

[6] M. C. Etter, *Acc. Chem. Res.*, 1990, **23**, 120-126

[7] M. C. Etter, *J. Phys. Chem.*, 1991, **95**, 4601-4610

[8] S. C. Nyburg, W. Wong-Ng, *Proc. R. Soc. London Ser. A*, 1979, **367**, 29

[9] S. L. Price. A. J. Stone, J. Lucas, R. S. Rowland, A. Thornley, *J. Am. Chem. Soc.*, 1994, **116**, 4910

[10] D. E. Williams, L. -Y. Hsu, *Acta Crystallogr. Sect. A*, 1985, **41**, 296

[11] V. R. Pedireddi, D. S. Reddy, B. S. Goud, D. C. Craig, A. D. Rae, G. R. Dcsiraju, *J. Chem. Soc. Perkin Trans. 2*, 1994, 2353

[12] P. Metrangolo, H. Neukirch, T. Pilati, G. Resnati, *Acc. Chem. Res.* 2005, **38**, 386-395

[13] P. Metrangolo, G. Resnati, *Chem. Eur. J.*, 2001, **7**, 2511-2519

[14] S. Grimme, *Angew. Chem. Int. Ed.*, 2008, **47**, 3430-3434

[15] W. Ostwald, *Z. Phys. Chem.*, 1897, **22,** 289-330

[16] J. A. R. P. Sarma, G. R. Desiraju, Polymorphism and Pseudopolymorphism in Organic Crystals: a Cambridge Structural Database study. *Crystal Engineering: the design and application of functional solids*, M. J. Zaworotko, K. R. Seddon, Eds., Kluwer, Dordrecht, 1999; pp 325-356.

[17] G. M. Day, A. V. Trask, W. D. S. Motherwell, W. Jones, *Chem. Commun.*, 2006, 54–56

[18] A. Nangia and G. R. Desiraju, *Design of Organic Solids*, E. Weber, Ed., Springer-Verlag., Berlin, 1998, p87.

[19] T. R. Schneider, *Acta Crystallogr., Sect. D*, 2002, **58**, 195–208

[20] M. C. Etter, J. C. MacDonald and J. Bernstein, *Acta Crystallogr., Sect. B*, 1990, **46**, 256–262

[21] V. A. Blatov, Acta Crystallogr., Sect. A, 2006, 62, 356–364

[22] H. Zabrodsky, S. Peleg and D. Avnir, *J. Am. Chem. Soc.*, 1992, **114**, 7843–7851

[23] M. A. Spackman and P. G. Byrom, *Chem. Phys. Lett.*, 1997, **267**, 215–220

[24] J. J. McKinnon, A. S. Mitchell and M. A. Spackman, *Chem.–Eur. J.*, 2002, **4**, 2136–2141

[25] T. Gelbrich, M. B. Hursthouse, *CrystEngComm*, 2005, **7**, 324-336

[26] A. W. Star, T. J. Marby, *Phytochemistry*, 1971, **10**, 2812–2817

[27] K. Satyanarayna, M. N. A. Rao, *Indian Drugs*, 1993, **30**, 313–318

[28] D. N. Dhar, *The Chemistry of Chalcones and Related Compounds*, Wiley, New York, 1981, p213

[29] T. Torigoo, M. Arisawa, S. Iloch, M. Fujiu, H. B. Mayuyama, *Biochem. Biophys. Res. Commun.*, 1983, **112**, 833–842

[30] R. J. Anto, K. Sukumaran, G. Kuttan, M. N. A. Rao, V. Subbaraju, R. Kuttan, *Cancer Lett.*, 1995, **97**, 33–37

[31] L. Deffet, *Repertoire des Compose's Organique Polymorphs*, Desoor, Liege, Belgium, 1942

[32] C. Weygand, *Lieb. Ann.*, 1929, **472**, 143

Chapter 2 : Experimental Techniques

In this chapter the techniques used in this study will be described. Special attention will be paid to the single crystal x-ray diffraction technique and the XPac crystal packing analysis program[1]. Additionally, database mining and other crystallographic analysis techniques will be described.

In essence, this thesis is a crystal packing analysis of the group of organic compounds described in the previous chapter. This involved two phases: the primary data collection; namely the crystal structures of the compounds studied, were collected by single crystal x-ray diffraction from crystals grown by Dr. T. Threlfall. Additionally, the Cambridge Structural Database[2] was mined for candidate structures. The second phase is derived data creation, namely the analysis of the crystal structures with the XPac algorithm, using the primary data in CIF format.

Synthesis and Crystallisation

All compounds used in this study were synthesised and crystallised by Dr. T. Threlfall according to the following reaction scheme.

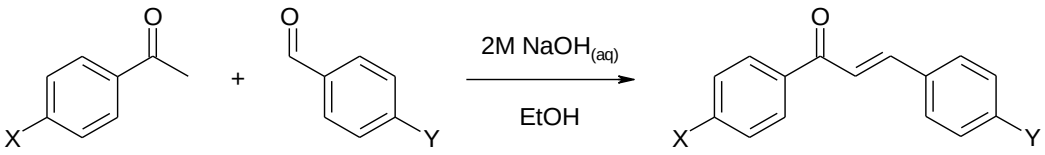

Recrystallisation of many of these compounds proved extremely problematic. In many cases only poor quality crystals could be obtained, despite several recrystallisation attempts and in some cases crystals of suitable quality were never obtained. This unfortunately, has resulted in some gaps in the set of compounds studied which it would be desirable to fill.

Structure Determination

Crystal Structure

A perfect crystal is composed of a number of atoms, ions, or molecules arranged in a periodic manner that is repeated by translation in all directions to yield a highly ordered, generally close packed structure. This translational periodicity in crystal structures may be conveniently described, by considering the geometry of the repetition rather than the identities of the motif repeated. Thus, if the intervals of repeat in a crystal are *a*, *b* and *c* along three non-coplanar directions, the repetition geometry can be described by a series of points at *a*, *b* and *c* intervals along these same three directions. This collection of points is called a lattice. It should be realised that changing the position of the lattice points with respect to defining the repeating motif does not change the lattice.

By defining an arbitrary lattice point as the origin, three vectors **a**, **b** and **c** may be described between the origin and the three nearest, non-coplanar lattice points. These are the unit vectors for the lattice and the translation vector, **t**, between the origin and any other lattice point may be described in terms of them such that:

$$\mathbf{t} = u\mathbf{a} + v\mathbf{b} + w\mathbf{c} \qquad \textbf{Equation 2-1}$$

where *u*, *v* and *w* are integers. Thus the geometry of the lattice can be completely described by these unit vectors; however to do this with pure numbers we must define the lengths of the unit vectors, and angles between each. By standard convention, the lengths of the three unit vectors are called *a*, *b* and *c* and the angles between each of the three pairs of unit vectors are called α, β and γ, such that α is the angle between **b** and **c**, β is the angle between **a** and **c** and γ is the angle between a and **b**. These three unit vectors (and the nine others equivalent to them) define a parallelepiped, which is called the unit cell and the vector lengths and angles between them are called the unit cell or lattice parameters.

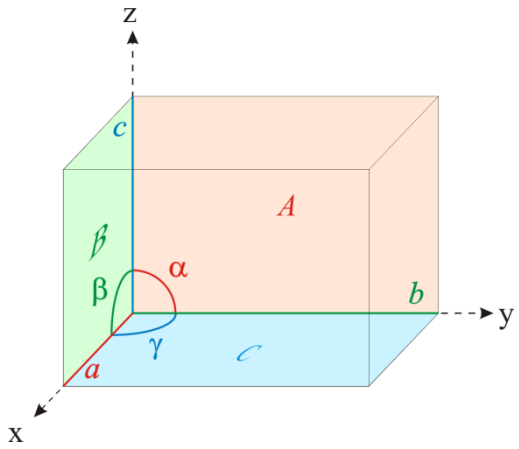

Figure 2-1: *Diagram of unit cell showing labelling of vectors, interaxial angles and faces.*

The unit cell described above has a lattice point at each intersection giving a total of eight lattice points; however, each of these lattice points is shared by eight unit cells and thus the cell contains a total of one lattice point and is thus described as primitive (*P*). In many crystal structures, due to symmetry elements present (see below), it is more convenient and conventional to consider unit cells that contain more than one lattice point and these are known as centred cells. There are six types of centring that unit cells may have: lattice points present at the centres of opposite faces (*A*, *B* or *C*, depending on which faces are centred) or at the body centre (*I*) and these contain two lattice points; unit cells with lattice points at the centres of all their faces (*F*) contain four lattice points and rhombohedrally centred unit cells (*R*) contain three. When considering centred unit cells, Equation 2-1 above is modified, such that *u*, *v* and *w* are rational numbers.

Up until now only the translational aspects of crystallographic periodicity have been considered. However as has been touched on above, the symmetry elements present within the unit cell also provide constraints and conventions on the choice and geometry of unit cells. If a molecule has symmetry in components of point groups, it is possible that this symmetry contributes to the development of repetition e.g. if a molecule has 3-fold symmetry, it is possible for repetition to develop in three related directions. Alternatively, if a molecule has no symmetry which is by far the dominant situation, then molecules pack together via the use of new types of symmetry using a point operation plus translation (see below).

There are two types of symmetry element which individual molecules may possess: proper rotations, which are rotations about an axis by a certain fraction of 360° and improper rotations, which are rotations followed by reflection in the plane perpendicular to the rotation axis and at the centre of the molecule. These symmetry operations come from the Schoenflies convention as used in spectroscopy. Crystallographers, however use the Hermann-Maugin convention, which defines an improper rotation as a rotation followed by an inversion through a point at the centre of the molecule. The equivalent notations for each convention are listed for symmetry elements and operations relevant to crystallography in Table 2-1.

	Proper Rotations					Improper Rotations				
Hermann-Maugin	1	2	3	4	6	$\bar{1}$	$\bar{2}$ (or m)	$\bar{3}$	$\bar{4}$	$\bar{6}$
Schoenflies	C_1 (or E)	C_2	C_3	C_4	C_6	S_2 (= i)	S_1 (=σ)	S_6	S_4	S_3

Table 2-1: *Symmetry element and operation notations in the Hermann-Maugin and Schoenflies conventions. The proper rotation '1' is called the identity operation; the improper rotation* $\bar{\mathbf{1}}$ *is the inversion and the improper rotation* $\bar{\mathbf{2}}$ *is the reflection.*

Whilst individual molecules, in principle, may have any order rotation axis, the constraints of the translation symmetry of the unit cell mean that within the environment of the crystal (i.e. the unit cell) only the orders of rotation listed in Table 2-1 are possible. The symmetry elements present within a unit cell place constraints on the geometry of the unit cell and these give rise to the seven crystal systems listed, along with their essential symmetry and geometrical restrictions in Table 2-2.

Crystal system		Unit cell restrictions	Essential symmetry
Triclinic		None	None
Monoclinic		$\alpha = \gamma = 90°$	One 2-fold axis and/or mirror plane
Orthorhombic		$\alpha = \beta = \gamma = 90°$	Three 2-fold axes and/or mirror planes
Tetragonal		$\alpha = \beta = \gamma = 90°$; a = b	One 4-fold axis
Trigonal	Rhombohedral	$\alpha = \beta = \gamma$; a = b = c	One 3-fold axis
	Hexagonal	$\alpha = \beta = 90°$, $\gamma = 120°$; a = b	One 6-fold axis
Cubic		$\alpha = \beta = \gamma = 90°$; a = b = c	Four 3-fold axes

Table 2-2: *The seven crystal systems with their cell parameter restraints and essential symmetry. The essential symmetry axes may be proper or improper rotation axes as well as screw axes and glide planes, in the case of the crystal structure symmetry..*

When the seven crystal systems are combined with the different types of cell centring (*P*, *A*, *B*, *C*, *I*, *R*, *F*) described above, fourteen geometrical combinations are found and these are known as the Bravais lattices and are shown in figure 2-2.

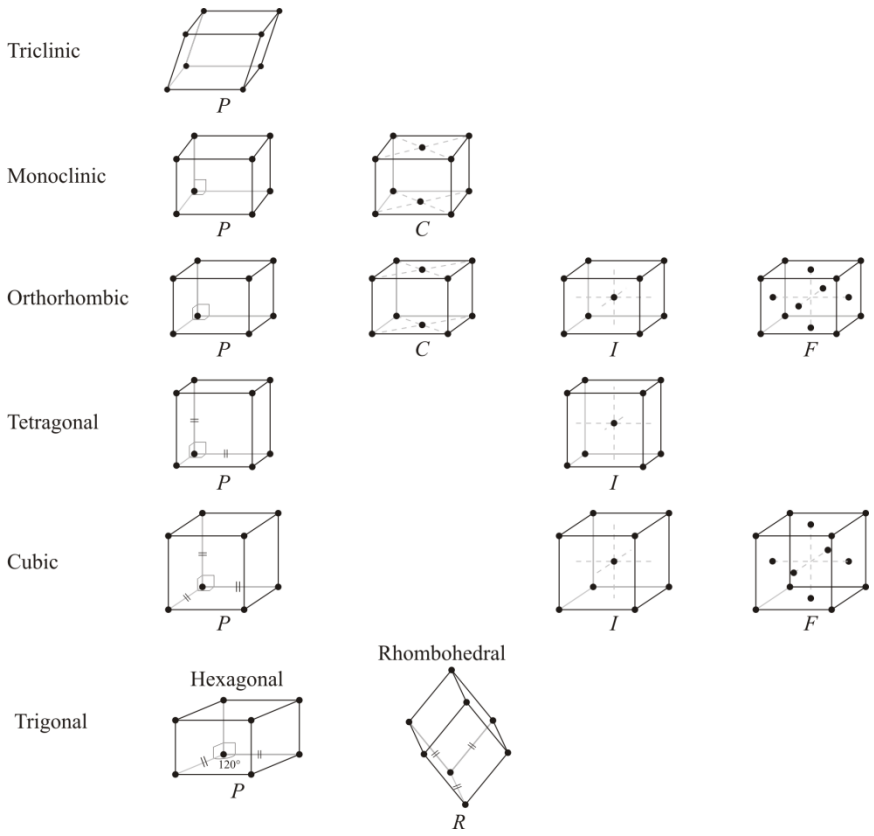

Figure 2-2: *The fourteen Bravais Lattices. Equal cell lengths are marked '=' and 90° angles are marked '┐'.*

With these considerations, it is apparent that a number of unit cells may be selected from a given lattice. In practice, the unit cell normally selected is that with the highest symmetry, shortest vector lengths and interaxial angles closest to 90°.

So far, only the point group symmetry of individual molecules has been discussed and it is so named because all of the symmetry elements present in a given molecule must pass through a single point in space. A property of point group symmetry is that repeated application of a symmetry operation will eventually return a molecule to its original position in space. However, the translational periodicity within the crystalline environment removes this restriction and allows consideration of other types of symmetry operations.

Thus, a space symmetry operation is simply a symmetry operation of one of the types considered above followed by a translation and there are two types: screw axes which are proper rotations followed by a translation and glide planes which are reflections followed by a translation. The translation in each case is by a fraction of the unit cell vectors, such that repeated application of the symmetry operation places the molecule in an equivalent position in the next unit cell along the translation vector. Table 2-3 summarises the possible types of screw axes and glide planes.

Screw Axes (rotations)		Glide Planes (reflections)	
Order	Notation	Translation vector	Notation
2-fold	2_1	Parallel to cell axis	*a b c*
3-fold	3_1 3_2	Parallel to diagonals	*n*
4-fold	4_1 4_2 4_3	Between corner and centred lattice points	*d*
6-fold	6_1 6_2 6_3 6_4 6_5		

Table 2-3: *Possible types of screw axes and glide planes. Screw axes subscript values denote the multiplier to the minimum translation which is 1/rotation order.*

The symmetry elements and operations so far discussed are all those that can occur in a crystalline solid however, because of the constraints of the lattice symmetry, only 230 combinations are possible. These are the crystallographic space groups, where each space group represents a particular combination of point and space symmetry elements in an arrangement compatible with the geometry of the lattice. The complete crystal structure may be obtained by application of the appropriate space group symmetry operations to the contents of the asymmetric unit. Each space group is classified according to its crystal system and is denoted by an upper case letter denoting its lattice type followed by a list of applicable symmetry elements. Some combinations of symmetry elements necessarily imply the presence of others and so not all symmetry elements are listed. The rules for which symmetry elements take precedence vary according to crystal system. The International Tables for Crystallography list all 230 space groups along with diagrams and other information for each. The distribution of crystal structures is far from even amongst the 230 space groups; whilst higher symmetry space groups predominate for inorganic ionic and network structures and minerals, the vast majority of molecular materials tend to

crystallise in lower symmetry triclinic, monoclinic and orthorhombic space groups

Single Crystal X-ray Diffraction

X-rays are a form of electromagnetic radiation with a wavelength in the range of 0.1 – 100Å lying between the UV and gamma ray wavelengths in the electromagnetic spectrum. Although discovered in1895 by Wilhelm Röntgen, it was not until 1912 that Max von Laue recognised their ability to be diffracted by crystals. This is because the wavelength of x-rays is of the same order of magnitude as the interatomic distances in crystals. X-rays are generated by bombarding a metal target with high-energy electrons. A continuous range of wavelengths is produced from the deceleration of the electrons deflected by the metal atomic nuclei, known as Bremsstrahlung. This bombardment also causes some 1s electrons from the inner atomic orbital of the metal nuclei to be displaced and these are replaced by electrons dropping from higher energy 2s and 3s orbitals with the corresponding releases of x-ray photons of specific wavelengths dependent on the metal target. The desired wavelength is then selected by passing the radiation through a suitable monochromator, such as a graphite crystal. For x-ray crystallography the metal targets typically used to generate x-rays are Mo ($\lambda = 0.71073$Å) and Cu ($\lambda=1.5418$Å).

From his work, Max von Laue derived three equations, the Laue equations, to describe the necessary conditions for constructive interference (i.e. a diffraction spot) of x-rays by crystals. Although physically rigorous, they are cumbersome to use and in 1913, father and son, W. H. and W. L. Bragg developed a far simpler model to describe the diffraction of x-rays by crystals. The Bragg model regards a crystal as a stack of lattice planes of separation d_{hkl}, each of which acts as a mirror. This model makes it simple to calculate the glancing or 'Bragg' angle, θ, such that constructive interference occurs, as shown in Figure 2-3 and Equation 2-2.

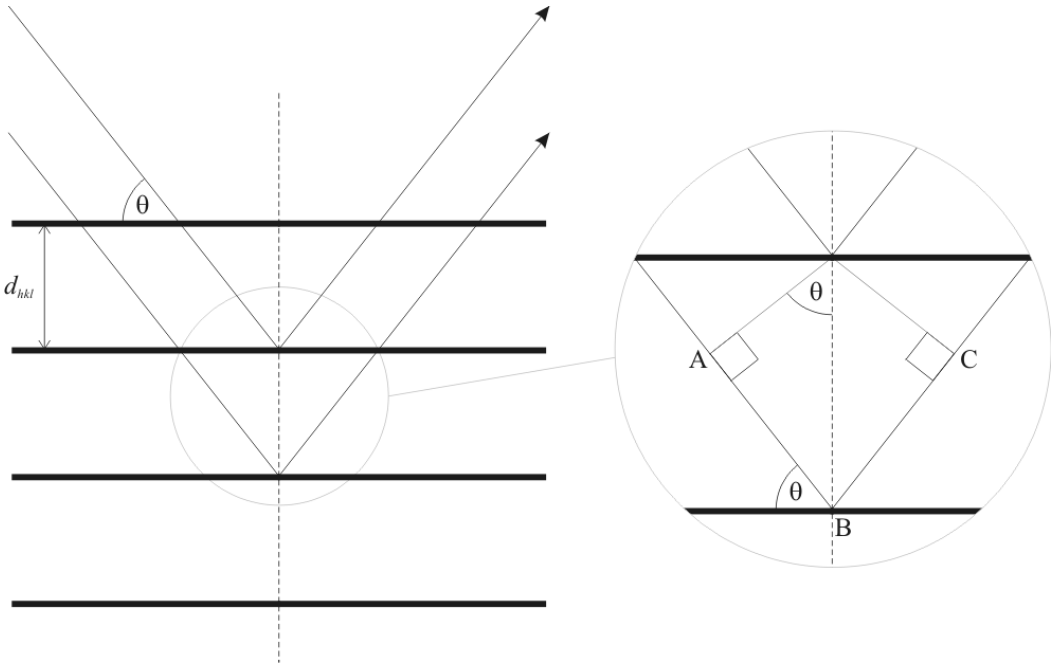

Figure 2-3: *Derivation of Bragg's Law; for constructive interference or a 'reflection' to occur, the difference in path length between the two rays, AB+BC=2d_{hkl} sinθ, must equal an integer number of wavelengths.*

Thus for constructive interference to occur between lattice planes (*h, k, l*):

$$n\lambda = 2d_{hkl} \sin\theta \qquad \textbf{Equation 2-2}$$

n = integer

λ = x-ray wavelength

d_{hkl} = lattice plane spacing

θ = 'Bragg' angle

Reflections of n^{th}-order, where n >1, are usually regarded as arising from planes (*nh, nk, nl*) and thus Equation 2-2 can be rewritten thus:

$$\lambda = 2d_{hkl} \sin\theta \qquad \textbf{Equation 2-3}$$

The Bragg equation describes the diffraction process for a simple atomic lattice but to fully understand the diffraction process it is necessary to go further. The diffraction of x-rays by an atom is due to the electrons associated with that atom. Thus the scattering factor, *f*, of an atom depends on its electron density distribution and also the incident angle of the x-rays. For 2θ = 0, *f* = number of electrons associated with atom and as 2θ increases, *f* decreases; this is because at higher angles the x-rays begin to become out of phase with each other. As the diffraction pattern of a crystal is derived from the whole crystal, the scattering

factors of all the atoms must be taken into account. The summation of the scattering factors of a group of atoms (in the unit cell), including their relative changes in phase due to distance from the origin, for a reflection *h*, *k*, *l*, is called the structure factor, F_{hkl}; it is a complex number with amplitude and phase and is defined thus:

$$F_{hkl} = \sum_{j=1}^{unit\ cell} f_j\, e^{-2\pi i\left(hx_j + ky_j + lz_j\right)} \qquad \textbf{Equation 2-4}$$

This extends over all atoms, *j*, with fractional coordinates, *x*, *y*, *z*. If all the structure factors F_{hkl}, were known, the electron density distribution of the unit cell, $\rho(xyz)$, could be found by a Fourier transform of Equation 2-4 thus:

$$\rho(xyz) = \frac{1}{V}\sum_{hkl} F_{hkl}\, e^{-2\pi i\left(hx_j + ky_j + lz_j\right)} \qquad \textbf{Equation 2-5}$$

However, the intensity of a reflection, I_{hkl}, is proportional to the square modulus of F_{hkl}, $|F_{hkl}|^2$. From this, the amplitude of F_{hkl} may be found but the phase information is lost and this is known as the phase problem. Much of the task of solving a crystal structure is recovering this lost phase information, at least to an approximation that allows the Fourier transform of Equation 2-5 to be carried out. There are two widely-used techniques for this, direct methods and Patterson synthesis. Direct methods rely on the possibility of treating the electron distribution of the unit cell as virtually random and then use statistical techniques to compute the probability that the phases have a particular value. This is mathematically intensive and is processed by computer but a good dataset will yield the electron density map for the whole structure, which is then ready for refinement. Direct methods work well for organic compounds where the atoms have approximately equal electron densities and were used for the structure solution of all the compounds in this project. The alternative to direct methods is Patterson synthesis and it is a modification of Equation 2-5. It is useful for structures with a few heavy atoms and relies on the fact that these heavy atoms dominate the scattering and are quite easy to locate. This is an iterative process and when the heavy atoms are located, the phase information can be used to calculate the positions of the lighter atoms and the structure is then ready for refinement.

The final stage of crystal structure determination is refinement and involves systematically altering the parameters of the model to give the best multidimensional least squares fit between the observed data for each reflection, $|F_o|$, and that calculated for the model, $|F_c|$. An atom is initially refined with four parameters; three for its positional coordinates and an atomic displacement parameter, *U*, which represents the isotropic motion of the atom due to thermal vibration. In the final stages of refinement, *U* is modelled with six parameters and the thermal motion of the atom is modelled anisotropically. This usually leads to a marked improvement in the fitting between $|F_o|$ and $|F_c|$. Additional parameters may be necessary during refinement, dependent on the crystal structure, to achieve a reasonable fit between the model and observed data. Progress during the refinement is measured by the residual (R) factor, which is a measure of the deviation of the model data $|F_c|$, with the observed data, $|F_o|$ and is defined thus:

$$R = \frac{\sum\big||F_o| - |F_c|\big|}{\sum|F_c|} \qquad \textbf{Equation 2-6}$$

During refinement the R-factor generally decreases to a stationary minimum of between 0.02 - 0.10, depending on the quality of the data and when this occurs, refinement is complete. Once the refinement is complete the positions of the atoms in the unit cell are known along with an estimate of the errors in these positions and this data can be used to derive intermolecular bond lengths and angles between atoms.

Experimental Procedure

For most of the structures reported in this thesis intensity data were collected using Mo *Kα* radiation (λ=0.71073) monochromated by either a graphite crystal or 10mm confocal mirrors, on a Bruker-Nonius Kappa CCD diffractometer with a Bruker-Nonius FR591 rotating anode. Data reduction and cell refinement was carried out with COLLECT[3] and DENZO[4] and absorption correction was applied to the data using SADABS[5]. Some crystals were too small or weakly diffracting to provide useful data from the above instrumentaton and intensity data for these were collected using synchrotron radiation at Station 9.8, Daresbury on a Bruker AXS APEX2 diffractometer. Data reduction and cell

refinement was carried out with SAINT[6] and absorption correction was applied to the data using SADABS[5]

The structures were solved by direct methods[7,8] and refined on F^2 by least-squares procedures[7]. The H atoms were located in difference maps and those attached to C were treated as riding. Positions of H atoms attached to N were refined using DFIX instruction in SHELXL.

Database Mining

As well as obtaining crystal structures directly from single crystal X-ray diffraction experiments the Cambridge Structural Database (CSD)[2] was searched for structures relevant to the thesis project that were already available. The CSD is a comprehensive database of small molecule organic and organometallic structures containing to-date more than 400 000 structures. Search, retrieval, analysis and display of information are achieved using the interface software ConQuest, which allows searching on a variety of fields. Structure searching based on chemical drawings and queries may be combined using standard logical operators allowing finely-tuned searches to be run. Further refinement of results is possible through combining search results.

For this study a simple structural search based on chemical drawings of the core molecules was sufficient. This was refined by visual examination of the search result.

Assessment of Structural Results

XPac Crystal Packing Analysis

The XPac algorithm[1] was developed by Dr. T. Gelbrich and enables the comparison of crystal packing structures of polymorphs and families of similar compounds in terms of their common 0-D, 1-D, 2-D or 3-D components. These components are termed 'supramolecular constructs' and are fundamental to the understanding of the XPac technique.

A supramolecular construct (SC) is defined simply as any assembly of atoms, ions or molecules that occurs in two or more crystal structures of related polymorphs or similar molecules. Similar molecules may be different species but must have approximately the same shape as represented by the families of compounds studied in this project. These assemblies may be 3-D, in the case of isostructurality; 2-D, where identical sheets are stacked differently; 1-D, where identical chains are bundled differently or 0-D, where isolated assemblies such as dimers are differently packed. This definition is different from that of the widely-used term 'supramolecular synthon'[9], employed in crystal engineering, insofar as supramolecular synthons focus on the specific molecular bonding interactions of the component assemblies; whereas for SCs, no bonding interactions are necessarily implied within an assembly, only a geometrical closeness. Thus the scope of SCs is much wider, encompassing assemblies based on more directionally-diffuse intermolecular interactions, such as ionic or van der Waals forces, as well as those linked through the more simply-characterised, directional interactions, such as H-bonds, described by supramolecular synthons. The existence of an SC in two or more crystal structures may be interpreted as a possible indication of a preferred mode of nucleation or crystal-growth irrespective of any bonding interactions that may be present and this may then be a starting point for further investigation of these processes.

The basis of the XPac procedure is the use of 'similarity' to identify SCs within sets of structures, thus assemblies of molecules in different crystals are similar (and hence SCs) if they consist of the same type of molecules, assembled in the same way. It should again be stressed that these assemblies are based on the geometrical configuration of their component molecules and not on the connectivity of them. The types and relationships possible for SCs is illustrated

in Figure 2-4 by a hypothetical set of crystal structures of five similar compounds, A-E, where C delivers two polymorphic forms C^{I} and C^{II} (this situation is analogous to the work undertaken in this project).

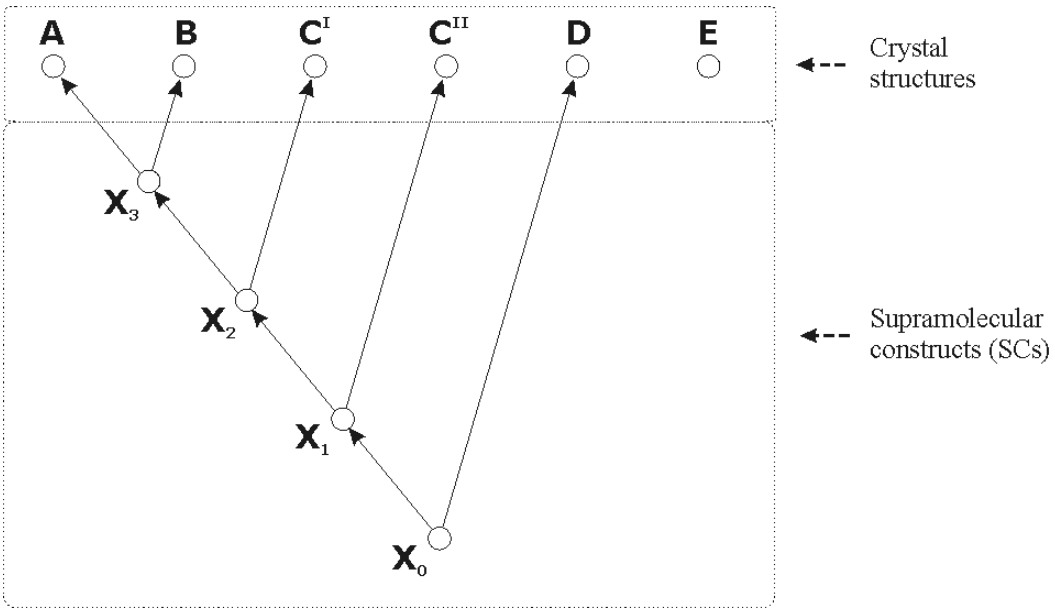

Figure 2-4: *Possible SC relationships, $X_0 - X_3$, in a hypothetical family of five compounds, **A**-**E**, which deliver the six crystal structures shown.*

A and B are isostructural and thus the entire 3D structure of these two crystal structures is similar and this is represented by SC, X_3. Conversely E is unique and contains no arrangement of two neighbouring molecules in common with the other structures of the group and thus contains no SCs. X_0 represents such an arrangement, a discrete 0-dimensional SC such as an H-bonded dimer and this is a common feature of all the structures A-D. These 0-dimensional SCs are arranged in two distinct ways in this group of structures represented by the crystal structure D and the SC X_1, which itself is a 1-dimensional arrangement, such as a chain or stack, of X_0 SCs, and is common to the remaining structures. Likewise, there are two arrangements of X_1, crystal structure C^{II} and the 2-dimensional SC, X_2, the arrangement common to A, B and C^{I}. Finally, there are two different 3-dimensional arrangements of X_2 SCs, represented by crystal structure C^{1} and SC X_3.

The XPac method of identifying SCs relies on the idea that a whole crystal structure (and thus its subcomponents) may be represented by a 'cluster' of molecules within it, defined by an arbitrary central molecule (the 'kernel') and

the group of its nearest neighbours (the 'shell') which is analogous to its coordination sphere. This representation of crystal structure is independent of conventional crystal descriptors, i.e. space group, unit cell parameters, Z', etc. and thus such representations of different structures are always comparable with each other. To enable direct comparison between crystal structures of different compounds their molecular shape must also be parameterised and this is facilitated with XPac by representing the molecular component(s) of the asymmetric unit of a crystal structure as an ordered set of points (OSP) where the OSP is a suitable selection of representative atoms. The consistency (similarity) of corresponding ordered sets of points (COSP) from two or more structures may be tested by comparing lists of sufficiently large, i.e. representative, numbers of internal coordinates – distances, angles, torsion angles etc. If *N* single pairs of corresponding entries x_i and x'_i are present in two such lists, then the mean value δ of all *N* absolute differences $|x_i - x'_i|$

$$\delta = \frac{1}{N}\sum_{i=1}^{N}|x_i - x'_i| \qquad \textbf{Equation 2-7}$$

is an indicator for the consistency of the COSP. This test is applied initially by XPac using lists of intermolecular angles to test the consistency and thus suitability of the COSP under investigation (δ_{con} will be close to 0° for suitable COSP) and subsequently throughout the comparison process. To compare a set crystal structures, a cluster is generated using the COSP as the kernel and a shell of symmetry generated OSP for each structure and each cluster is then compared pair-wise with every other cluster. The comparison is carried out in two stages: firstly, all possible double sub-units are generated, each comprising of the kernel molecule and one shell molecule, for both clusters and the each double sub-unit of one cluster is compared to every double sub-unit of the other. A typical cluster consists of a kernel molecule plus fourteen shell molecules so for two Z'=1 structures 196 comparisons are performed. For each double sub-unit pair δ_{amg}, δ_{dhd} and δ_{tor} are calculated (Equation 2-7) based on lists of intermolecular angles, dihedrals and torsion angles respectively and filtered based on user-defined values (default values are ang = 7°, dhd = 18° and tor = 18°). Any double sub-unit pair which passes all filters is deemed similar and passed to the second stage where *s* similar double sub-unit are pair-wise combined to give

$(s^2 - s)/2$ triple sub-units each comprising of the kernel and two shell molecules. These are compared and filtered as above and the resulting similar triple sub-units are assembled to give the seed of a SC which may then be characterised from the crystallographic information contained in the seed. For structures with Z'>1, the above procedure is slightly modified insofar as COSP are selected for each set of independent molecules from which clusters are generated. Each cluster is the subjected to the above procedure and it may be necessary to merge any SC seeds that result from each cluster.

To summarize, the XPac procedure is as follows:

1. Crystal structure data is input in CIF format and suitable COSP are selected for each independent molecule in the asymmetric unit.
2. From each kernel, shell molecules are generated according to crystal symmetry and intermolecular distance < sum of the van der Waals radii + 1.5Å to form a cluster.
3. All double sub-units of a cluster, each comprising of the kernel plus a shell molecule are compared to all double sub-units of a second cluster and each pair is assessed for similarity. Similar pairs are passed to the next stage.
4. If more than one similar pair is present the component double sub-units are combined in pairs to form a set of triple sub-units, each comprised of the kernel and two shell molecules.
5. Triple sub-unit pairs are compared and assessed and similar pairs are used to construct the primary seed of the SC from each cluster. For Z'>1 structures, primary seeds may need to be merged. These seeds can be readily characterised according to dimensionality and orientation to the original structure.

Step 1 is carried out by the user and at this stage, δ_{con} may be tested for COSP, allowing the general suitability for comparison of structures to be assessed and also the filter parameter values may be adjusted if necessary. Steps 2-5 are automated and seeds are output as collections of molecules using the ARU notation of many crystallographic software packages including Platon[10]. Seeds may also be visualised using XPac.

Identification of Packing Similarity

The set of n = 50 structures and $(n^2 - n)/2$ = 1225 structure pairs was investigated for packing similarity, using the XPac program as described above

with standard filter parameters. In order to rationalize procedures once the complete three-dimensional arrangements of molecules in two structures were found to be isostructural, only one was kept for subsequent investigations, the assumption being that the same results would be obtained from both structures when compared to a third. All comparisons were carried out with parameter lists derived from corresponding ordered sets of points. These were obtained from the atoms highlighted in Figure 2-5. The geometry of the selected points highlights the essential shape of the molecules whilst being unaffected by any rotation of the benzene/pyridine rings.

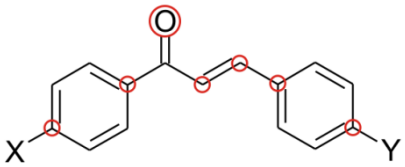

Figure 2-5: *COSP for chalcones; atoms used for COSP are highlighted with red circles.*

[1] T. Gelbrich and M. B. Hursthouse, *CrystEngComm.*, 2005, **7**, 324-336

[2] CSD V5.29 (2007); F. H. Allen, *Acta Crystallogr.*, 2002, **B58**, 380

[3] COLLECT: Data Collection Software, R. Hooft, B. V. Nonius, 1998

[4] Z. Otwinowski, W. Minor, *Macromol. Crystallogr., PartA,* 1997, **276**, 307-326

[5] G. M. Sheldrick, SADABS v.2.10, Bruker AXS Inc., Madison, Wisconison, USA., 2003

[6] SAINT, Bruker AXS Inc. Madison, Wisconison, USA, 2004.

[7] SHELX97 [Includes SHELXS97, SHELXL97, CIFTAB (and SHELXA?)] - Programs for Crystal Structure Analysis (Release 97-2). G. M. Sheldrick, Institüt für Anorganische Chemie der Universität, Tammanstrasse 4, D-3400 Göttingen, Germany, 1998.

[8] SIR2002. M. C. Burla, M. Camalli, B. Carrozzini, G. L. Cascarano, C. Giacovazzo, G. Polidori and R. Spagna. *J. Appl. Cryst.*, 2003, **36**, 1103.

[9] G. R. Desiraju, *Angew. Chem. Int. Ed. Engl.*, 1995, **34**, 2311

[10] A. L. Spek, *J. Appl. Cryst*., 2003, **36**, 7

Chapter 3 : Chalcone Results and Discussion

In this chapter the chalcone crystal structures obtained in this study and the results of their comparison and classification with XPac are described and discussed. The hierarchy and relationships of the supramolecular constructs found with XPac are illustrated using various methods including Hasse diagrams which give a graphical representation of the similarity relationships present.

The 4,4'-disubstituted chalcones were the largest of the three groups in this study comprising 46 compounds which yielded 50 crystal structures. Their crystallographic parameters are summarised below and because the packing arrangements of these structures are so fundamental to this study, diagrams of each of their unit cells are also shown.

The notation for solid forms used throughout this chapter is X-C-Y where X and Y represent the 4 and 4' benzyl substituents respectively and C represents the core chalcone moiety ($C_{15}H_{10}O$). Polymorphs, where present, are denoted with a suffixed, bracketed number. All substituents except for OMe are rotationally symmetrical or pseudo-symmetrical, which reduces the options for different packing owing to group rotation. Additionally, none of the substituents are strong hydrogen bond donors and thus no classical H-bonds are present in any of these crystal systems.

Chalcone Crystal Structures

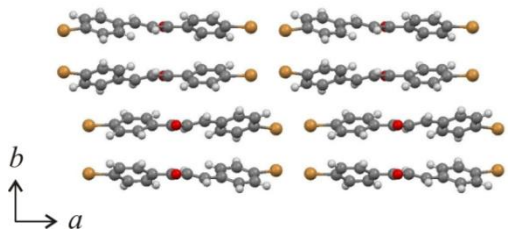

1. Br-C-Br

monoclinic $P2_1/c$ (14)

a = 15.724(3)Å b = 13.948(5)Å c = 16.635(4)Å

α = 90° β = 92.33(1)° γ = 90°

V = 1277.6(5)Å^3

Z'= 1

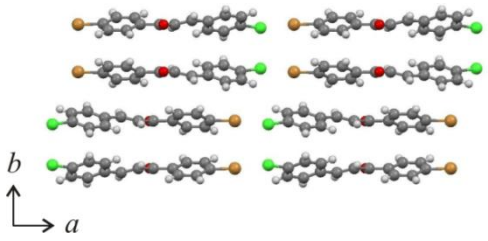

2. Br-C-Cl

monoclinic $P2_1/c$ (14)

a = 15.6116(8)Å b = 13.9778(7)Å c = 5.8184(2)Å

α = 90° β = 92.756(3)° γ = 90°

V = 1268.2(1)Å^3

Z'= 1

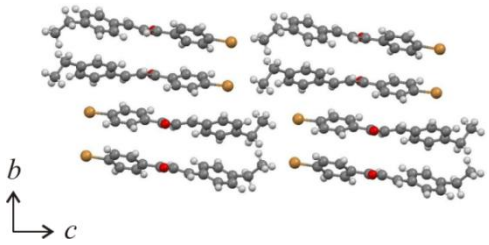

3. Br-C-Et

triclinic $P\bar{1}$ (2)

a = 5.859(1)Å b = 14.308(2)Å c = 5.8184(2)Å

α = 91.88(1)° β = 91.91(2)° γ = 90.61(1)°

V = 1329.9(5)Å^3

Z'= 2

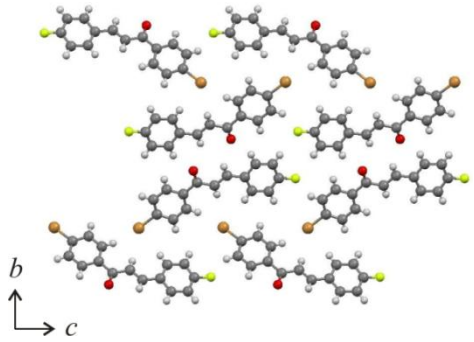

4. Br-C-F

monoclinic $P2_1/n$ (14)

a = 4.0137(1)Å b = 23.1253(8)Å c = 13.5057(4)Å

α = 90° β = 96.349(2)° γ = 90°

V = 1245.88(6)Å^3

Z'= 1

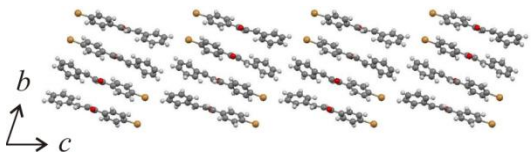

5. Br-C-H

monoclinic $P2_1/c$ (14)

a = 15.10(1)Å a = 5.90(1)Å a = 31.13(2)Å

α = 90° β = 108.6(1)° γ = 90°

V = 2628.5(1)Å^3

Z'= 2

CSD entry BRCHAL[1]

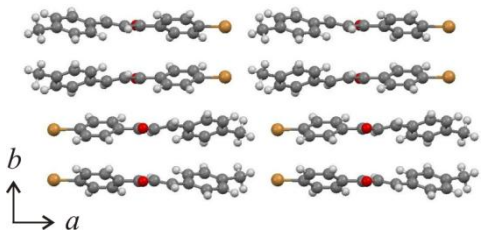

6. Br-C-Me

monoclinic $P2_1/c$ (14)

a = 15.6425(7)Å b = 14.4138(8)Å c = 5.8990(3)Å

α = 90° β = 92.269(4)° γ = 90°

V = 1329.0(1)Å^3

Z'= 1

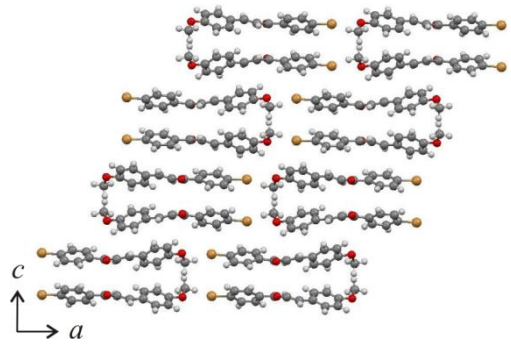

7. Br-C-OMe

monoclinic $P2_1/n$ (14)

a = 15.776(2)Å b = 5.9141(3)Å c = 29.012(3)Å

α = 90° β = 90.421(3)° γ = 90°

V = 2706.7(4)Å^3

Z'= 2

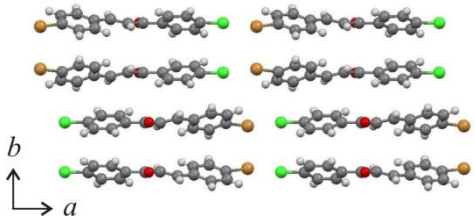

8. Cl-C-Br

monoclinic $P2_1/c$ (14)

a = 15.5178(8)Å b = 14.2137(6)Å c = 5.9113(2)Å

α = 90° β = 92.515(2)° γ = 90°

V = 1302.6(1)Å^3

Z'= 1

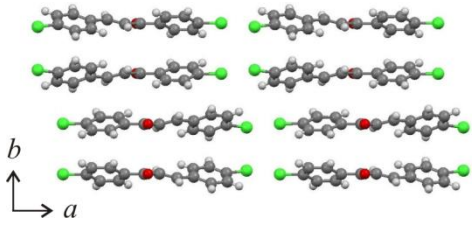

9. Cl-C-Cl

monoclinic $P2_1/c$ (14)

a = 15.3734(9)Å b = 14.2123(7)Å c = 5.8906(3)Å

α = 90° β = 92.928(2)° γ = 90°

V = 1285.4(1)Å^3

Z'= 1

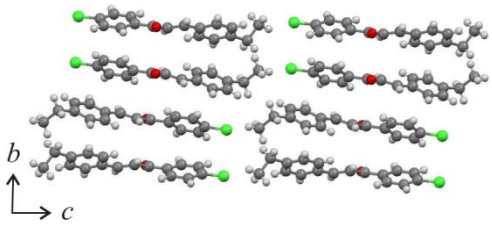

10. Cl-C-Et

triclinic $P\bar{1}$ (2)

a = 5.8727(3)Å b = 14.2193(8)Å c = 16.343(1)Å

α = 91.600(2)° β = 91.997(2)° γ = 90.598(4)°

V = 1363.3(1)Å^3

Z'= 2

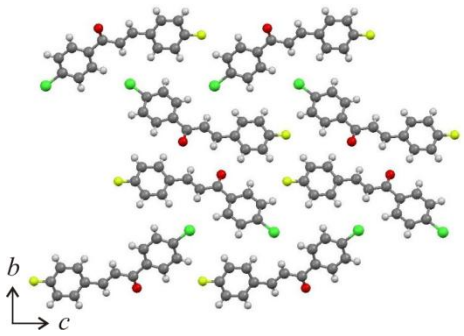

11. Cl-C-F

monoclinic $P2_1/n$ (14)

a = 3.9499(1)Å b = 23.0419(6)Å c = 13.3737(4)Å

α = 90° β = 96.145(1)° γ = 90°

V = 1210.19(6)Å^3

Z'= 1

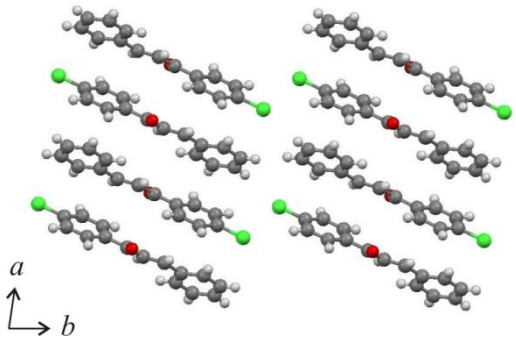

12. Cl-C-H

triclinic $P\bar{1}$ (2)

a = 7.565(2)Å b = 14.060(2)Å c = 5.858(1)Å

α = 90.09(2)° β = 92.15(2)° γ = 81.70(2)°

V = 616.12(1)Å^3

Z'= 1

CSD entry PUQSOJ[2]

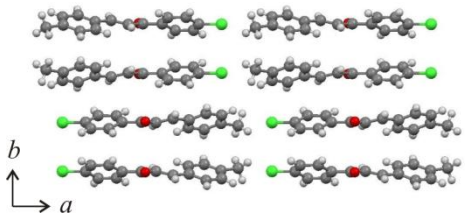

13. Cl-C-Me

monoclinic $P2_1/c$ (14)

a = 15.351(2)Å b = 14.352(2)Å c = 5.9070(6)Å

α = 90° β = 92.283(4)° γ = 90°

V = 1300.4(3)Å^3

Z' = 1

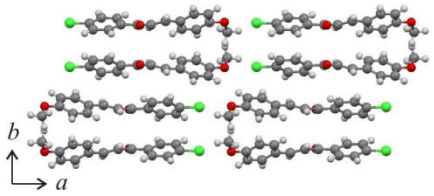

14. Cl-C-OMe (1)

monoclinic $P2_1/c$ (14)

a = 15.6425(9)Å b = 14.1207(9)Å c = 5.8452(2)Å

α = 90° β = 90.362(4)° γ = 90°

V = 1291.1(1)Å^3

Z' = 1

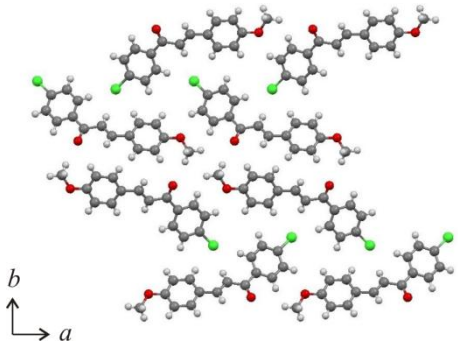

15. Cl-C-OMe (2)

orthorhombic $Pna2_1$ (33)

a = 12.8179(4)Å b = 25.5550(6)Å c = 3.9175(1)Å

α = 90° β = 90° γ = 90°

V = 1283.2(2)Å^3

Z' = 1

CSD entry MEGYON01[3]

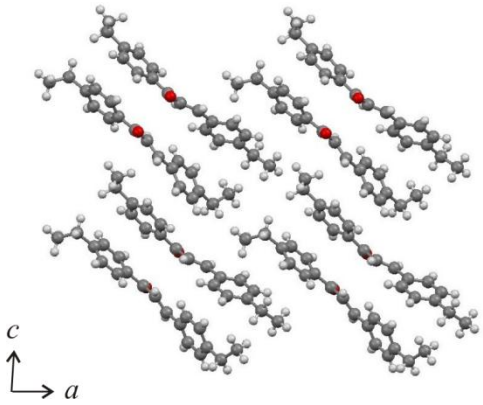

16. Et-C-Et

monoclinic *P*c (7)

a = 12.4084(9)Å *b* = 5.8324(2)Å *c* = 20.586(2)Å

α = 90° *β* = 93.475(2)° *γ* = 90°

V = 1487.1(2)Å^3

Z'= 2

The second disorder components (54:46) of the ethyl substituents of both molecules of the asymmetric unit are omitted for clarity.

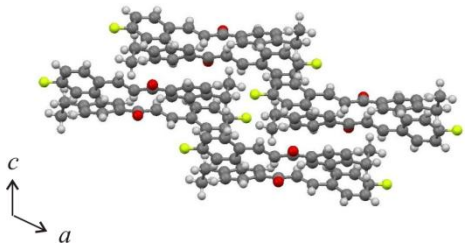

17. Et-C-F

monoclinic $P2_1/n$ (14)

a = 10.7987(2)Å *b* = 11.0025(2)Å *c* = 12.1139(2)Å

α = 90° *β* = 115.244(1)° *γ* = 90°

V = 1301.83(4)Å^3

Z'= 1

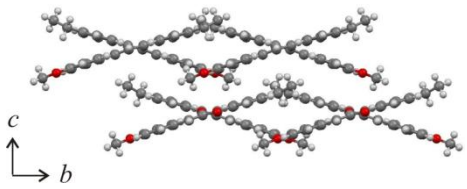

18. Et-C-OMe

orthorhombic $Pna2_1$ (33)

a = 11.0822(2)Å *b* = 12.0699(3)Å *c* = 10.7018(3)Å

α = 90° *β* = 90° *γ* = 90°

V = 1431.48(6)Å^3

Z'= 1

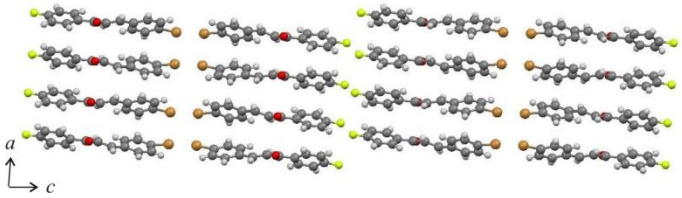

19. F-C-Br

monoclinic $P2/c$ (13)

a = 7.1418(8)Å b = 5.856(1)Å c = 58.137(9)Å

α = 90° β = 94.279(8)° γ = 90°

V = 2424.8(7)Å^3

Z'= 2

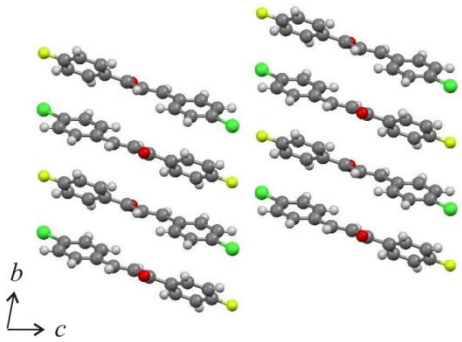

20. F-C-Cl

triclinic $P\bar{1}$ (2)

a = 5.9477(5)Å b = 7.6501(8)Å c = 13.784(1)Å

α = 79.263(7)° β = 85.379(6)° γ = 83.884(4)°

V = 611.5(1)Å^3

Z'= 1

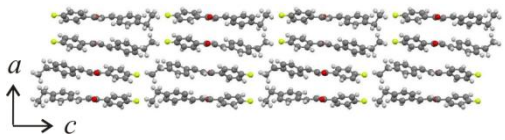

21. F-C-Et

monoclinic $P2_1/c$ (14)

a = 14.377(7)Å b = 5.918(3)Å c = 30.55(2)Å

α = 90° β = 90.169(7)° γ = 90°

V = 2599.6(2)Å^3

Z'= 2

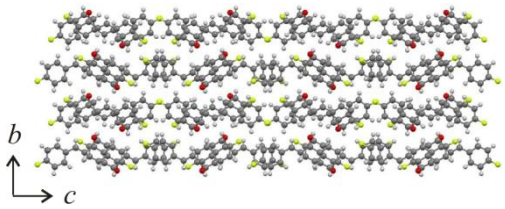

22. F-C-F

orthorhombic $Pbca$ (61)

a = 7.0669(7)Å b = 22.218(2)Å c = 28.787(3)Å

α = 90° β = 90° γ = 90°

V = 4519.9(7)Å^3

Z'= 2

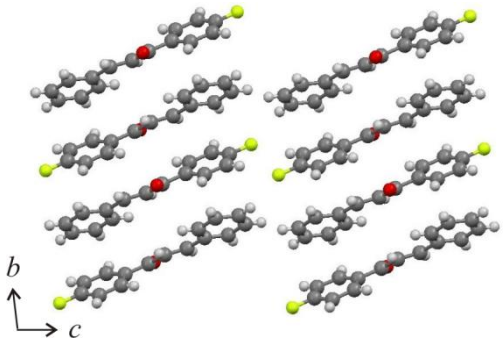

23. F-C-H

triclinic $P\bar{1}$ (2)

a = 5.8428(8)Å b = 7.4454(1)Å c = 13.040(2)Å

α = 96.784(8)° β = 93.78(1)° γ = 93.61(1)°

V = 560.6(2)Å^3

Z'= 1

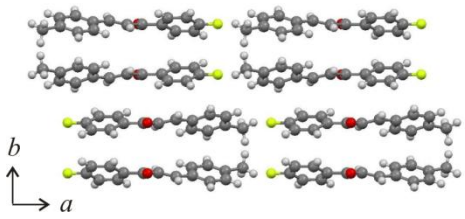

24. F-C-Me

monoclinic $P2_1/c$ (14)

a = 14.530(1)Å b = 14.104(1)Å c = 5.8514(3)Å

α = 90° β = 92.074(4)° γ = 90°

V = 1198.4(1)Å^3

Z'= 1

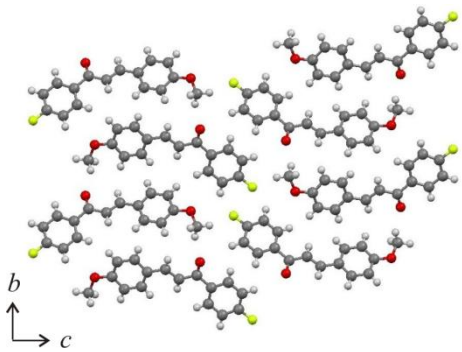

25. F-C-OMe

orthorhombic $P2_12_12_1$ (19)

a = 3.9167(2)Å b = 10.1905(4)Å c = 30.804(2)Å

α = 90° β = 90° γ = 90°

V = 1229.5(1)Å^3

Z'= 1

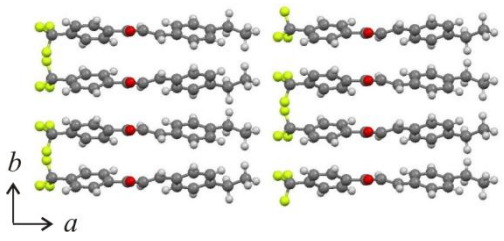

26. F_3C-C-Et

monoclinic Cc (9)

a = 34.534(4)Å b = 7.1295(8)Å c = 5.8776(5)Å

α = 90° β = 96.275(7)° γ = 90°

V = 1438.5(3)Å^3

Z'= 1

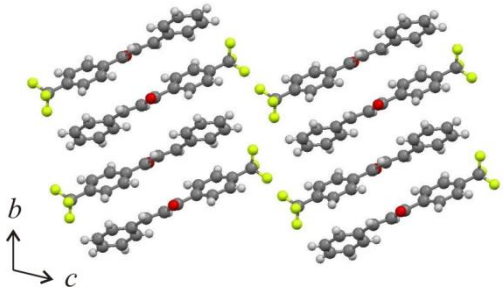

27. F_3C -C-H

triclinic $P\bar{1}$ (2)

a = 5.7791(8)Å b = 7.388(1)Å c = 15.415(5)Å

α = 103.46(2)° β = 92.24(2)° γ = 92.08(2)°

V = 638.9(2)Å^3

Z'= 1

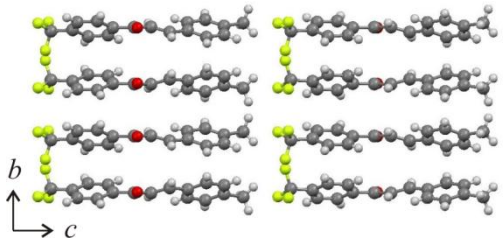

28. F_3C-C-Me

orthorhombic $Pca2_1$ (29)

a = 5.8907(4)Å b = 7.1826(5)Å c = 31.682(2)Å

α = 90° β = 90° γ = 90°

V = 1340.5(2)Å^3

Z'= 1

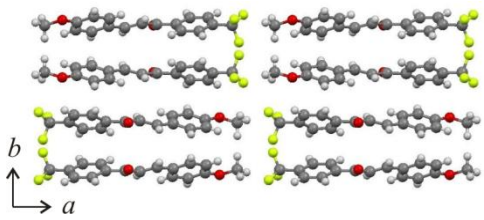

29. F_3C-C-OMe

monoclinic $P2_1/c$ (14)

a = 16.769(2)Å b = 14.132(2)Å c = 5.8388(8)Å

α = 90° β = 91.95(1)° γ = 90°

V = 1382.8(3)Å^3

Z'= 1

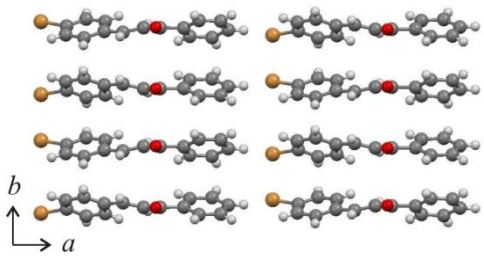

30. H-C-Br

monoclinic *Cc* (9)

a = 29.027(7)Å *b* = 7.26(2)Å *c* = 5.917(3)Å

α = 90° *β* = 101.38(3)° *γ* = 90°

V = 1222.4(1)Å^3

Z'= 1

CSD entry TARCIY[4]

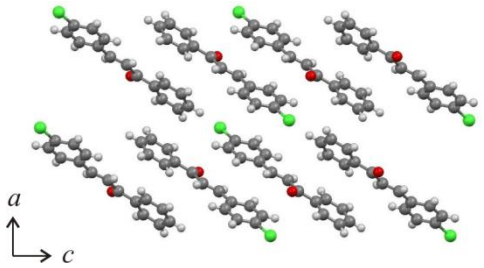

31. H-C-Cl

monoclinic $P2_1/c$ (14)

a = 8.211(2)Å *b* = 5.869(2)Å *c* = 25.291(5)Å

α = 90° *β* = 99.18° *γ* = 90°

V = 1203.1(7)Å^3

Z'= 1

CSD entry LEBGUU[5]

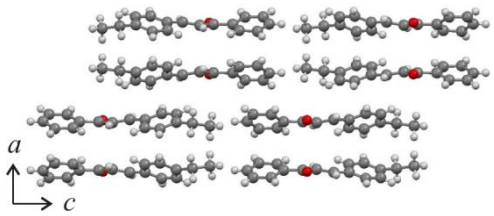

32. H-C-Et

orthorhombic *Pbca* (61)

a = 14.584(1)Å *b* = 5.8361(4)Å *c* = 30.549(2)Å

α = 90° *β* = 90° *γ* = 90°

V = 2600.2(3)Å^3

Z'= 1

The second disorder component (54:46) of the phenyl ring at the carbonyl end is omitted for clarity.

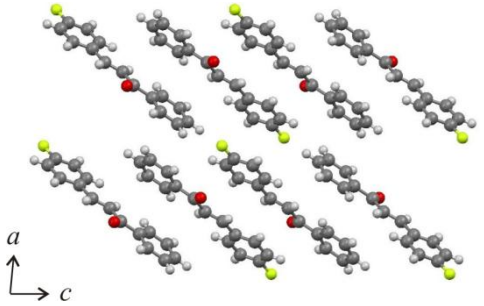

33. H-C-F

monoclinic $P2_1/c$ (14)

a = 8.7015(4)Å *b* = 5.9395(3)Å *c* = 22.664(2)Å

α = 90° *β* = 95.371(2)° *γ* = 90°

V = 1166.2(1)Å^3

Z'= 1

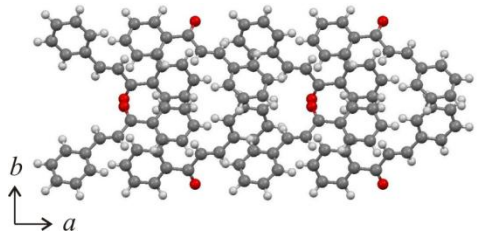

34. H-C-H (1)

orthorhombic $Pbc2_1$ (29)

a = 12.747(2)Å b = 11.553(2)Å c = 7.689(2)Å

α = 90° β = 90° γ = 90°

V = 1132.3(3)Å^3

Z'= 1

CSD entry BZYACO[6]

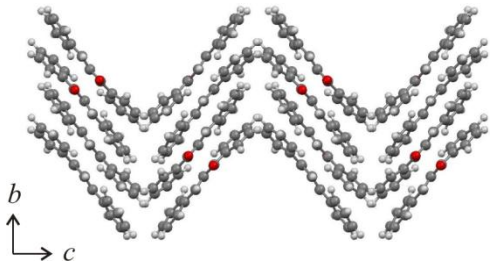

35. H-C-H (2)

orthorhombic $Pbcn$ (29)

a = 10.90(2)Å b = 11.90(1)Å c = 17.93(1)Å

α = 90° β = 90° γ = 90°

V = 2325.7(8)Å^3

Z'= 1

CSD entry BZYACO01[7]

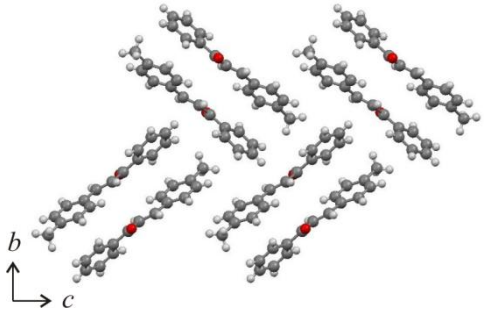

36. H-C-Me (1)

monoclinic $P2_1/c$ (14)

a = 5.8601(6)Å b = 16.732(2)Å c = 12.536(2)Å

α = 90° β = 93.522(9)° γ = 90°

V = 1226.8(8)Å^3

Z'= 1

CSD entry CERYAA[8]

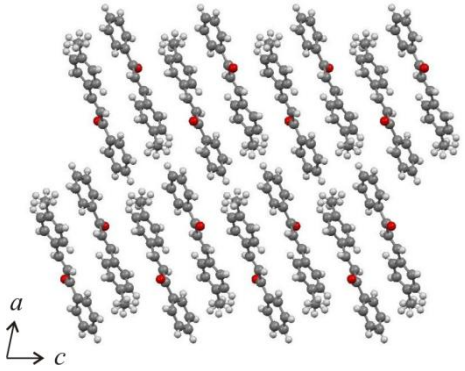

37. H-C-Me (2)

monoclinic $C2/c$ (15)

a = 26.2365(9)Å b = 5.8236(2)Å c = 15.5412(5)Å

α = 90° β = 101.807(1)° γ = 90°

V = 2324.3(1)Å^3

Z'= 1

CSD entry CERYAA03[9]

38. H-C-Me (3)

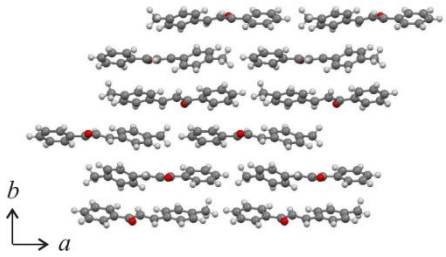

monoclinic $P2_1$ (4)

a = 14.1639(3)Å b = 21.8749(2)Å c = 5.91297(9)Å

α = 90° β = 89.947(1)° γ = 90°

V = 1832.03(5)Å^3

Z'= 3

CSD entry CERYAA01[9]

39. H-C-OMe

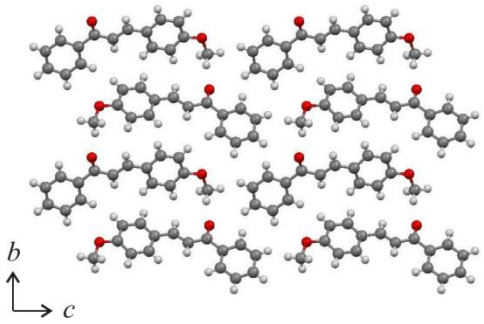

monoclinic $P2_1$ (4)

a = 4.070(6)Å b = 9.926(8)Å c = 15.12(3)Å

α = 90° β = 91.6(1)° γ = 90°

V = 610.4(1)Å^3

Z'= 1

40. Me-C-Br

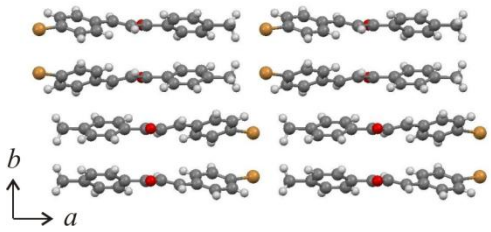

monoclinic $P2_1/c$ (14)

a = 15.408(7)Å b = 14.039(7)Å c = 5.914(3)Å

α = 90° β = 90.964(8)° γ = 90°

V = 1279.1(1)Å^3

Z'= 1

41. Me-C-F

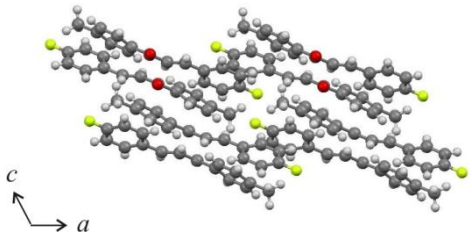

monoclinic $P2_1/c$ (14)

a = 11.0063(5)Å b = 10.7409(7)Å c = 11.4333(7)Å

α = 90° β = 117.783(3)° γ = 90°

V = 1195.8(1)Å^3

Z'= 1

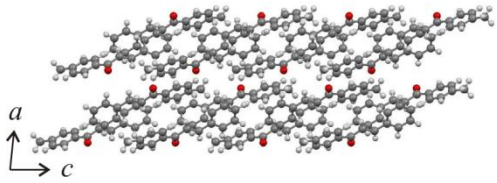

42. Me-C-H

monoclinic $C2/c$ (15)

a = 14.976(4)Å b = 9.843(3)Å c = 17.561(3)Å

α = 90° β = 105.83(2)° γ = 90°

V = 2490.5(1)Å^3

Z'= 1

CSD entry PUQSUP[2]

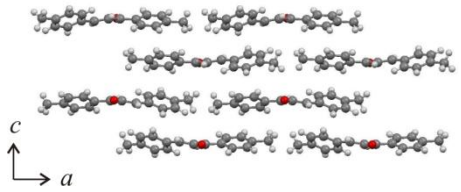

43. Me-C-Me

orthorhombic $P2_12_12_1$ (19)

a = 15.2464(3)Å b = 5.9059(5)Å c = 14.6283(5)Å

α = 90° β = 90° γ = 90°

V = 1317.2(1)Å^3

Z'= 1

CSD entry DMCHAL[10]

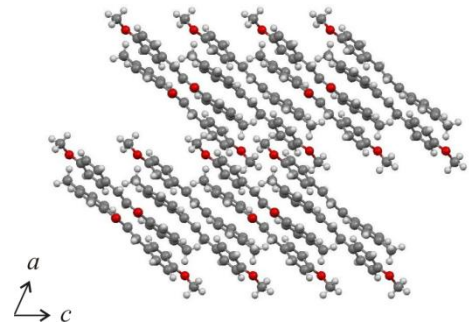

44. Me-C-OMe

monoclinic $P2_1/c$ (14)

a = 11.476(7)Å b = 10.910(7)Å c = 11.431(7)Å

α = 90° β = 114.305(6)° γ = 90°

V = 1304.3(1)Å^3

Z'= 1

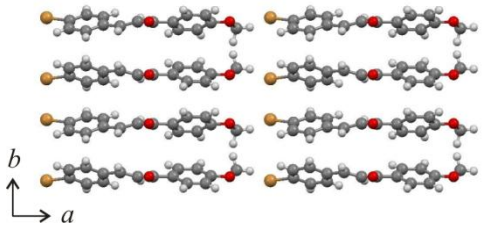

45. MeO-C-Br

monoclinic Pc (7)

a = 15.869(3)Å b = 7.146(2)Å c = 5.991(1)Å

α = 90° β = 82.85(1)° γ = 90°

V = 674.10(1)Å^3

Z'= 1

CSD entry KORROY[11]

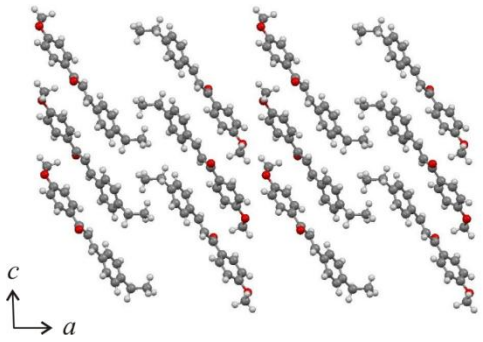

46. MeO-C-Et

monoclinic $P2_1/c$ (14)

a = 19.531(2)Å b = 5.8433(4)Å c = 13.081(1)Å

α = 90° β = 92.205(5)° γ = 90°

V = 1491.7(2)Å^3

Z'= 1

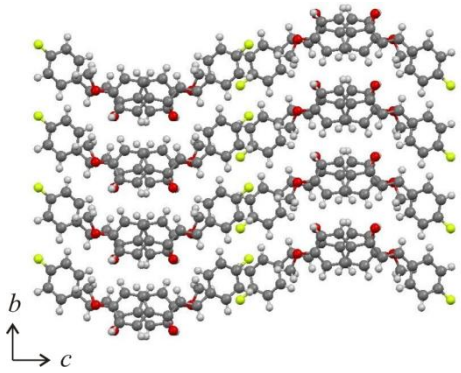

47. MeO-C-F

orthorhombic *P*bca (61)

a = 7.2901(1)Å b = 11.0074(3)Å c = 31.0779(7)Å

α = 90° β = 90° γ = 90°

V = 2493.85(9)Å^3

Z'= 1

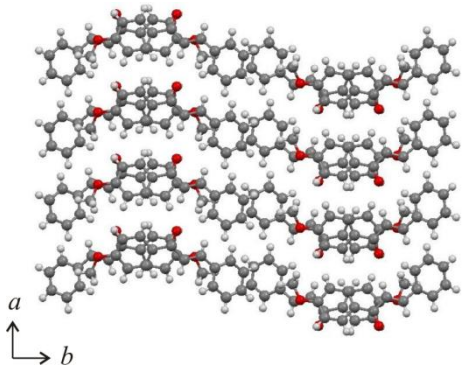

48. MeO-C-H

orthorhombic *P*bca (61)

a = 10.891(2)Å b = 30.507(2)Å c = 7.499(3)Å

α = 90° β = 90° γ = 90°

V = 2491.6(1)Å^3

Z'= 1

CSD entry KOTSER[12]

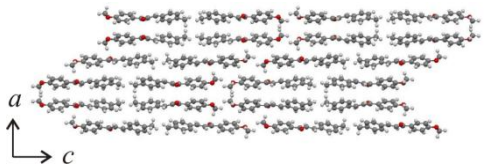

49. MeO-C-Me

orthorhombic *P*bca (61)

a = 21.421(2)Å b = 5.8286(5)Å c = 62.472(6)Å

α = 90° β = 90° γ = 90°

V = 7799.8(1)Å^3

Z'= 3

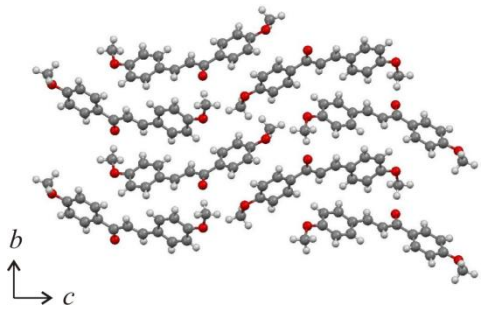

50. MeO-C-OMe

orthorhombic $P2_12_12_1$ (19)

a = 5.1547(2)Å b = 8.6377(4)Å c = 30.533(1)Å

α = 90° β = 90° γ = 90°

V = 1359.5(1)Å^3

Z'= 1

The crystallographic data from the structures above is summarised in Table 3-1 below.

ID	Phase	SG	Z	a (Å)	b (Å)	c (Å)	α (°)	β (°)	γ (°)	V (Å^3)
1	Br-C-Br	$P2_1/c$	4	15.724(3)	13.948(5)	5.8302(4)	90	92.329(10)	90	1277.6(5)
2	Br-C-Cl	$P2_1/c$	4	15.6116(8)	13.9778(7)	5.8184(2)	90	92.756(3)	90	1268.2(1)
3	Br-C-Et	$P\bar{1}$	4	5.859(1)	14.308(2)	16.635(4)	91.88(1)	91.91(2)	90.61(1)	1329.9(5)
4	Br-C-F	$P2_1/n$	4	4.0137(1)	23.1253(8)	13.5057(4)	90	96.349(2)	90	1245.88(6)
5	Br-C-H[1]	$P2_1/c$	8	15.10(1)	5.90(1)	31.13(2)	90	108.6(1)	90	2628.5(1)
6	Br-C-Me	$P2_1/c$	4	15.6425(7)	14.4138(8)	5.8990(3)	90	92.269(4)	90	1329.0(1)
7	Br-C-OMe	$P2_1/n$	8	15.776(2)	5.9141(3)	29.012(3)	90	90.421(3)	90	2706.7(4)
8	Cl-C-Br	$P2_1/c$	4	15.5178(8)	14.2137(6)	5.9113(2)	90	92.515(2)	90	1302.6(1)
9	Cl-C-Cl	$P2_1/c$	4	15.3734(9)	14.2123(7)	5.8906(3)	90	92.928(2)	90	1285.4(1)
10	Cl-C-Et	$P\bar{1}$	4	5.8727(3)	14.2193(8)	16.343(1)	91.600(2)	91.997(2)	90.598(4)	1363.3(1)
11	Cl-C-F	$P2_1/n$	4	3.9499(1)	23.0419(6)	13.3737(4)	90	96.145(1)	90	1210.19(6)
12	Cl-C-H[2]	$P\bar{1}$	2	7.565(2)	14.060(2)	5.858(1)	90.09(2)	92.15(2)	81.70(2)	616.12(1)
13	Cl-C-Me	$P2_1/c$	4	15.351(2)	14.352(2)	5.9070(6)	90	92.283(4)	90	1300.4(3)
14	Cl-C-OMe(1)	$P2_1/c$	4	15.6425(9)	14.1207(9)	5.8452(2)	90	90.362(4)	90	1291.1(1)
15	Cl-C-OMe(2)[3]	$Pna2_1$	4	12.8179(4)	25.5550(6)	3.9175(1)	90	90	90	1283.2(2)
16	Et-C-Et	Pc	4	12.4084(9)	5.8324(2)	20.586(2)	90	93.475(2)	90	1487.1(2)
17	Et-C-F	$P2_1/n$	4	10.7987(2)	11.0025(2)	12.1139(2)	90	115.244(1)	90	1301.83(4)
18	Et-C-OMe	$Pna2_1$	4	11.0822(2)	12.0699(3)	10.7018(3)	90	90	90	1431.48(6)
19	F-C-Br	$P2/c$	8	7.1418(8)	5.856(1)	58.137(9)	90	94.279(8)	90	2424.8(7)
20	F-C-Cl	$P\bar{1}$	2	5.9477(5)	7.6501(8)	13.784(1)	79.263(7)	85.379(6)	83.884(4)	611.5(1)
21	F-C-Et	$P2_1/c$	8	14.377(7)	5.918(3)	30.55(2)	90	90.169(7)	90	2599.6(2)
22	F-C-F	$Pbca$	16	7.0669(7)	22.218(2)	28.787(3)	90	90	90	4519.9(7)
23	F-C-H	$P\bar{1}$	2	5.8428(8)	7.4454(1)	13.040(2)	96.784(8)	93.78(1)	93.61(1)	560.6(2)
24	F-C-Me	$P2_1/c$	4	14.530(1)	14.104(1)	5.8514(3)	90	92.074(4)	90	1198.4(1)
25	F-C-OMe	$P2_12_12_1$	4	3.9167(2)	10.1905(4)	30.804(2)	90	90	90	1229.5(1)
26	F3C-C-Et	Cc	4	34.534(4)	7.1295(8)	5.8776(5)	90	96.275(7)	90	1438.5(3)
27	F3C-C-H	$P\bar{1}$	2	5.7791(8)	7.388(1)	15.415(5)	103.46(2)	92.24(2)	92.08(2)	638.9(2)
28	F3C-C-Me	$Pca2_1$	4	5.8907(4)	7.1826(5)	31.682(2)	90	90	90	1340.5(2)
29	F3C-C-OMe	$P2_1/c$	4	16.769(2)	14.132(2)	5.8388(8)	90	91.95(1)	90	1382.8(3)
30	H-C-Br[4]	Cc	4	29.027(7)	7.26(2)	5.917(3)	90	101.38(3)	90	1222.4(1)
31	H-C-Cl[5]	$P2_1/c$	4	8.211(2)	5.869(2)	25.291(5)	90	99.18	90	1203.1(7)
32	H-C-Et	$Pbca$	8	14.584(1)	5.8361(4)	30.549(2)	90	90	90	2600.2(3)
33	H-C-F	$P2_1/c$	4	8.7015(4)	5.9395(3)	22.664(2)	90	95.371(2)	90	1166.2(1)
34	H-C-H(1)[6]	$Pbc2_1$	4	12.747(2)	11.553(2)	7.689(2)	90	90	90	1132.3(3)
35	H-C-H(2)[7]	$Pbcn$	8	10.90(2)	11.90(1)	17.93(1)	90	90	90	2325.7(8)
36	H-C-Me(1)[8]	$P2_1/n$	4	5.8601(6)	16.732(2)	12.536(2)	90	93.522(9)	90	1226.8(8)
37	H-C-Me(2)[9]	$C2/c$	8	26.2365(9)	5.8236(2)	15.5412(5)	90	101.807(1)	90	2324.3(1)
38	H-C-Me(3)[9]	$P2_1$	6	14.1639(3)	21.8749(2)	5.91297(9)	90	89.947(1)	90	1832.03(5)
39	H-C-OMe	$P2_1$	2	4.070(6)	9.926(8)	15.12(3)	90	91.6(1)	90	610.4(1)
40	Me-C-Br	$P2_1/c$	4	15.408(7)	14.039(7)	5.914(3)	90	90.964(8)	90	1279.1(1)
41	Me-C-F	$P2_1/c$	4	11.0063(5)	10.7409(7)	11.4333(7)	90	117.783(3)	90	1195.8(1)
42	Me-C-H[2]	$C2/c$	8	14.976(4)	9.843(3)	17.561(3)	90	105.83(2)	90	2490.5(1)
43	Me-C-Me[10]	$P2_12_12_1$	4	15.2464(3)	5.9059(5)	14.6283(5)	90	90	90	1317.2(1)
44	Me-C-OMe	$P2_1/c$	4	11.476(7)	10.910(7)	11.431(7)	90	114.305(6)	90	1304.3(1)
45	MeO-C-Br[11]	Pc	2	15.869(3)	7.146(2)	5.991(1)	90	82.85(1)	90	674.10(1)
46	MeO-C-Et	$P2_1/c$	4	19.531(2)	5.8433(4)	13.081(1)	90	92.205(5)	90	1491.7(2)
47	MeO-C-F	$Pbca$	8	7.2901(1)	11.0074(3)	31.0779(7)	90	90	90	2493.85(9)
48	MeO-C-H[12]	$Pbca$	8	10.891(2)	30.507(2)	7.499(3)	90	90	90	2491.6(1)
49	MeO-C-Me	$Pbca$	24	21.421(2)	5.8286(5)	62.472(6)	90	90	90	7799.8(1)
50	MeO-C-OMe	$P2_12_12_1$	4	5.1547(2)	8.6377(4)	30.533(1)	90	90	90	1359.5(1)

Table 3-1: *Crystallographic parameters for chalcone structures;*

XPac Analysis

The XPac analysis of these 50 chalcone crystal structures was carried out as described in Chapter 2 and this generated 1225 comparisons between all possible pairs of structures within the group. Each of these comparisons describes the similarity between a pair of structures which may range from no similarity, through 0, 1 and 2-D SCs, to isostructurality. Each of these relationships was then examined, collated and compiled to form an overall picture of the similarity relationships within the group of structures. It should be emphasised that this was not a trivial task. The number of potential relationships for any given family is positively correlated to its size and a myriad of complex interrelationships between crystal structures and SCs is observed for a large set of crystal structures such as this.

To refer to the possible relationships between SCs, the following notation is used: (a) "X $\rightarrow$ Y" for SC X is a subset of SC Y" and (b) "Z $\rightarrow$ X $\times$ Y" for "SC Z is a subset of both SC X and SC Y". Additionally SCs are 0-D, 1-D, 2-D or 3-D and thus have 0, 1, 2 or 3 bases vectors, ***t,*** associated with them. A brief description of each of the SCs discovered in the chalcone family and the base vectors of periodic SCs associated with each structure is given in Tables 3-2 and 3-3 below.

SC	*D*	*Description*	*Figs*	*#*	*Base*	*Dependencies*
A	1	Row of molecules related by translation	3-3	34	***t1***	Primary SC
A1	1	Double row with 2 A rows related by a glide plane	3-4	23	***t1***	A1 → A
A2	1	Double row with 2 A rows related by inversion	3-5	19	***t1***	A2 → A
A3	1	Double row with 2 A rows related by a 2 rotation axis	3-6	2	***t1***	A3 → A
A4	1	'Slipped' double row with 2 A rows related by a 2_1 axis	3-7	8	***t1***	A4 → A
A5	1	'Slipped' double row with 2 A rows related by a 2_1 axis	3-8	5	***t1***	A5 → A
A6	1	Two double rows with 2 A1 rows related by a 2 rotation axis	3-9	2	***t1***	A6 → A1
A7	1	Two 'slipped' triple rows related by inversion	3-10	2	***t1***	A7 → A4
A8	1	Quadruple row with 2 A1 rows related by inversion	3-11	14	***t1***	A8 → A1 × A2
A9	1	'Slipped' quadruple row with 2 A1 rows related by a 2_1 axis	3-12	2	***t1***	A9 → A1 × A5
A10	2	Single layer sheet with A rows related by translation	3-13	20	***t1, t2***	A10 → A
A11	2	Single layer sheet with A rows related by a 2_1 axis	3-14	6	***t1, t3***	A11 → A
A12	2	Double layer sheet with A1 rows related by translation	3-15	13	***t1, t2***	A12 → A1 × A10
A13	2	Double layer sheet with A2 rows related by translation	3-16	16	***t1, t2***	A13 → A2 × A10
A14	2	'Slipped' double layer sheet with A4 rows related by translation	3-17	3	***t1, t2***	A14 → A4 × A5 × A10
A15	2	Double layer sheet with A1 rows related by a 2_1 axis	3-18	4	***t1, t3***	A15 → A1 × A11
A16	2	'Slipped' double layer sheet with A4 rows related by inversion	3-19	3	***t1, t3***	A16 → A4 × A11
A17	2	Quadruple layer sheet with A8 rows related by translation (A12 sheets related by inversion)	3-20	12	***t1, t2***	A17 → A8 × A12
A18	2	Single layer sheet with A8 rows related by translation	3-21	13	***t1, t4***	A18 → A8
A19	2	Single layer sheet with A1 rows related by translation	3-22	5	***t1, t5, t8***	A19 → A1 × D
B	0	'Trimer'	3-23	5		Primary SC
B1	1	Corrugated row of molecules related by a 2_1 axis	3-24	4	***t6***	B1 → B
C	1	Corrugated row of molecules related by a 2_1 axis	3-25	4	***t7***	Primary SC
C1/D1	2	Single layer sheet of C rows related by a D translation	3-26	3	***t7, t8***	C1/D1 → C × D
D	1	Row of molecules related by translation	3-27	6	***t8***	Primary SC
D2	2	Single layer sheet of D rows related by translation	3-28	4	***t8, t9***	D2 → D
D3	2	Double layer sheet of D2 layers related by a glide plane	3-29	3	***t8, t9***	D3 → D2
E	1	Row of molecules related by translation	3-30	4	***t10***	Primary SC
isostructural: 1/2/3/6/8/9/10/13/14/24/40, 4/11, 12/20/23/27, 17/41/44, 26/30, 31/33, (47/48)						
Structures unrelated by these SCs: 34, 47/48						

Table 3-2: *Similarity relationships amongst chalcones studied (D = dimensionality, # = number of structures).*

Str.	***t1***	d1	***t2***	d2	***t3***	d3	***t4***	d4	***t5***	d5	∠(***t1, t2***)	∠(***t1, t3***)	∠(***t1, t4***)	∠(***t1, t5***)
1	001	5.8302	-100	15.724			0-10	13.948			87.671		90	
2	00-1	5.8184	-100	15.6116			010	13.9778			87.244		90	
3	-100	5.8592	001	16.635			0-10	14.3077			88.089		89.389	
5	010	5.9					-100	15.1					90	
6	00-1	5.899	100	15.6425			0-10	14.4138			87.731		90	
7	0-10	5.9141	100	15.776							90			
8	001	5.9113	-100	15.5178			0-10	14.2137			87.485		90	
9	00-1	5.8906	-100	15.3734			0-10	14.2123			87.072		90	
10	100	5.8727	00-1	16.3431			010	14.2193			88.003		90.598	
12	00-1	5.858	-110	14.9735							91.0015			
13	001	5.907	-100	15.351			010	14.352			87.717		90	
14	00-1	5.8452	100	15.6425			010	14.1207			89.638		90	
16	0-10	5.8324			-20-1	33.1905						90		
19	0-10	5.8564							-100	7.1418				90
20	100	5.9477	011	14.4649							88.8297			
21	010	5.918			00-1	30.554	-100	14.377				90	90	
23	100	5.8428	0-11	14.2316							95.3585			
24	00-1	5.8514	100	14.5304			010	14.1036			87.926		90	
26	001	5.8776							010	7.1295				90
27	-100	5.7791	01-1	15.6547							86.7718			
28	100	5.8907			001	31.682			0-10	7.1826		90		90
29	00-1	5.8388	100	16.769							88.047			
30	001	5.917							0-10	7.26				90
31	010	5.869			-20-1	27.8711						90		
32	010	5.8361			00-1	30.5486								
33	010	5.9395			201	27.2523						90		
36	-100	5.8601												
37	0-10	5.8236			-10-1	27.6228						90		
38	001	5.91297	-100	14.1639							90.0351			
40	001	5.914	-100	15.408			010	14.039			89.036		90	
43	0-10	5.9059	-100	15.2464							90			
45	00-1	5.991	-100	15.869					0-10	7.146	82.85			90
46	010	5.8433												
49	010	5.8286												
Str.	***t6***	d6	***t7***	d7	***t8***	d8	***2t8***	2d8	***t9***	d9	***t10***	d10	∠(***t7, t8***)	∠(***t8, t9***)
4					100	4.0137	200	8.0274	00-1	13.5057				83.651
11					-100	3.9499	-200	7.8998	00-1	13.3737				83.855
15					00-1	3.9175	00-2	7.835	10-1	13.4032				73.054
17	0-10	11.0025									100	10.7987		
18											0-10	12.0699		
19[a]							-110	9.2360						
25			0-10	10.1905	100	3.9167	200	7.8334					90	
26[a]							0-1-1	9.2398						
28[a]							-110	9.2898						
30[a]							0-1-1	9.3658						
35	100	10.9									010	11.9		
39			-100	9.926	-100	4.07	-200	8.14	00-1	15.12			90	91.68
41	010	10.7409									-100	11.0063		
42			0-10	9.843										
44	010	10.91									10-1	12.4249		
45[a]							0-11	9.3251						
50			0-10	8.6377	-100	5.1547	-200	10.3094					90	
[a] Data refer to SC D														
22,34,47/48 have no common 1-D and 2-D SCs with remaining chalcone structures and are therefore excluded from this table														

Table 3-3: *Data for base vectors **t** in 1-D and 2-D SCs (lengths in Å and angles in °)*

In order to discuss the similarity relationships in detail, it is first useful to describe a method for their graphical representation. Each SC provides a connection between at least two crystal structures and a SC may itself be derived from one or more SCs (its sub SCs). This complexity necessitates a special visualisation method to allow these relationships to be viewed simultaneously and efficiently. Figure 3-1 below meets these demands, showing the full set of relationships for the series of chalcones studied. It is generated by the application of rules derived from Hasse diagrams[13], a method in set theory for the

rendering of a partially ordered set. Each node represents the elements of a family, i.e. crystal structures and SCs, whereas each edge connecting the nodes represents the dependencies between these elements. There is a strict vertical hierarchy within this diagram such that for connected nodes, the lower node is a sub-group of the higher node. Conversely, the horizontal arrangement of nodes is arbitrary, but arrangements that provide the least number of crossing lines are preferable for ease of readability.

The order of elements from bottom to top is thus 0-D SCs < 1-D SCs < 2-D SCs < 3-D SCs < crystal structures and the SC nodes are also colour coded according to their dimensionality. The nodes of the crystal structures are arranged in a horizontal line at the top and isostructural crystals with the same arrangement of base molecules are represented by a joint node, such as 1+, 4+, 12+, 17+, 26+, 31+ and 47+ and the crystal structures represented by these nodes are shown in the key.

Due to the strict vertical hierarchy in Figure 3-1, to find all of the crystal structures that contain a particular SC, all of the branches radiating *upwards* from its node are followed to the crystal structure level. Thus with the SC A node as the starting point, this leads eventually (via the remaining A SCs) to 19 nodes (representing the 34 crystal structures that contain SC A). Similarly, the same operation carried out for SC A9 leads to just two nodes for **7** and **32**. Dependencies between SCs are found in a similar fashion. For example it is easy to see that the relationship between SC A and SC A9 is $\{A9 \rightarrow A5 \times A1, A5 \rightarrow A, A1 \rightarrow A\}$.

The common SC of two crystal structures is found by following branches radiating *downwards*, beginning at the respective nodes, until they meet at a common node. For example **7** and **36** are both connected to SC A2. Conversely, *pure downward* connections starting at **7** and **15** do not meet at all, indicating that these structures have no common SC.

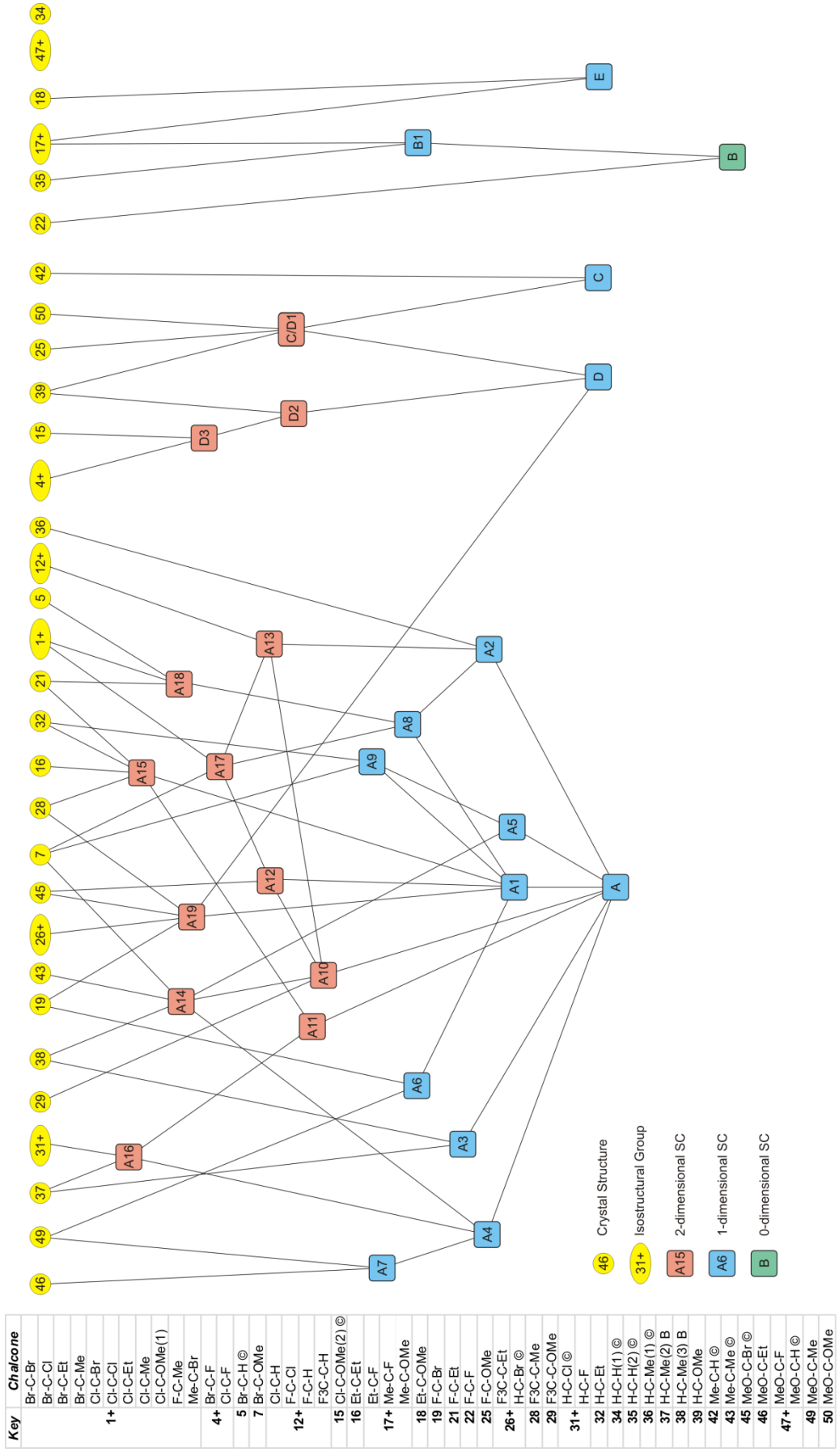

Figure 3-1: *Chalcone structure relationship diagram*

The diagram of the chalcone structure relationships (Figure 3-1) shows that there are five groups of SCs, which relate 47 of the 50 structures studied along with an additional two unrelated structural forms which encompass the remaining three structures. Each group of SCs comprises a primary SC, which is a SC that cannot be obtained by combination of any other discovered SCs, and a number of higher order SCs derived from the primary SC. The primary SCs are labelled alphabetically and these labels are also applied to each of their related groups; thus the A group includes all the chalcone structures related by SCs which have SC A as their primary SC. The higher order derived SCs are labelled according to their primary SC along with a numeric suffix, the assignment of which is somewhat arbitrary, but in general, higher numbers denote more complex relationships. At this juncture it is worth pointing out that although SCs have been referred to as rows or stacks in the case of 1-D SCs and sheets or layers in the case of 2-D SCs, these simple descriptors mask a level of complexity. Thus, a 1-D SC is any SC that is infinite in one direction and may consist of single or multiple, discrete 1-D components which themselves may also be simpler 1-D SCs. Likewise, a 2-D SC is any SC that is infinite in two directions and may consist of multiple, discrete sub-layers, which themselves may be simpler 2-D SCs. As can be seen from Figure 3-1, there are several examples of these types of interrelationships within the group of chalcone crystal structures.

Chalcone Supramolecular Constructs

To enable more detailed exploration of the similarity relationships between the chalcone structures studied, each of the SCs shown in the chalcone structure relationship diagram (Figure 3-1) are described and illustrated with a representative structure below. A Mercury[14] packing diagram of each of the structures with SCs highlighted is included on the supplementary CD included with this thesis and the reader is strongly advised to refer to this as an aid to visualisation. Because of the variance in orientation of unit cells for the large number of structures studied, it is often cumbersome and difficult to discuss the orientation of a particular SC with respect to a group of structures in terms of their unit cell axes. However, the geometry of the chalcone moiety readily allows simple definition of three molecular axes: long, mid and short, as shown

in Figure 3-2 below and these are used as references to provide generally applicable orientation information for each SC, independent of unit cell axes.

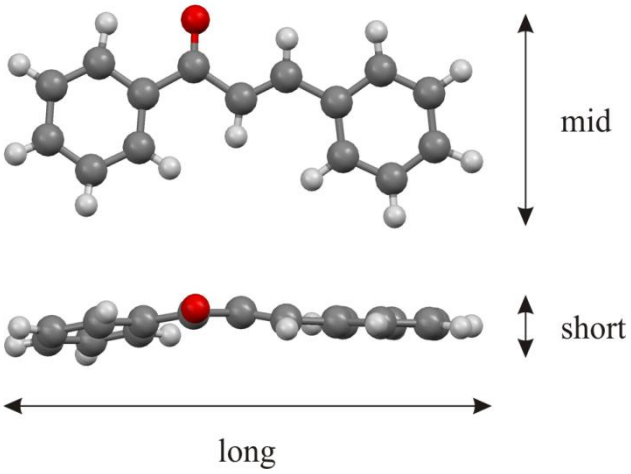

Figure 3-2: *Chalcone molecular axes*

A group

The A group of structures is by far the most numerous and complex comprising 20/28 SCs found using the XPac procedure with 34/50 structures exhibiting these types of arrangements. All of the structures of this group contain primary SC A.

Primary SC A

This SC is simply a 1-D, close-packed, single row of molecules related by translation along the direction of the mid molecular axis as shown in Figure 3-3 below. The length of the translation vector in each of the structures ranges from 5.779(1)-5.991(1) Å. Although the SC is a close-packed assembly, in the majority of structures there are no close-contacts, i.e. distances between atoms that are less than the sum of the van der Waals radii, between its constituent molecules and for those structures where close-contacts occur between the constituent molecules of the SC, they are limited to a single minor contact in each case. Additionally, it should be noted that there are no direct links between this SC and any of the chalcone crystal structures, thus in all of the structures that this SC occurs, it occurs not as an independent SC but as a sub-assembly of a more complex SC. This SC is the fundamental 'building-block' of the A group of structures and thus conversely each of the structures of this group represents a different 2-D arrangement of this SC.

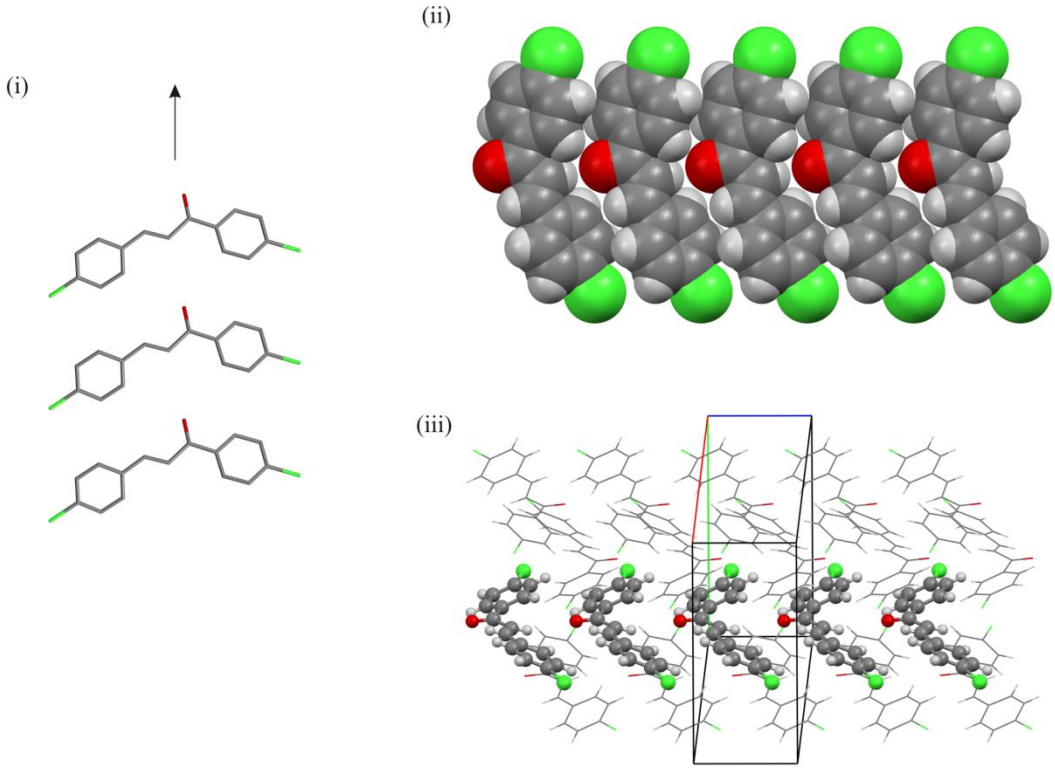

Figure 3-3: *SC A, Cl-C-Cl is shown as a representative structure; (i) spatial arrangement of molecules in SC A, translation vector is indicated by arrow; (ii) space-filling diagram clearly shows close-packed structure of SC A and lack of close contacts between molecules of the SC; (iii) SC A within the crystal structure of Cl-C-Cl (highlighted as ball and stick structure).*

SC A1

SC A1 is a 1-D, close-packed, double (SC A) row of molecules related by a glide along the direction of the mid molecular axis as shown in Figure 3-4 below. It should be noted that in the structures with Z'>1 (with the exception of MeO-C-Me) in which this SC occurs, the components of the SC are crystallographically independent molecules related by an approximate glide.

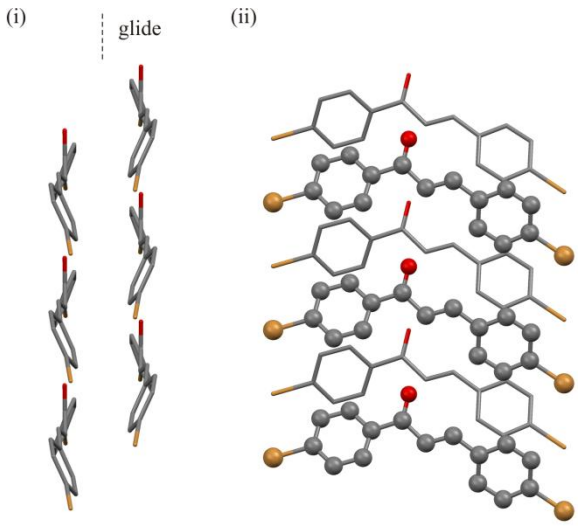

Figure 3-4: *SC A1, Br-C-Br is shown as a representative structure; (i) spatial arrangement of molecules in SC A1, glide plane is indicated by dashed line; (ii) alternate view of SC A1 with component SC A rows highlighted, the different rows are highlighted as ball and stick and stick representations.*

SC A2

SC A2 is a 1-D, close-packed, double (SC A) row of molecules related by inversion, and in all the structures that it is present the symmetry element is crystallographic. It is shown in Figure 3-5 below.

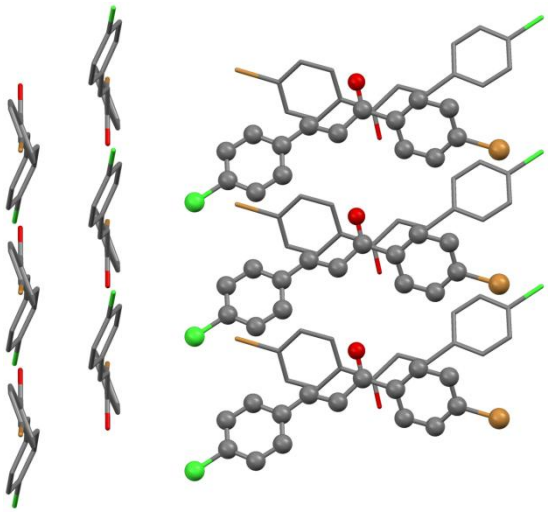

Figure 3-5: *SC A2, Br-C-Cl is shown as a representative structure; two alternate views showing the inversion relationship between the two rows. Different layers are highlighted with different molecular representations.*

SC A3

SC A3 is a 1-D, close-packed, double (SC A) row of molecules related by a 2 rotation axis along the direction of the mid molecular axis as shown in Figure 3-6 below. A point to note is that this SC only occurs between polymorphs 2 and 3 of H-C-Me and that for H-C-Me(3) the rotation axis is approximate as the two rows of the SC in this structure are composed of crystallographically independent molecules.

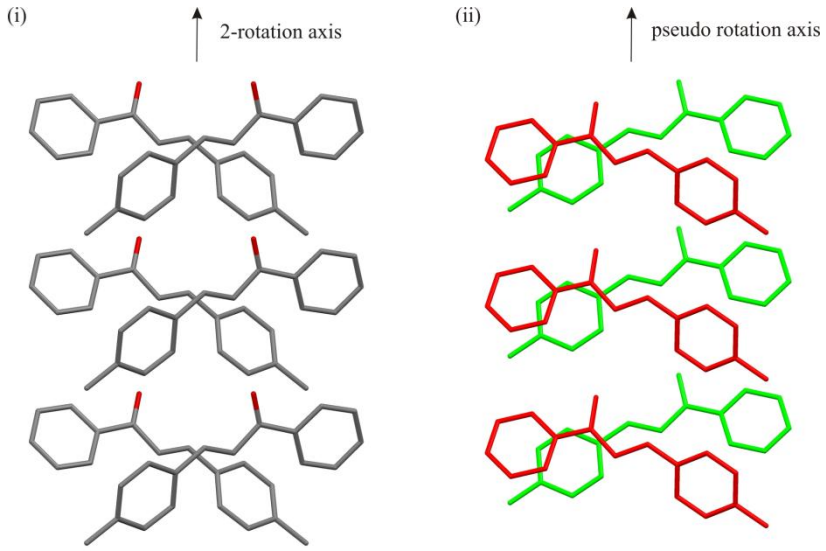

Figure 3-6: *SC A3, (i) H-C-Me(2); the 2-rotation axis is shown by the arrow; (ii) H-C-Me(3); the pseudo-rotation axis is shown by the arrow; crystallographically independent molecules are shown in red and green (only two of the three crystallography independent molecules in this structure are involved in this SC).*

SC A4

SC A4 is a 1-D, close-packed, double (SC A) row of molecules related by a 2_1 screw axis along the direction of the mid molecular axis as shown in Figure 3-7 below. This SC occurs in H-C-Me(3) and MeO-C-Me, both structures with Z'=3 and in these cases the screw axis is approximate as the two rows of the SC in these structure are composed of crystallographically independent molecules.

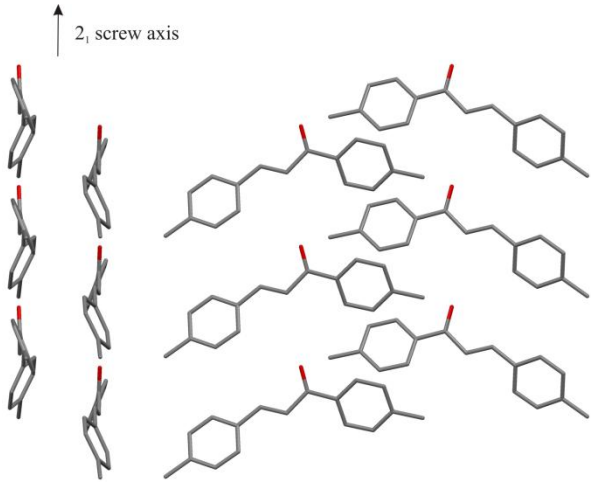

Figure 3-7: *SC A4, Me-C-Me is shown as a representative structure; two alternate views are shown, the 2_1 screw axis is shown by the arrow.*

SC A5

SC A5 is a 1-D, close-packed, double (SC A) row of molecules related by a 2_1 screw axis along the direction of the mid molecular axis as shown in Figure 3-8 below. This SC occurs in H-C-Me(3) with Z'=3 and in this case the screw axis is approximate as the two rows of the SC in this structure are composed of crystallographically independent molecules.

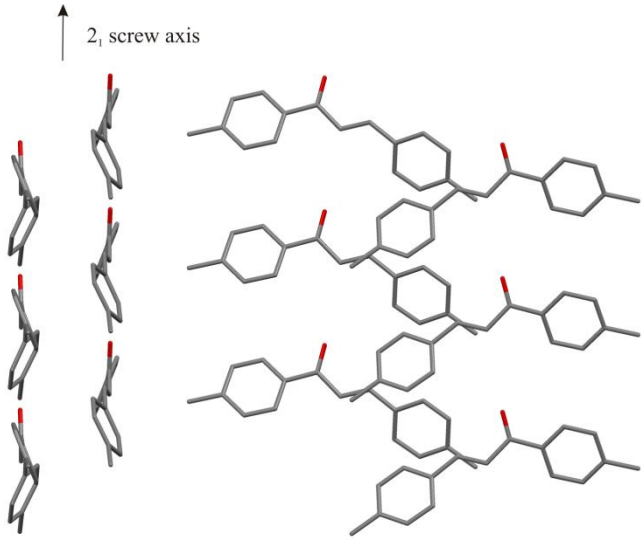

Figure 3-8: *SC A5, Me-C-Me is shown as a representative structure; two alternate views are shown, the 2_1 screw axis is shown by the arrow.*

SC A6

SC A6 is a 1-D, close-packed, pair of double (SC A) rows of molecules. It is equivalent to a pair of SC A1 rows related by a 2 rotation axis along the direction of the mid molecular axis as shown in Figure 3-9 below. This SC occurs in two structures, F-C-Br, a Z'=2 structure and MeO-C-Me which is a Z'=3 structure and in this case the rotation axis is approximate as the two rows of the SC in these structure are composed of crystallographically independent molecules.

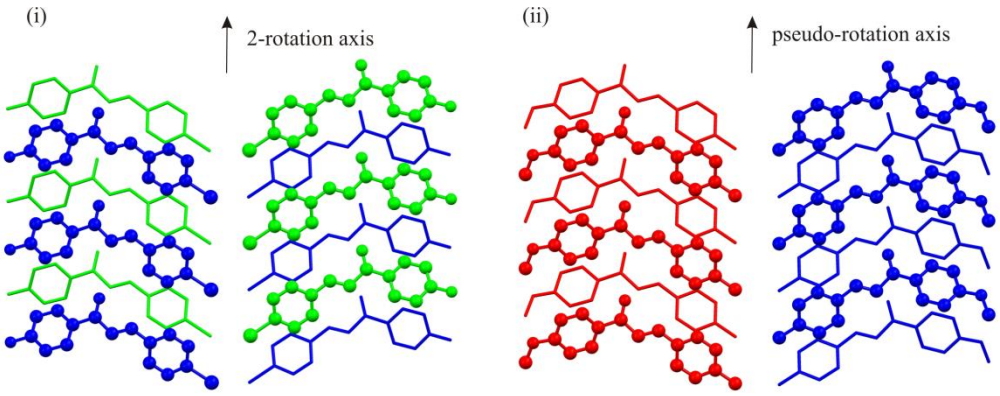

Figure 3-9: *SC A6, (i) F-C-Br; the 2-rotation axis is shown by the arrow; (ii) MeO-C-Me the pseudo-rotation axis is shown by the arrow. For both structures different layers are indicated by different molecular representations and crystallographically independent molecules are indicated by different colours (only two of the three crystallography independent molecules in MeO-C-Me are involved in this SC).*

SC A7

SC A7 is a 1-D, close-packed, pair of triple (SC A) rows of molecules. It relates two structures, MeO-C-Et and MeO-C-Me and is a subset of SC A4. In MeO-C-Et each of the triple rows are related by a glide and the pair of triple rows are related to each other by inversions and 2_1 screw axes along the direction of the mid molecular axis. In MeO-C-Me, each of the triple rows is made up of crystallographically independent molecules and they are related to the second pair by inversion as shown in Figure 3-10 below.

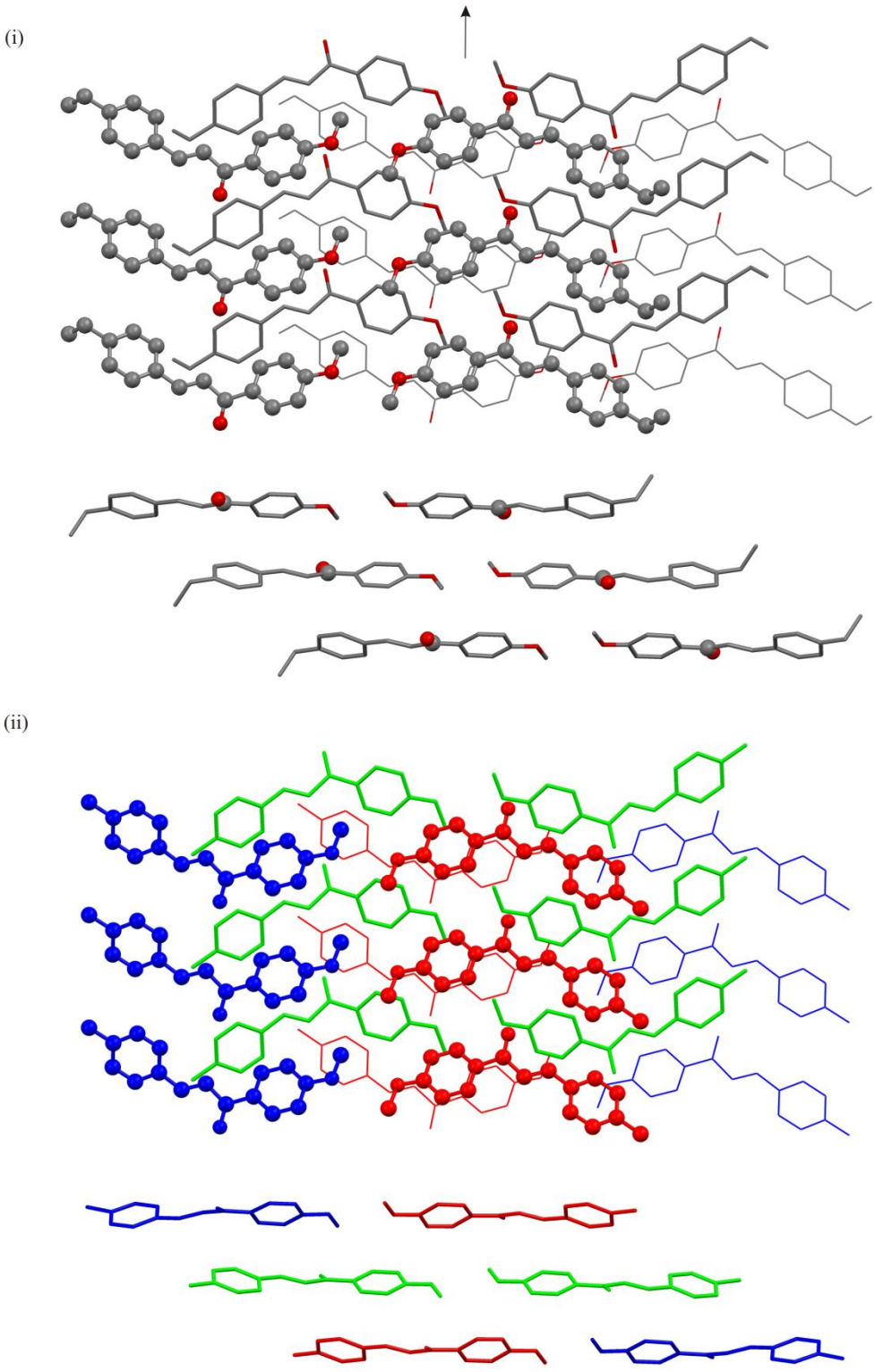

Figure 3-10: *SC A7, (i) MeO-C-Et; the orientation of the 2_1 screw axes and translation vector is shown by the arrow; (ii) MeO-C-Me; the crystallographically independent molecules are shown in different colours; two alternate views are shown for each structure, in the top view the layers are differentiated so that the upper layer is shown as ball and stick, the mid layer is stick and the lower layer is wireframe;*

SC A8

SC A8 is a 1-D, close-packed, quad (SC A) row of molecules. It is equivalent to a pair of SC A1 rows related by inversion along the direction of the mid molecular axis as shown in Figure 3-11 below.

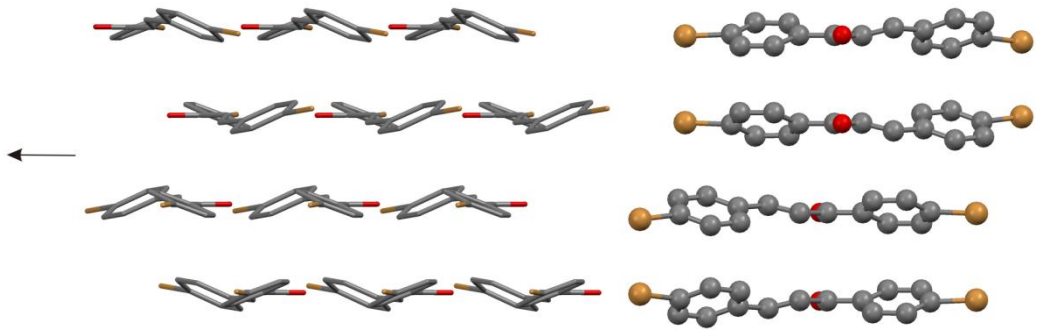

Figure 3-11: *SC A8, Br-C-Br is shown as a representative structure; two alternate views are shown; the translation vector of the SC is indicated by the arrow, the inversion centres are not shown.*

SC A9

SC A9 is a 1-D, close-packed, quad (SC A) row of molecules. It is equivalent to a pair of SC A1 rows related by a 2_1 screw axis along the direction of the mid molecular axis as shown in Figure 3-12 below.

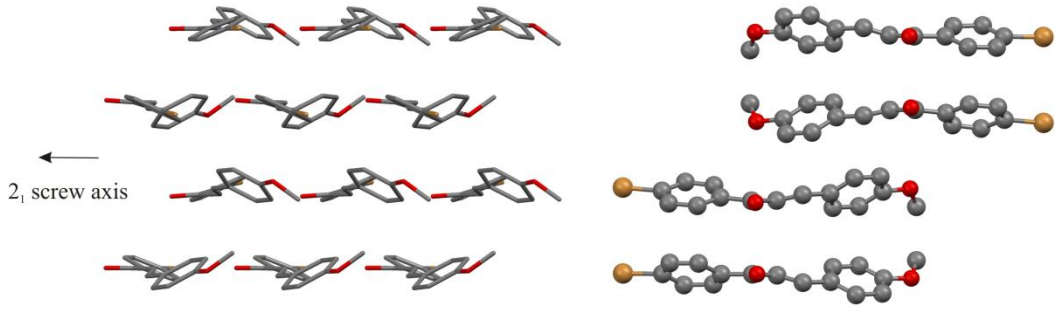

Figure 3-12: *SC A9, Br-C-OMe is shown as a representative structure; two alternate views are shown; the 2_1 screw axis and translation vector of the SC is indicated by the arrow.*

SC A10

SC A10 is a 2-D, close-packed, single layer of molecules, related by translation along both the mid and long molecular axes as shown in Figure 3-13 below. This SC is equivalent to SC A rows related by translation.

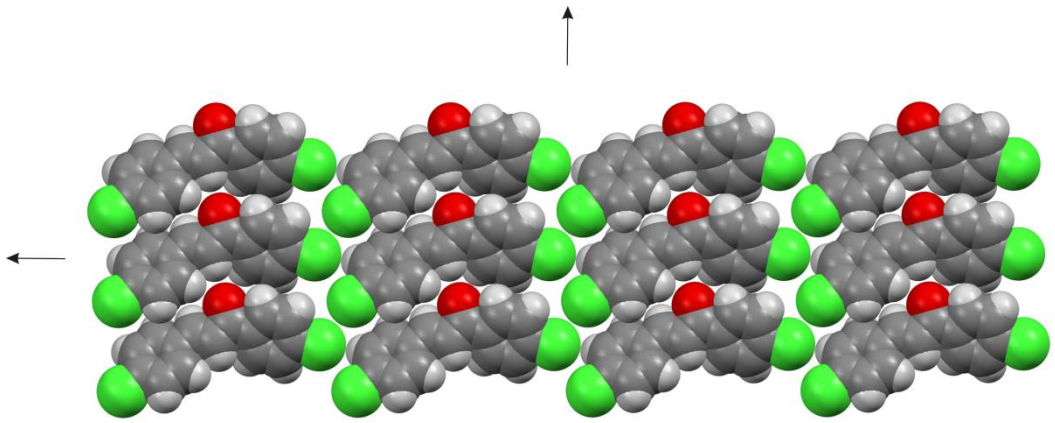

Figure 3-13: *SC A10, Cl-C-Cl is shown as a representative structure; the space-filling diagram indicates the close-packed structure of the SC; the translation vectors of the SC are indicated by the arrows.*

SC A11

SC A11 is a 2-D, close-packed, single layer of molecules, related by translation along the mid molecular axis and a glide along the long molecular axis as shown in Figure 3-14 below. This SC is equivalent to SC A rows related by a glide.

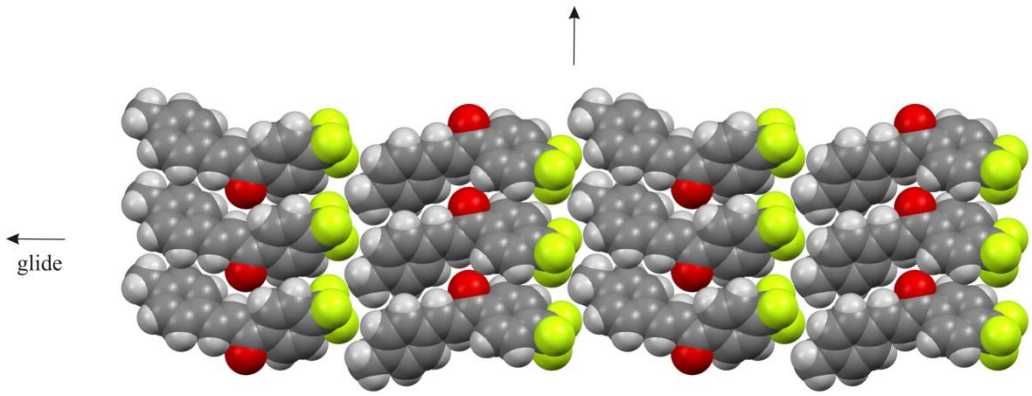

Figure 3-14: *SC A11, F3C-C-Me is shown as a representative structure; the space-filling diagram indicates the close-packed structure of the SC; the translation vectors of the SC are indicated by the arrows, additionally the direction of the glide is indicated.*

SC A12

SC A12 is a 2-D, close-packed, double layer of molecules, related by a glide along the mid molecular axis and translation along the long molecular axis as shown in Figure 3-15 below. This SC is equivalent to SC A1 rows related by translation.

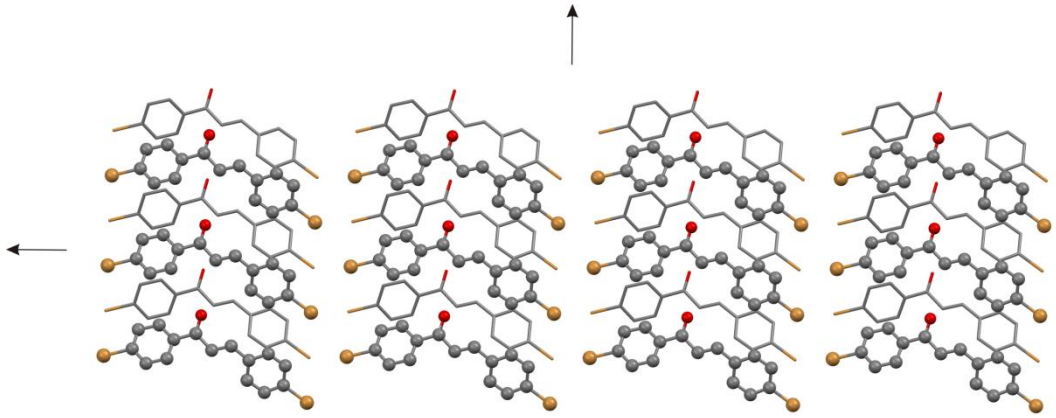

Figure 3-15: *SC A12, Br-C-Br is shown as a representative structure; this is a double layer structure, the upper layer is shown by ball and stick representation whilst the lower layer is shown by stick representation; the translation vector and direction of the glide of the SC are indicated by the arrows.*

SC A13

SC A13 is a 2-D, close-packed, double layer of molecules, related by inversion along the mid molecular axes and translation along the long molecular axis as shown in Figure 3-16 below. This SC is equivalent to SC A2 rows related by translation.

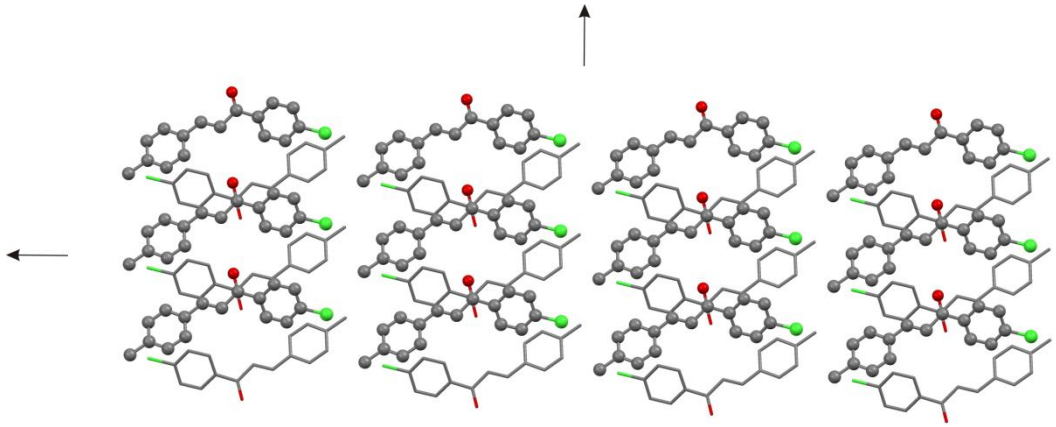

Figure 3-16: *SC A13, Cl-C-Me is shown as a representative structure; this is a double layer structure, the upper layer is shown by ball and stick representation whilst the lower layer is shown by stick representation; the translation vector of the SC and the direction of the axes on which the inversions lie are indicated by the arrows.*

SC A14

SC A14 is a 2-D, close-packed, double layer of molecules, related by 2_1 screw axes along the mid molecular axis and translation along the long molecular axis as shown in Figure 3-17 below. This SC is equivalent to SC A4 rows related by translation.

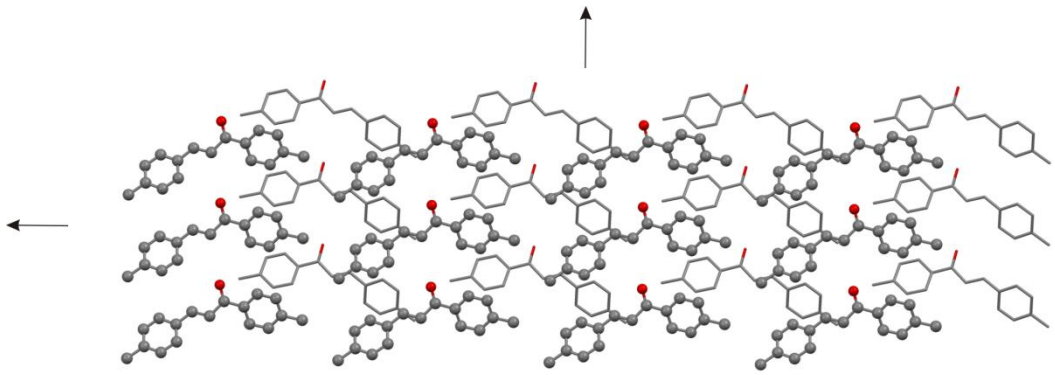

Figure 3-17: *SC A14, Me-C-Me is shown as a representative structure; this is a double layer structure, the upper layer is shown by ball and stick representation whilst the lower layer is shown by stick representation; the translation vector and direction of the 2_1 screw axes of the SC are indicated by the arrows.*

SC A15

SC A15 is a 2-D, close-packed, double layer of molecules, related by glides along the mid and long molecular axis as shown in Figure 3-18 below. This SC is equivalent to SC A1 rows related by a glide. Two of the structures displaying this SC, namely Et-C-Et and F-C-Et, are Z'=2 structures and each of the layers are made up of crystallographically independent molecules and are thus related by a 'pseudo'-glide plane.

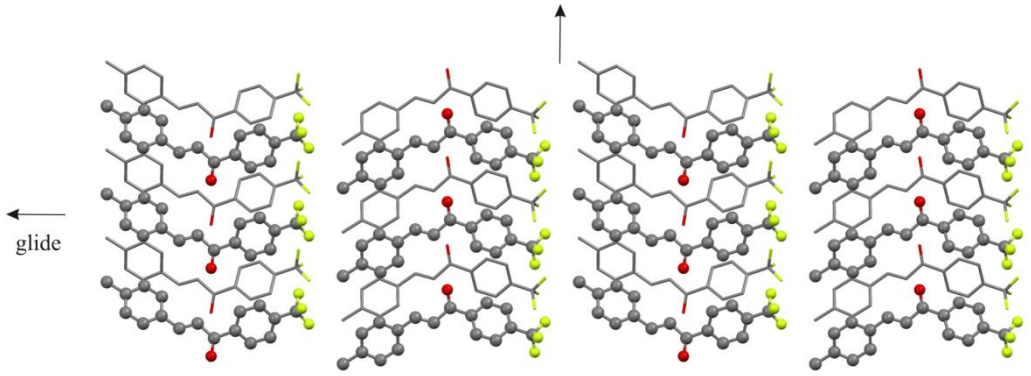

Figure 3-18: *SC A15, F3C-C-Me is shown as a representative structure; this is a double layer structure, the upper layer is shown by ball and stick representation whilst the lower layer is shown by stick representation; the directions of the glides of the SC are indicated by the arrows.*

SC A16

SC A16 is a 2-D, close-packed, double layer of molecules, related by translation along the mid molecular axis and glide planes along the long molecular axis as shown in Figure 3-19 below.

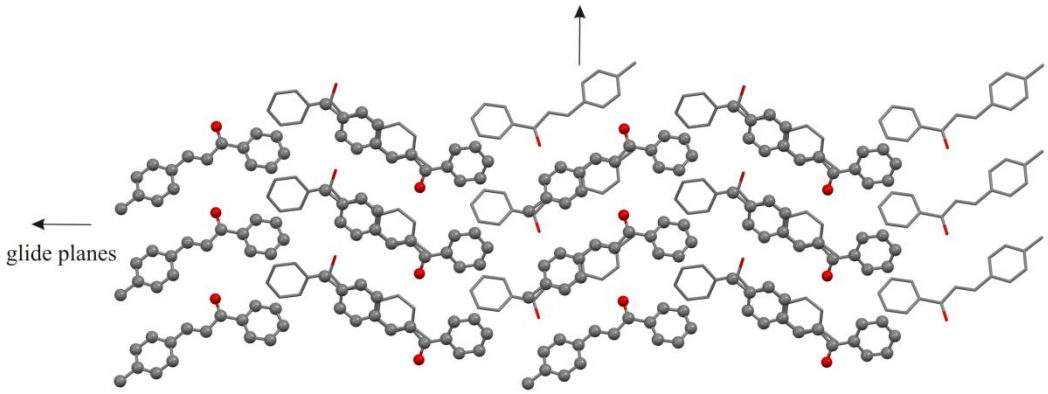

Figure 3-19: *SC A16, H-C-Me(2) is shown as a representative structure; this is a double layer structure, the upper layer is shown by ball and stick representation whilst the lower layer is shown by stick representation; the translation vectors and orientation of the glide planes of the SC are indicated by the arrows.*

SC A17

SC A17 is a 2-D, close-packed, quad layer of molecules, related by translation along the mid and long molecular axis as shown in Figure 3-20 below. This SC is equivalent to SC A8 rows related by translation.

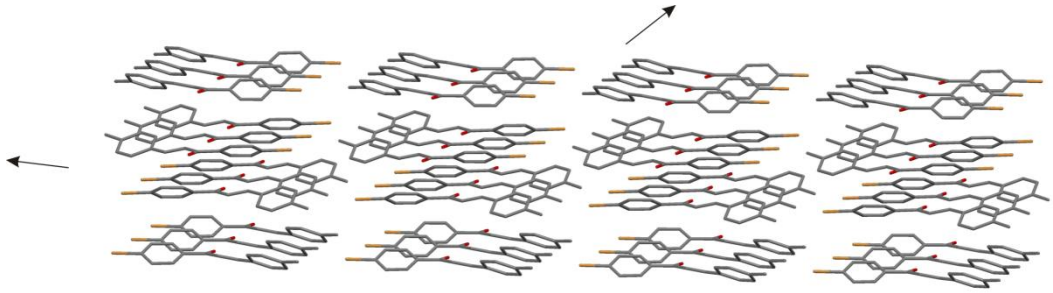

Figure 3-20: *SC A17, Br-C-Me is shown as a representative structure; this is a quad layer structure, the translation vectors of the SC are indicated by the arrows.*

SC A18

SC A18 is a 2-D, close-packed, single, 'stacked' layer of molecules, related by translation along the mid molecular axis and an alternating series of (pseudo-) glides and inversions along the short molecular axis and is shown in Figure 3-21 below. This SC is equivalent to stacks of SC A8 rows related by translation.

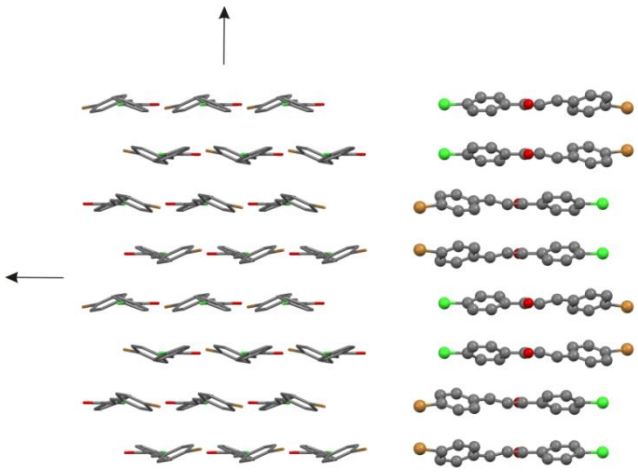

Figure 3-21: *SC A18, Cl-C-Br is shown as a representative structure; this is a single layer (stack) structure and two alternative views are shown; the translation vectors of the SC are indicated by the arrows.*

SC A19

SC A19 is a 2-D, close-packed, single, 'stacked' layer of molecules, related by translation along the mid molecular axes and glides along the short molecular axis and is shown in Figure 3-22 below. This SC is equivalent to stacks of SC A1 rows related by translation.

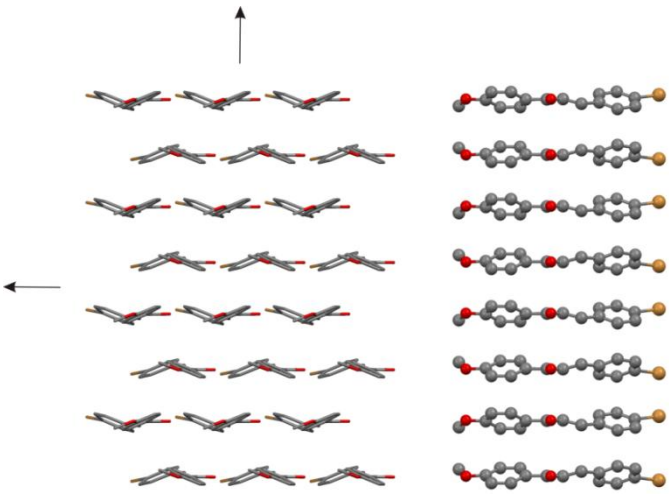

Figure 3-22: *SC A19, MeO-C-Br is shown as a representative structure; this is a single layer (stack) structure and two alternative views are shown; the translation vectors of the SC are indicated by the arrows.*

B Group

The B group of structures comprises 2/28 SCs found with the XPac procedure with 5/50 structures exhibiting these types of arrangements. All of the structures of this group contain primary SC B.

Primary SC B

SC B is a 0-D, close-packed 'trimer' as shown in Figure 3-23 below. It can be seen here and more clearly in SC B1 below that the relationship between the component molecules of this SC is based along the mid molecular axis. This 'trimer' does not exist as a discrete entity as most 0D SCs do, but as a repeating motif along a single dimension in all of the structures in which it is found. This SC relates a single structure, in this case F-C-F, with a group of structures, those related by SC B1 in this instance, which is quite a common occurrence amongst the group of chalcones studied.

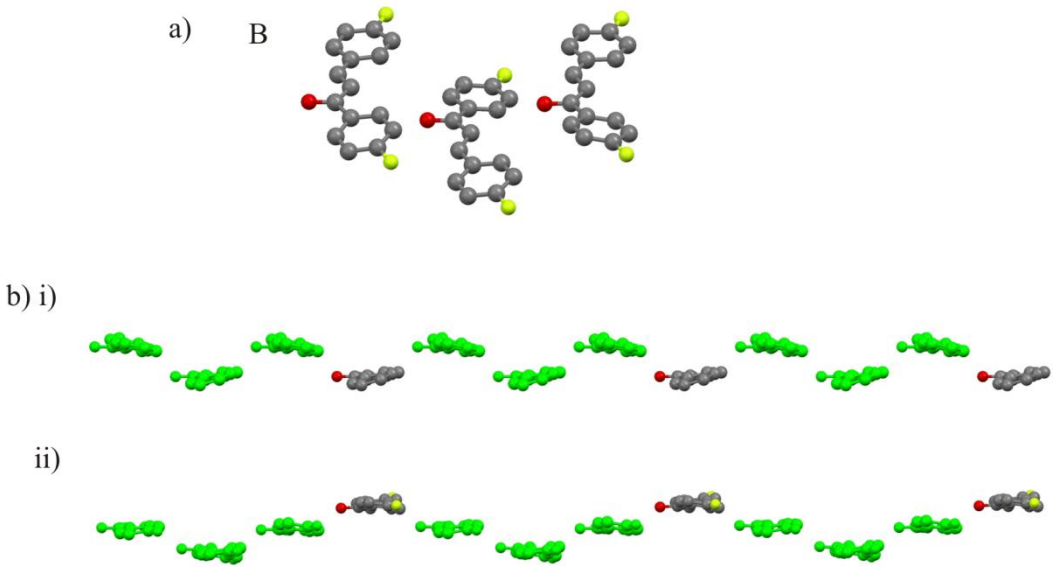

Figure 3-23: *SC B, a) F-C-F is shown as a representative structure; this is a 0-D close-packed trimer as shown; b) 1-D rows with instances of SC B highlighted in green from crystal structures i)H-C-H(2) and ii) F-C-F; the relative positioning of every 'fourth' molecule in the rows is the only significant difference between these two substructures.*

SC B1

SC B1 is a 1-D, close-packed, single, staggered row of molecules related by a 2_1 screw axis along the mid molecular axis as shown in Figure 3-24 below.

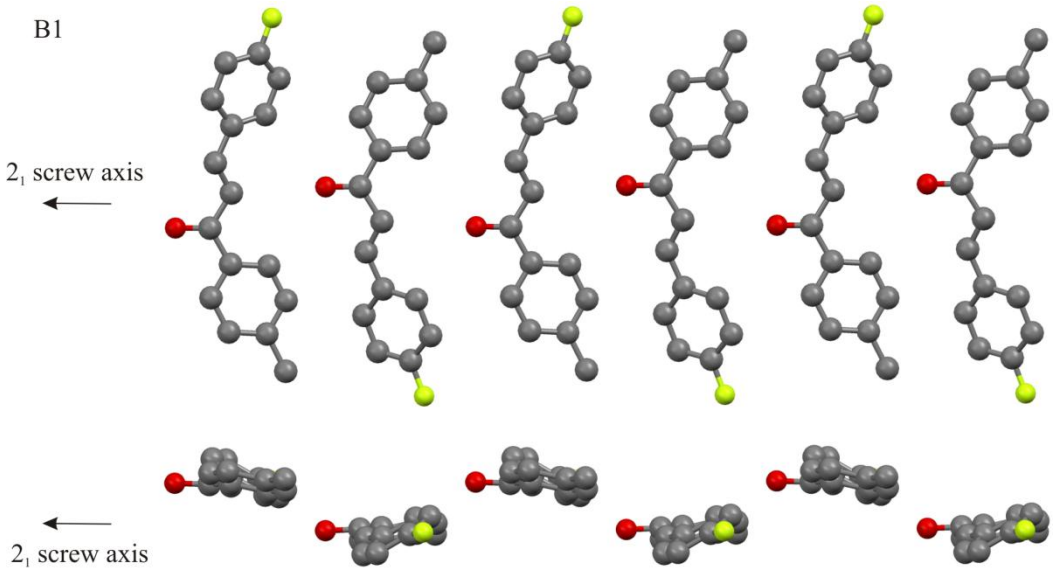

Figure 3-24: *SC B1, Me-C-F is shown as a representative structure; two alternative views are shown; and the orientation of the 2_1 screw axis of the SC is indicated by the arrows.*

C Group

The C group of structures comprises 2/28 SCs found with the XPac procedure with 4/50 structures exhibiting these types of arrangements. All of the structures of this group contain primary SC C.

Primary SC C

SC C is a 1-D, close-packed, single, staggered row of molecules related by a 2_1 screw axis along the mid molecular axis as shown in Figure 3-25 below. The similarity between this SC and SC B1 is immediately apparent, the most obvious differences being, the shift along the direction of the long molecular axis with respect to the two sub-layers of these SCs and the difference in orientation of the carbonyl groups with respect to the screw axis between the two SCs.

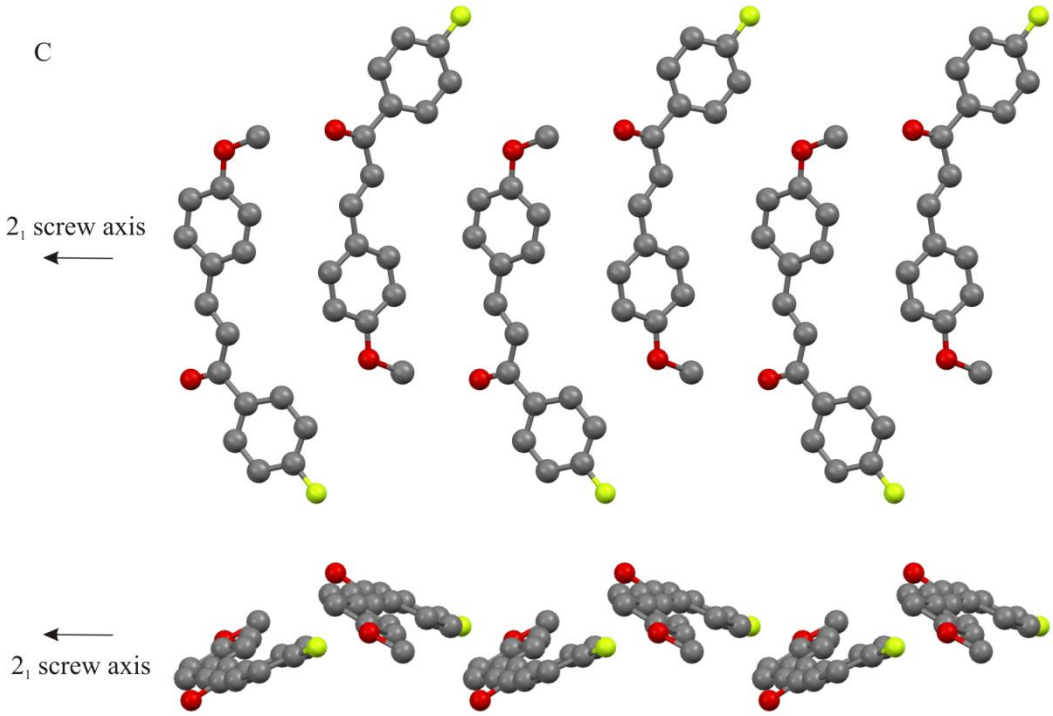

Figure 3-25: *SC C, F-C-OMe is shown as a representative structure; two alternative views are shown; and the orientation of the 2_1 screw axis of the SC is indicated by the arrows.*

SC C1/D1

SC C1/D1 is a 2-D, close-packed, single layer of molecules related by translation along the short molecular axis and a 2_1 screw axis along the mid molecular axis as shown in Figure 3-26 below. It is a combination of Primary SC C and Primary SC D (see below) and thus can be viewed as a 2-D arrangement of either of these 1-D SCs.

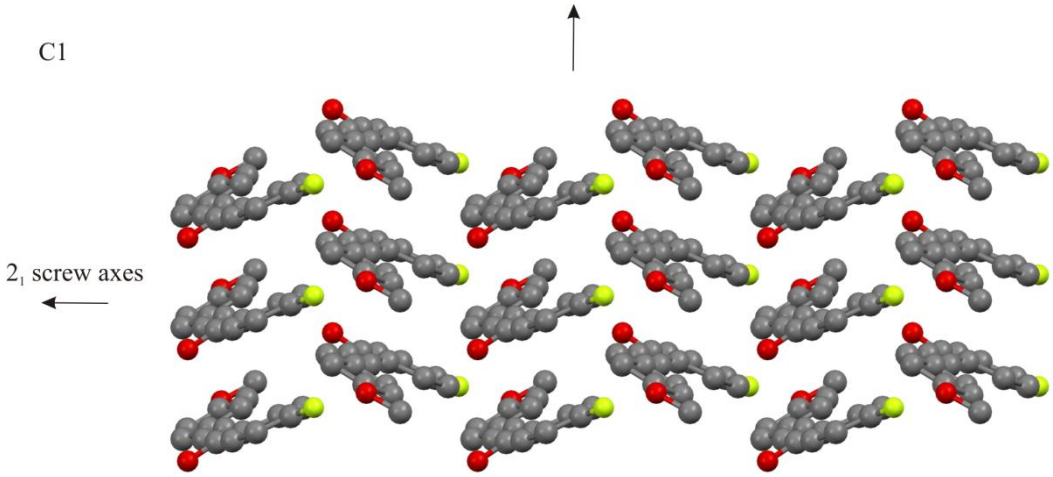

Figure 3-26: *SC C1/D1, F-C-OMe is shown as a representative structure; this is a single layer structure; the translation vectors and orientation of the 2_1 screw axes of the SC are indicated by the arrows.*

D Group

The D group of structures comprises 4/28 SCs found with the XPac procedure with 11/50 structures exhibiting these types of arrangements. All of the structures of this group contain primary SC D.

Primary SC D

SC D is a 1-D, close-packed, single, stack of molecules related by translation along the short molecular axis as shown in Figure 3-27 below.

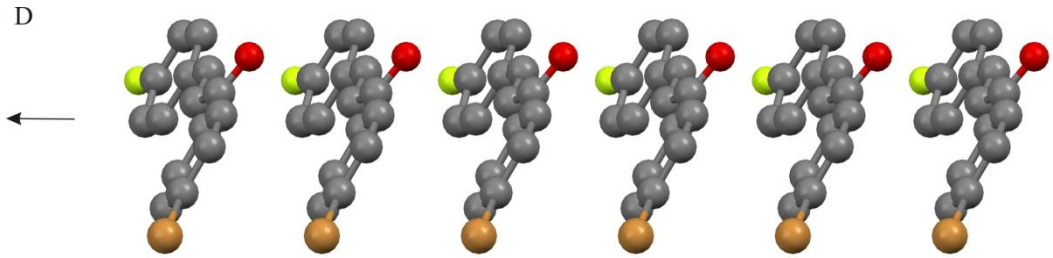

Figure 3-27: *SC D, Br-C-F is shown as a representative structure; the translation vector of the SC is indicated by the arrow.*

SC D2

SC D2 is a 2-D, close-packed, single, layer of molecules related by translation along the short and long molecular axes as shown in Figure 3-28 below. This is an alternative 2-D arrangement of 1-D SC D stacks compared with SC C1/D1 although not mutually exclusive as both of these SCs are present in the crystal structure of H-C-OMe.

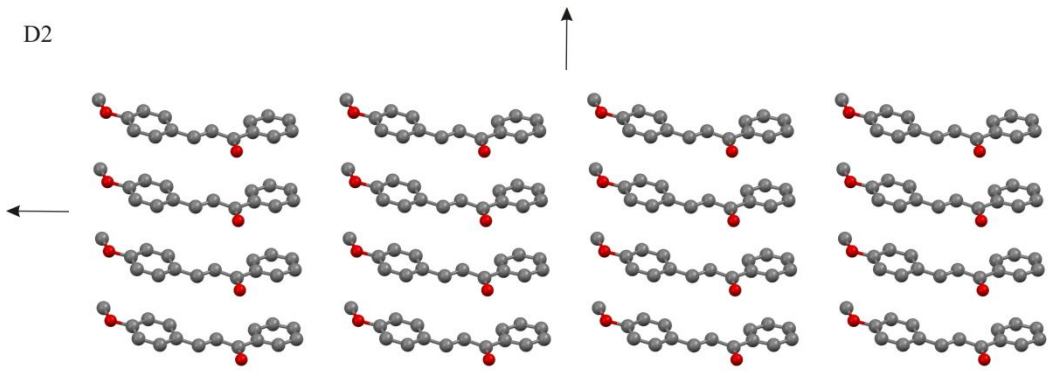

Figure 3-28: *SC D2, H-C-OMe is shown as a representative structure; the translation vectors of the SC are indicated by the arrows.*

SC D3

SC D3 is a 2-D, close-packed, double layer of molecules related by translation along the short and long molecular axes as shown in Figure 3-28 below. The layers are related by a glide.

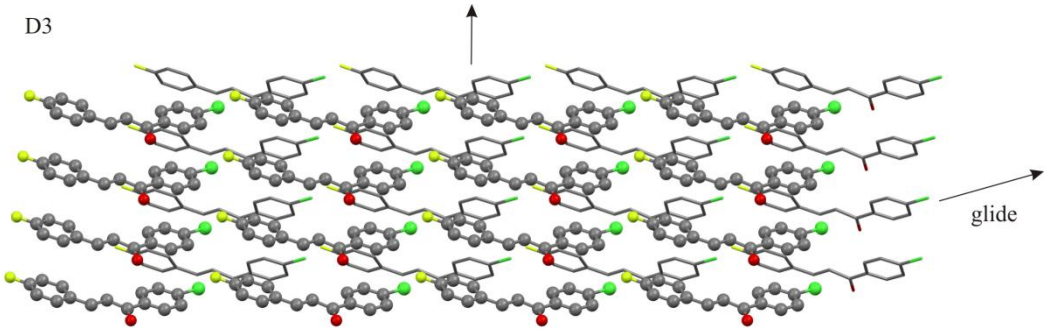

Figure 3-29: *SC D3, Cl-C-F is shown as a representative structure; this is a double layer structure, the upper layer is shown by ball and stick representation whilst the lower layer is shown by stick representation; the translation vectors and orientation of the glide planes of the SC are indicated by the arrows.*

E Group

The E group of structures comprises 1/28 SCs found with the XPac procedure with 4/50 structures exhibiting these types of arrangements. All of the structures of this group contain primary SC E.

Primary SC E

SC E is a 1-D, close-packed, single row of molecules related by translation along the long and short molecular axes as shown in Figure 3-30 below.

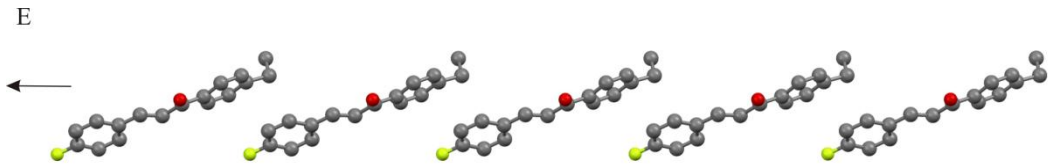

Figure 3-30: *SC E, Et-C-F is shown as a representative structure; the translation vector of the SC is indicated by the arrow.*

Discussion

From the chalcone structure relationship diagram (Figure 3-1), all of the nodes of the crystal structures, apart from those representing H-C-H(1) and the isostructural pair of MeO-C-F/MeO-C-H have an indirect downward connection to at least one of the five primary SCs, SC A (1-D), SC B (0-D), SC C (1-D), SC D (1-D) and SC E (1-D). This means that 47/50 chalcone structures studied are in fact composed of differently arranged occurrences of one or more of these five SCs. Thus it can be concluded that the low-dimensionality SCs A-E have a particular importance as they dominate the arrangement of molecules amongst this set of structures. The three structures which cannot be linked to a primary SC serve as a reminder that although the five primary SCs dominate the crystal packing of the group studied, they are not the only arrangements possible and that further study with an expanded group of structures may reveal further SCs with fundamentally different arrangements of molecules from those so far found. This is especially true of the MeO-C-F/MeO-C-H isostructural pair in which the overall geometrical arrangement of the molecules is sufficiently robust to occur in both these structures. However, the remainder of this discussion will concentrate on the 47 structures and the associated SCs that link them.

Consideration of the combinations of primary SCs exhibited by the chalcones studied shows that of all the theoretically possible combinations only A × D, B × E and C × D are observed. The absence of most of the other combinations may be rationalised by simply considering the molecular axis along which each SC is arranged. Thus SC A, SC B and SC C are different arrangements of molecules along the mid-molecular axis and these arrangements are incompatible with one another and therefore a combination of them cannot exist in the same crystal structure. Likewise, SC D is an arrangement of molecules along the short molecular axis and SC E is an arrangement along the short and long axes. Inspection of these two SCs clearly shows that they are incompatible and cannot exist in the same structure. By this simple consideration it is theoretically possible for A × E and C × E combinations of SCs to exist in a crystal structure, however no examples of these have been observed amongst the structures studied.

It is significant that three of the five primary SCs discovered are for molecular arrangements along the mid molecular axis of the molecule. The shape of the core chalcone molecule is essentially planar (although significant deviation from planarity is present in many of the crystal structures due to differences in the rotation of the substituted phenyl rings) and the only significant 'bump' and 'hollow' is formed by the carbonyl oxygen and the two rings along the mid molecular axis. It is thus only along this axis that the molecule is constrained in packing in the crystal structures and thus it is along this axis that robust packing motifs form.

Structures containing SC A

From the chalcone structure relationship diagram (Figure 3-1), it is immediately apparent that SC A is the most significant interaction amongst the chalcones studied. It is a 1-D row of molecules close-packed along the mid molecular axis of the chalcone molecule, which is present in 34/50 structures and 19/31 packing arrangements found amongst the chalcones and gives rise to 19 secondary SCs. The A group structures include four of the seven isostructural groups found amongst the chalcones studied, including the largest '1+' group of 11 structures. The A group SCs have been described and illustrated above and are summarised in Figure 3-31 below. All of SCs are viewed parallel to the ***t1*** translation vector of SC A, so that each molecule in the drawing represents a single SC A row. The colouring of each individual molecule indicates the orientation of the carbonyl with respect to the plane of the page (black = upwards, orange = downwards) and the position of the carbonyl oxygen atom is always indicted with a red ball. These representations allow easy comparison of the SCs, although it should be realised that these diagrams do not enable different height levels of SC A units of the same orientation to be distinguished.

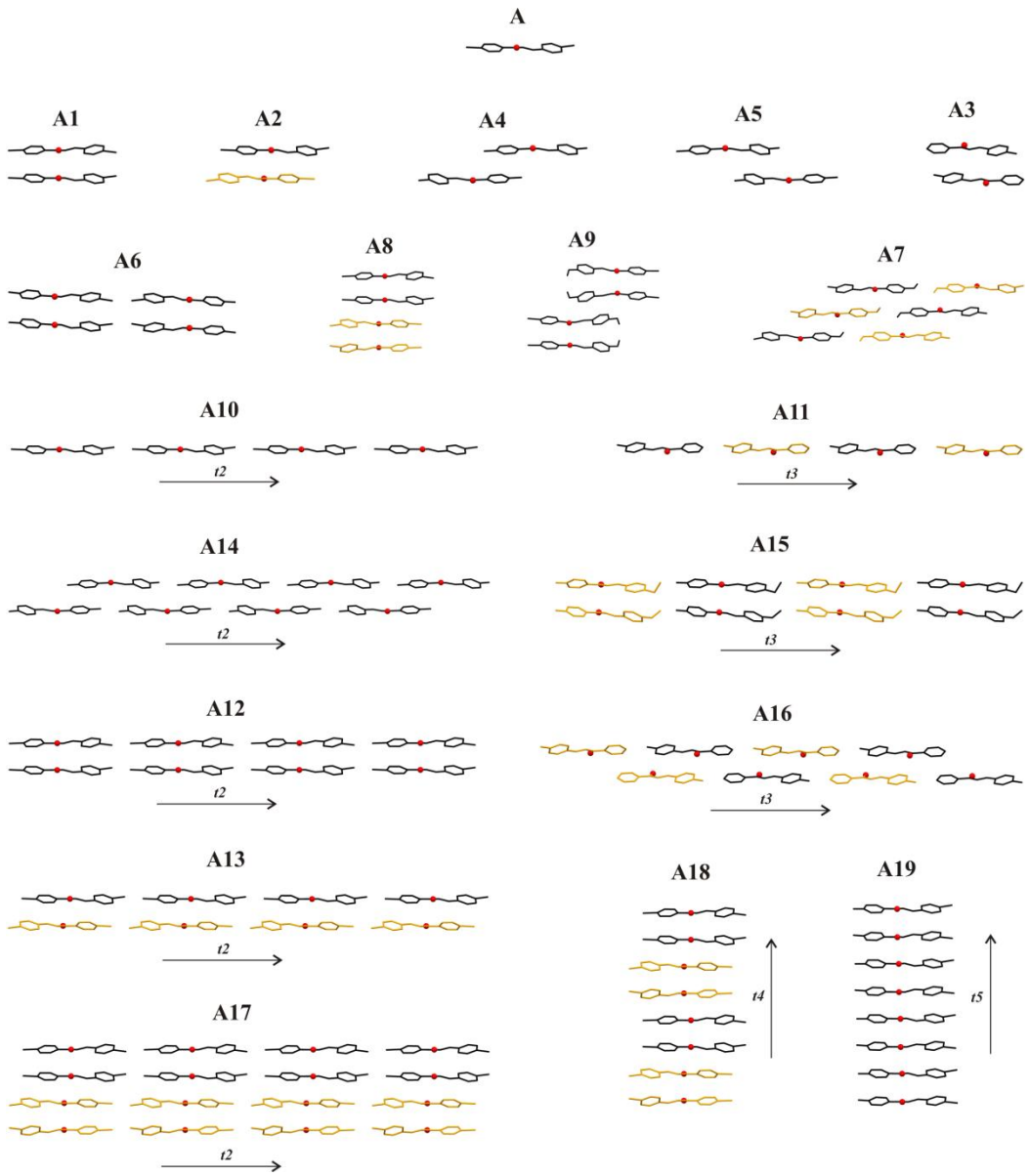

Figure 3-31: *Primary SC A and secondary SCs A1-A19 derived from it. All rows are viewed parallel to the t1 vector (see Table 3-3).*

Figure 3-32 below shows representations of the nineteen different principle packing arrangements that are composed of SC A. The same style as used for Figure 3-31 above is used for this and all subsequent figures.

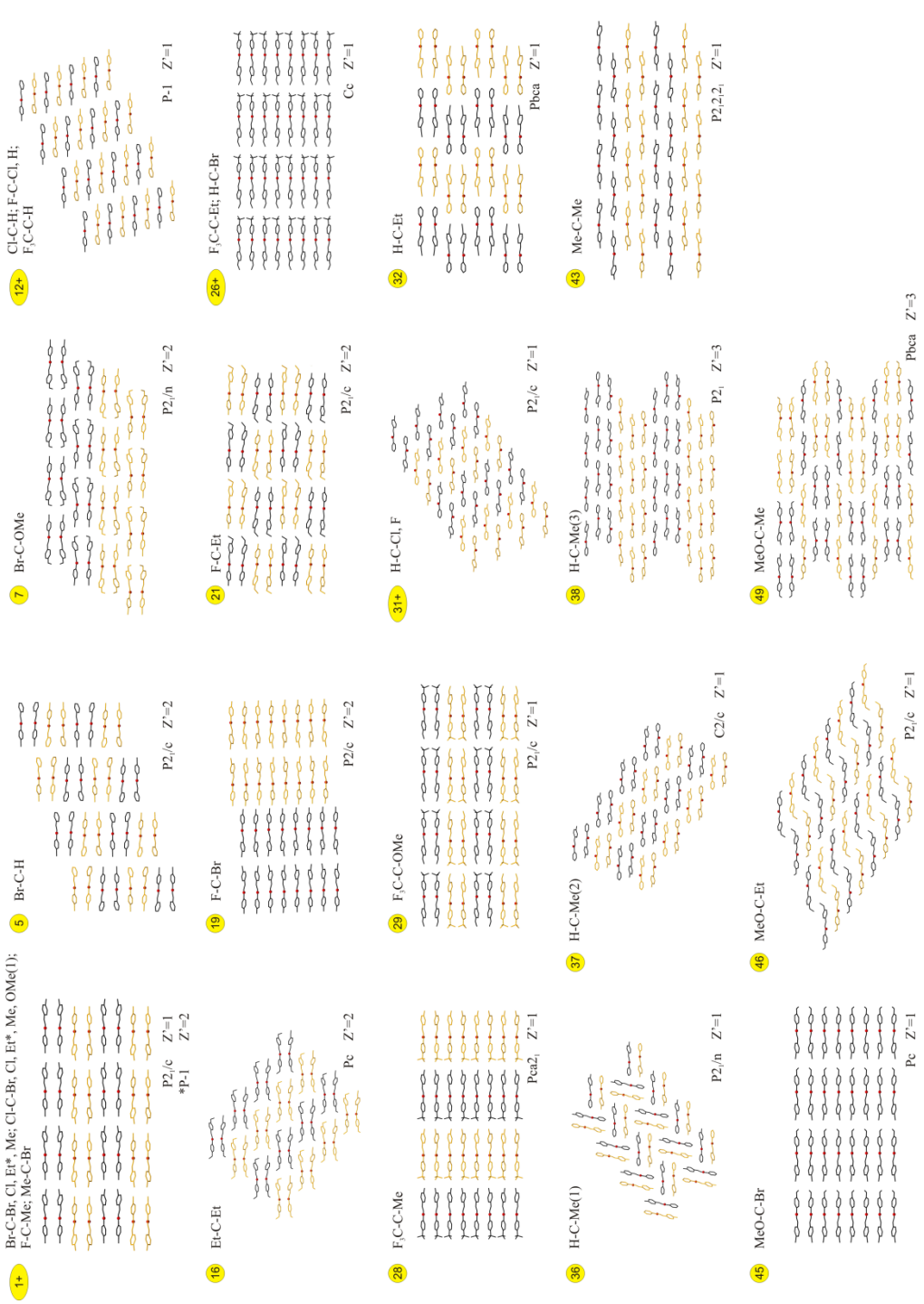

Figure 3-32: *Packing of chalcone molecules in structures containing SC A. Each of the structures is viewed parallel to its* ***t1*** *vector.*

From Figure 3-32 it can be seen that there are 19 packing arrangements based on SC A of which 16 of the packing arrangements also contain a secondary 2-D SC (SCs A10-A19). These 2-D SCs may be classified into four types based on their secondary translation vectors (see Tables 3-2 and 3-3 and Figure 3-31), thus SCs A10, A12, A13, A14 and A17 are 2-D arrangements of SC A based on the translation vector ***t2***. Likewise, SCs A11, A15 and A16 are 2-D arrangements of SC A based on ***t3***, SC A18 is based on ***t4*** and SC A19 is based on ***t5***. Translation vectors ***t2*** and ***t3*** are both parallel to the long molecular axis, but the SCs based on them have fundamentally different arrangements of molecules along these vectors. SCs based on ***t2*** are characterised by neighbouring (along ***t2***) instances of SC A related simply by translation, whereas those based on ***t3*** are characterised by neighbouring (along ***t3***) instances of SC A related by a glide. These differences of molecular arrangement along the translation vectors means that the SCs based on these vectors are mutually exclusive from each other and none of the crystal structures of the chalcones studied contain instances of both of these types of SCs. A similar situation exists between the SCs based on ***t4*** and ***t5***. Both of these translation vectors are parallel to the short molecular axis, but the molecular arrangements along each are also fundamentally different. SCs A18 and A19 (based on ***t4*** and ***t5*** respectively) are both subsets of SC A1, however in SC A18, pairs of SC A1 double rows of molecules are related by inversion to form SC A8 and these in turn are related by translation whereas in SC A19 instances of SC A1 are simply related by translation. Thus SCs A18 and A19 are mutually exclusive and incompatible in the same crystal structure. Whilst the SCs with different translation vectors parallel to the same molecular axis are mutually exclusive, this is not the case between SCs with translation vectors parallel to different molecular axis, thus different structures containing SCs based on ***t2*** occur that also contain SC A18 (***t4***) and SC A19 (***t5***) and this is also the same for different structures containing SCs based on ***t3***.

From Figures 3-1 and 3-31 it can be seen that SC A10 is the basic ‘building block’ of the ***t2*** group of SCs and in this sense is a 2-D analogue of SC A. In most of the structures that it occurs, it is as part of a more complex SC, the only exception to this is F_3C-C-OMe, but this is an unusual structure amongst the group studied as will be discussed later. Pairs of SC A10 sheets combine via

(pseudo-) glides, inversions and (pseudo-) 2_1 screws to form SCs A12, A13 and A14 respectively and SCs A12 and A13 are combined in SC A17. These relationships encompass 7/19 structural types and 20/34 crystal structures found amongst the A group and includes the large isostructural '1+' group of 11 crystal structures (Br-C-Br, Br-C-Cl, Br-C-Et, Br-C-Me, Cl-C-Br, Cl-C-Cl, Cl-C-Et, Cl-C-Me, Cl-C-OMe(1), F-C-Me, Me-C-Br). This isostructural group is by far the largest found amongst the chalcones studied and it can thus be assumed that the geometry of this arrangement of molecules is particularly stable, existing as it does over a large number of structures containing differently substituted molecular components . This structural group and the Br-C-OMe and MeO-C-Br structures are derived from SC A12 as shown in Figure 3-33 below.

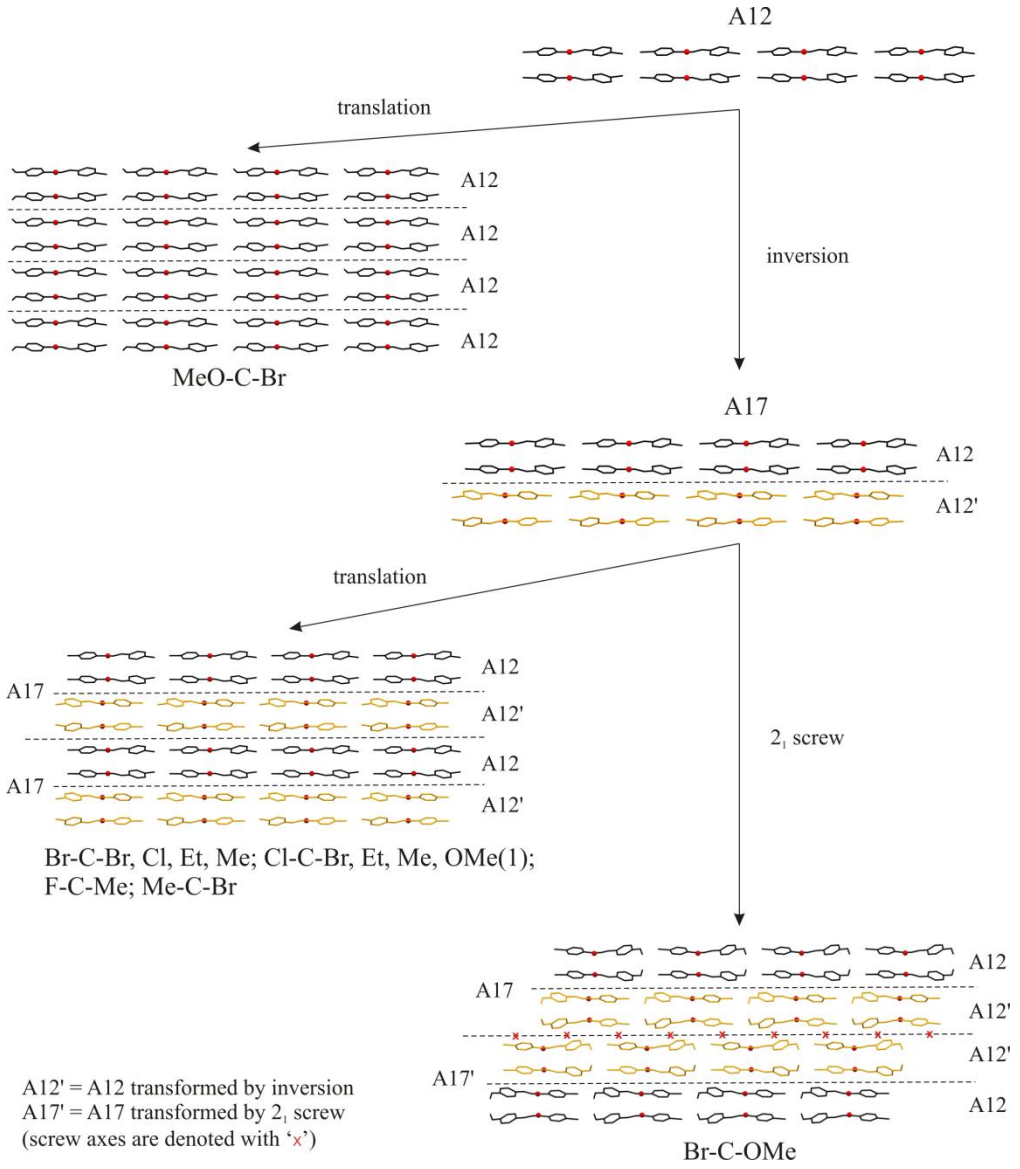

Figure 3-33: *The relationships between the '1+' structural group and the Br-C-OMe and MeO-C-Br structures.*

Although not explicitly labelled, it can be clearly seen from Figure 3-33 that in the '1+' group of structures and Br-C-OMe the inverse relationship of two occurrences of the double-layer SC A12 results in the SC A13 relationship. This SC is also displayed in the isostructural group 12+, which is the second largest of the isostructural groups with four structures (Cl-C-H, F-C-Cl, F-C-H, F_3C-C-H). Unlike the structures containing SC A17, these structures are made up of single layer sheets (SC A10) related by inversion to form SC A13, instances of which, related by translation, form the structures as can be seen in Figure 3-34 below. The SC A14 relationship is displayed in three structures, Br-C-OMe, H-C-Me(3) and Me-C-Me. It is composed of a pair of SC A10 sheets related by 2_1 screw axes, although in H-C-Me(3), these are non-crystallographic symmetry elements. In the Br-C-OMe structure this SC relates instances of SC A17 to give the overall crystal structure as has been shown above (see Figure 3-33). In the Me-C-Me structure pairs of SC A14 sheets are related by 2_1 screw axes to give the overall structure as shown in Figure 3-34 below.

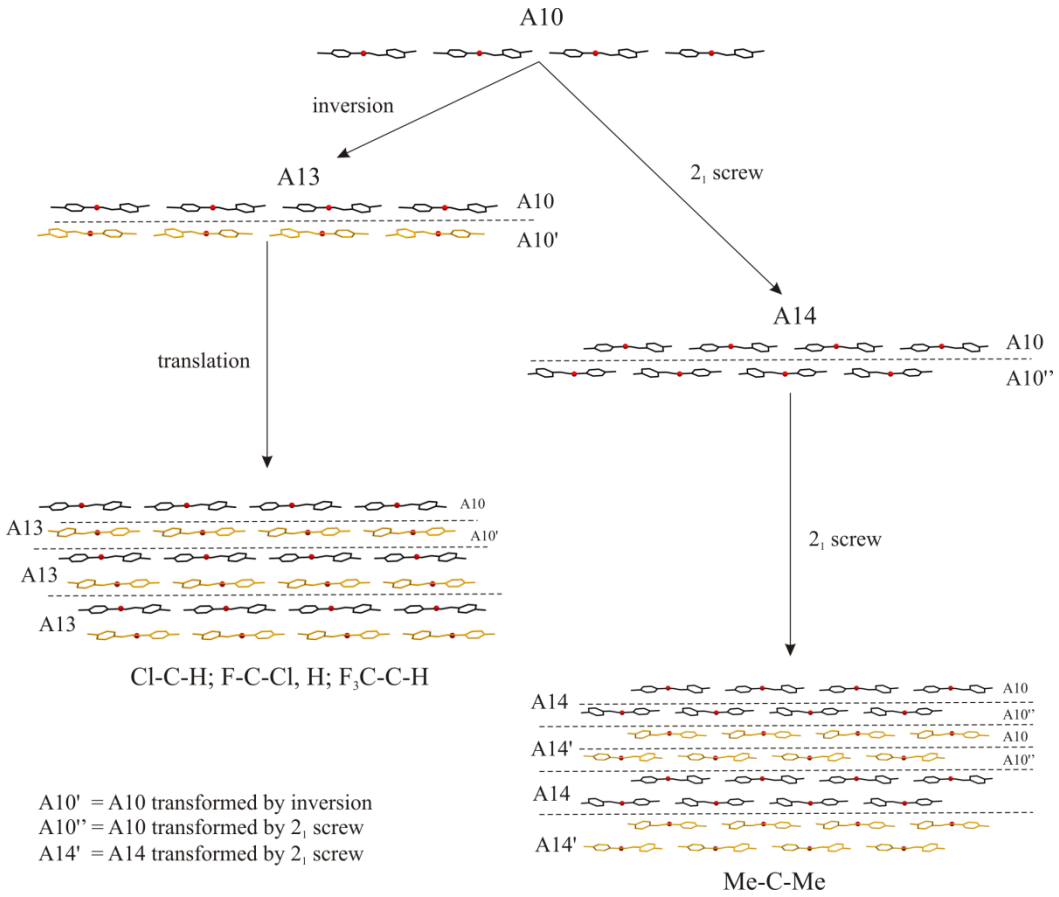

Figure 3-34: *SCs A13 and A14 relationships*

As was mentioned earlier F_3C-C-OMe is an unusual structure amongst the chalcones studied. At first glance, it appears to be isostructural with the '1+' group of structures with double layers of SC A10 sheets related by a glide to each other and with these double layers in turn related by inversion to give the overall structure. Whilst this is true for both structure types, close comparison of the double SC A10 sheets of F_3C-C-OMe and the '1+' isostructural group reveals that each of the component SC A10 sheets of the double layer of F_3C-C-OMe is of the opposite conformation to its equivalent in the '1+' isostructural group as shown in Figure 3-35 below.

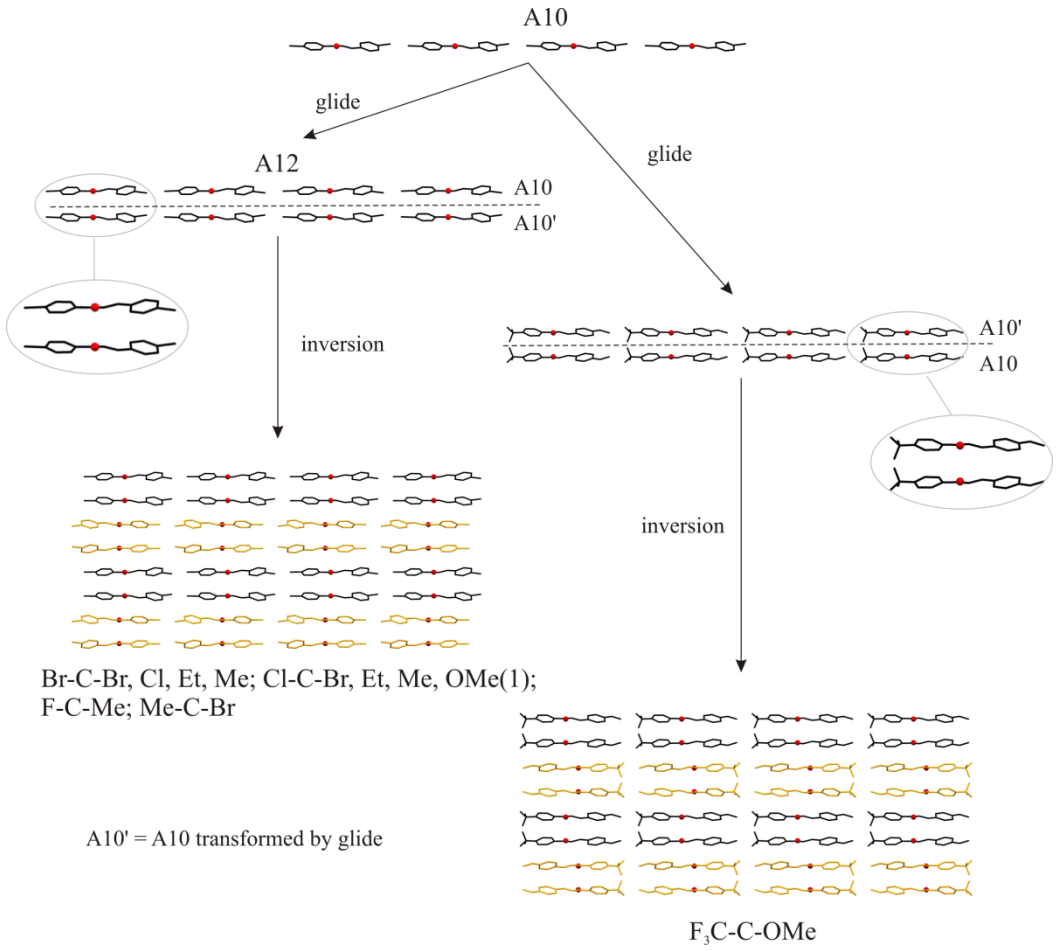

Figure 3-35: *Different packing arrangements of the '1+' structural group and F_3C-C-OMe due to subtle conformational differences highlighted in the enlarged parts of the structures.*

This conformational difference arises from slightly different packing arrangements of the aromatic rings of the core chalcone moiety. In F_3C-C-OMe and all of the structures that exhibit the SC A1 double-row relationship (SC A1 is the 1-D analogue of SC A12) the aromatic rings pack in a 'herring-bone' pattern to maximise packing efficiency. However, in all the structures exhibiting SC A1

the aromatic rings at the carbonyl end form a 'herring-bone' pattern with the apex aligned towards the oxygen atom of the carbonyl and the rings at the alkene end are aligned oppositely. Conversely, in the F_3C-C-OMe structure, this situation is reversed so that aromatic rings at the carbonyl end of the molecule form a herring-bone pattern with the apex aligned away from the carbonyl oxygen atom. This is illustrated in Figure 3-36 below.

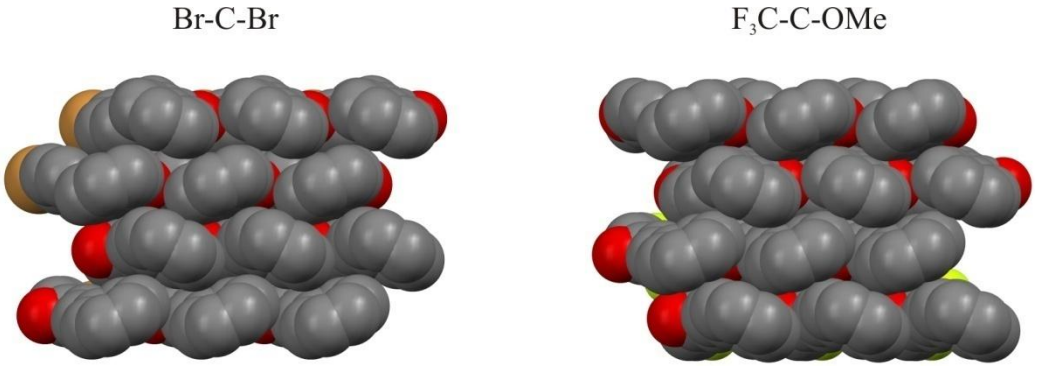

Figure 3-36: *Comparison of packing of aromatic rings in Br-C-Br, shown as a representative SC A1 structure and F_3C-C-OMe; the structures are viewed parallel to the **t2** vector (or equivalent) and hydrogen atoms and substituents are omitted for clarity. Two SC A1 double-rows related by inversion are shown for Br-C-Br and the equivalent arrangement of molecules is shown for F_3C-C-OMe and they are both viewed down the long molecular axis so that in the top two rows of each structure the aromatic rings at the carbonyl end of the molecule are in the foreground and in the bottom two rows it is those at the alkene end. From these views the 'opposite' alignments of the aromatic rings in these structures is clearly seen.*

This conformational difference of the F_3C-C-OMe structure caused difficulty with its placement in the chalcone structural relationship scheme (Figure 3-1) and thus not all of the SCs it displays can be derived from this scheme. The additional important SCs displayed by F_3C-C-OMe along with the structures it shares them with are as follows: SC A13 – isostructural group '12+' only, SC A2 – isostructural group '12+' and H-C-Me(1) only, additionally the 'opposite' SC A12 relationship displayed by F_3C-C-OMe and shown in Figure 3-35 is also displayed by MeO-C-Br.

From Figures 3-1 and 3-31 it can be seen that SC A11 is the basic 'building block' of the ***t3*** group of SCs. It is a single layer sheet made up of alternating SC A rows related by glide planes parallel to the ***t3*** axes and perpendicular to the mid-molecular axes in the structures in which it occurs. There are no direct links between SC A11 and any crystal structures, instead this

SC provides the link between two subsets of the A group chalcone structures based on SCs A15 and A16. SC A15 is a double-layer sheet consisting of two SC A11 layers related by a glide plane (this is analogous to the relationship between SCs A10 and A12 described above). It is displayed in four crystal structures: Et-C-Et, F-C-Et, F_3C-C-Me and H-C-Et, although in Et-C-Et and F-C-Et each of the SC A11 sub-layers of this SC consist of crystallographically independent molecules and thus the glide planes relating the two layers in these structures are approximate and non-crystallographic. Each of the four structures is generated from SC A15 with different crystallographic symmetry elements, thus the F_3C-C-Me structure is generated from translation, the F-C-Et structure from inversion and the Et-C-Et and H-C-Et structures from a glide and 2_1 screw respectively, as is shown in Figure 3-37 below.

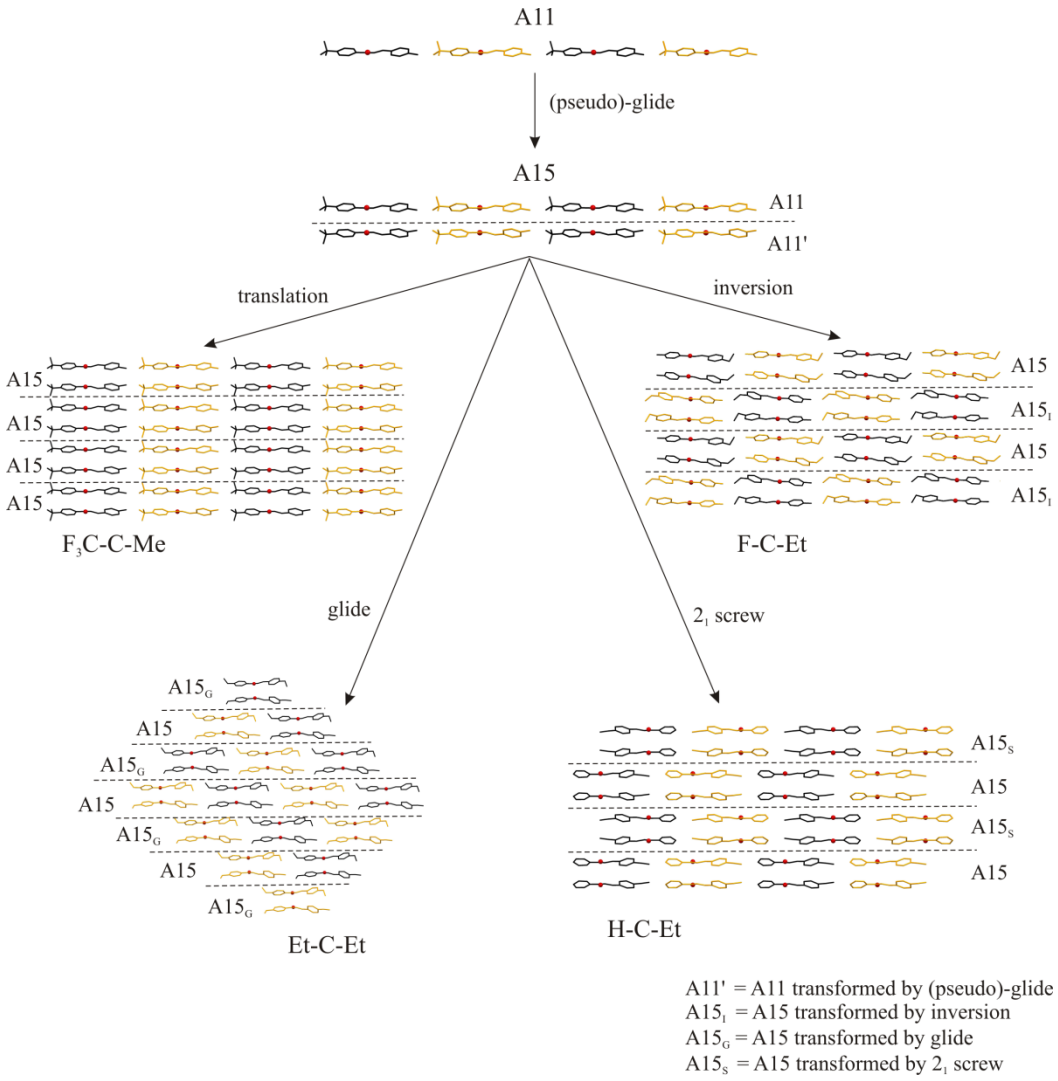

Figure 3-37: *Relationships between SC A15 and the structures displaying this SC.*

SC A16 is a double-layer sheet comprising two SC A11 layers related by 2_1 screw axes (this is analogous to the relationship between SCs A10 and A14 described previously). This SC is displayed in two structure types, the isostructural pair of H-C-Cl and H-C-F ('31+') and the H-C-Me(2) structure and both structure types are built up from repeated instances of SC A16 related by c glides as shown in Figure 3-38 below.

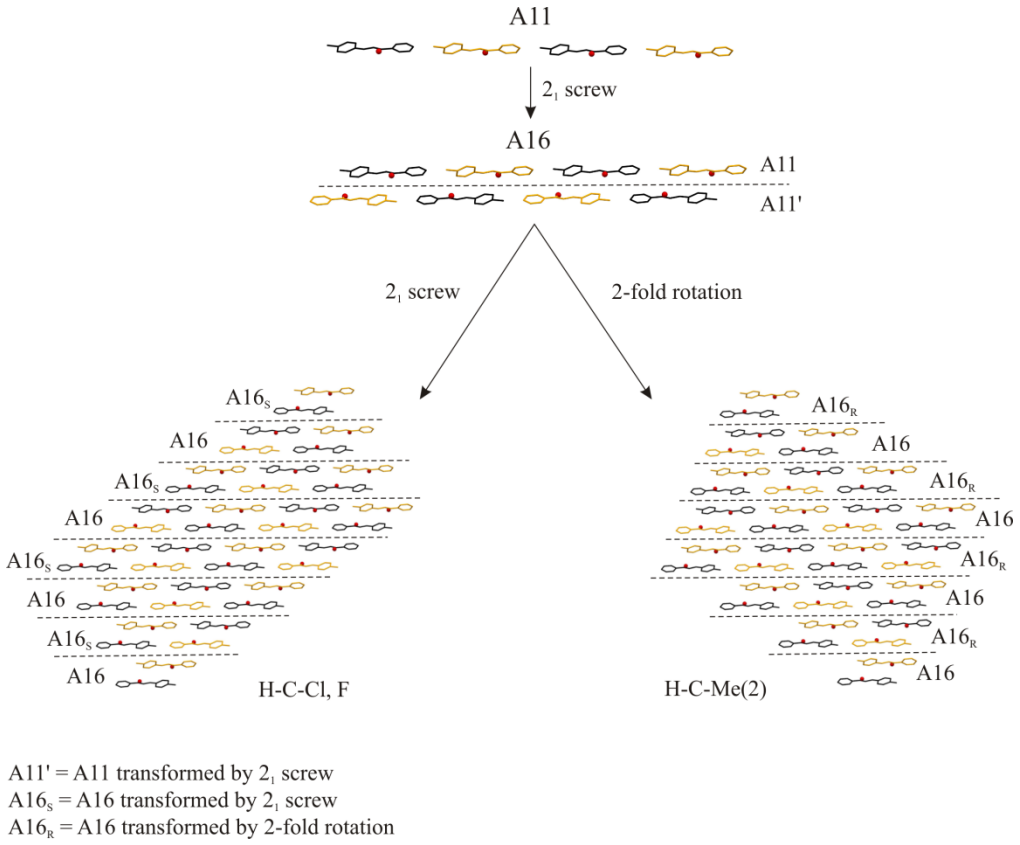

Figure 3-38: *Relationships between SC A16, and the structures displaying this SC*

It can be seen that both of these structures are very closely related and this is shown clearly in Figure 3-39 below. In this diagram four layers of the H-C-Cl and H-C-Me(2) structures, each composed of SC A16 and SC A16' double layers (see Figure 3-38), are shown overlaid with one another. The top two layers of each structure (SC A16) overlay each other both in position and conformation in very good agreement. The bottom two layers are displaced with respect to each other such that both phenyl rings of one molecule of the H-C-Cl structure are in approximately the same position as two adjacent phenyl rings from neighbouring molecules in the H-C-Me(2) structure. Whilst the unsubstituted ring of a molecule in the H-C-Cl structure maps with good

agreement to the position and conformation to the substituted ring of a molecule in the H-C-Me(2) structure, the substituted ring maps to a position between the unsubstituted rings of molecules in the H-C-Me(2) structure and in the opposite conformation. If the linker portion of the chalcone moiety is ignored, the position and conformation of the rings is overall very similar in both structures and this suggests it is the drive for efficient close-packing of the phenyl rings of the chalcone molecules that dominates packing interactions along the vector of the short molecular axis in these structures.

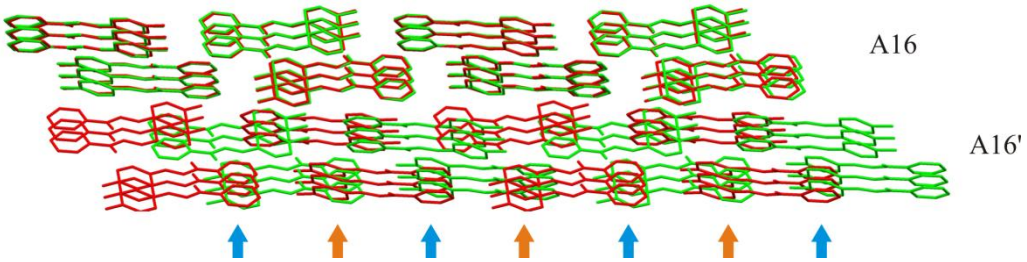

Figure 3-39: *Structure overlay of H-C-Cl (green) and H-C-Me(2) (red). The SC A16 rows overlay with very good agreement, however the A16' rows of each structure are shifted with respect to each other. The blue arrows indicate the ring portions of the A16' rows of both structures with close positional and conformational alignment and the orange arrows indicate the ring portions of both structures where the relative positions are shifted with respect to each other and with opposite conformations.*

There is only one SC based on the ***t4*** translation vector which is SC A18 (see Figures 3-1 and 3-31). It is displayed in 3/19 structure types including the large, eleven member '1+' isostructural group and the Br-C-H and F-C-Et structures and is composed of stacked SC A rows of molecules related by an alternating series of (pseudo-) glides (in the crystal structures of this group with Z'=2, the glides are non-crystallographic symmetry elements) and inversions. In the '1+' isostructural group, instances of SC A18, related by translation, result in the overall crystal structure, whereas in both the Br-C-H and F-C-Et structures, instances of SC A18 are related by c glides to give the overall structures. These relationships are illustrated in Figure 3-40 below.

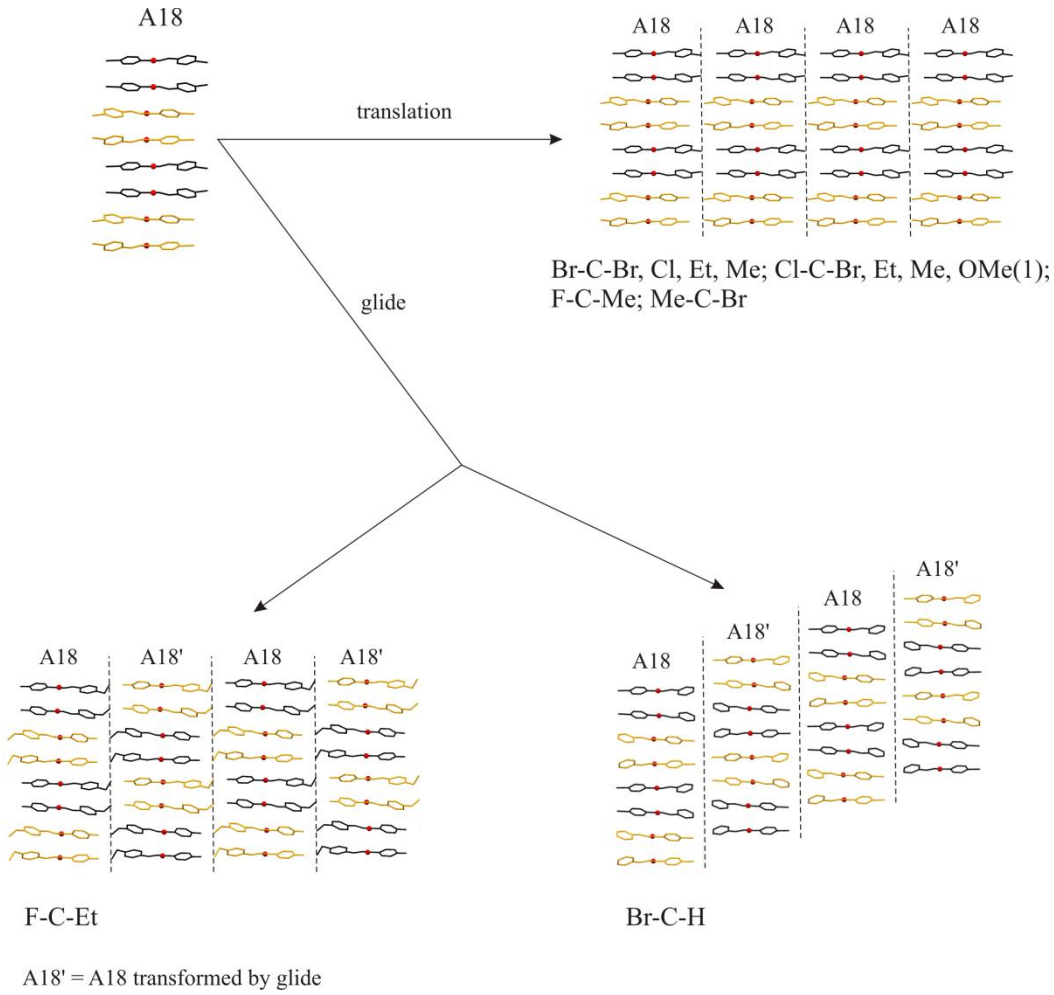

Figure 3-40: *SC A18 relationships. The relationship between the F-C-Et and Br-C-H structure is similar to the SC A16 relationship between the isostructural group '31+' and H-C-Me(2), both sets of structures are related by c glides.*

From Figure 3-40 it can be clearly seen that the Br-C-H structure is related to the F-C-Et structure by a simple shear parallel to the short molecular axis. The rows of molecules of SC A18 align with the interstices of the rows of molecules of neighbouring instances of SC A18' and it is presumed that this allows some degree of 'interleaving' of the adjacent rings of neighbouring SC A18 and SC A18' stacked rows and thus more efficient packing which results in the shear. Conversely, this cannot occur in the F-C-Et structure where the bulky ethyl substituents prevent this interleaving.

There is only one SC based on the ***t5*** translation vector which is SC A19 (see Figures 3-1 and 3-31). It is displayed in 4/19 structure types including the isostructural group '26+' (F_3C-C-Et, H-C-Br), F-C-Br, F_3C-C-Me and MeO-C-Br. It is composed of stacked SC A rows of molecules each related by a

(pseudo-) glide (F-C-Br is a Z'=2 structure and the glide is a non crystallographic symmetry element relating two crystallographically independent molecules). Each of the four structures is generated from SC A19 with different crystallographic symmetry elements, thus the MeO-C-Br structure is generated from translation, the F-C-Br structure from a 2 rotation and inversion, the F_3C-C-Et and H-C-Br structures from a glide and the F_3C-C-Me structure from a 2_1 screw, as is shown in Figure 3-41 below.

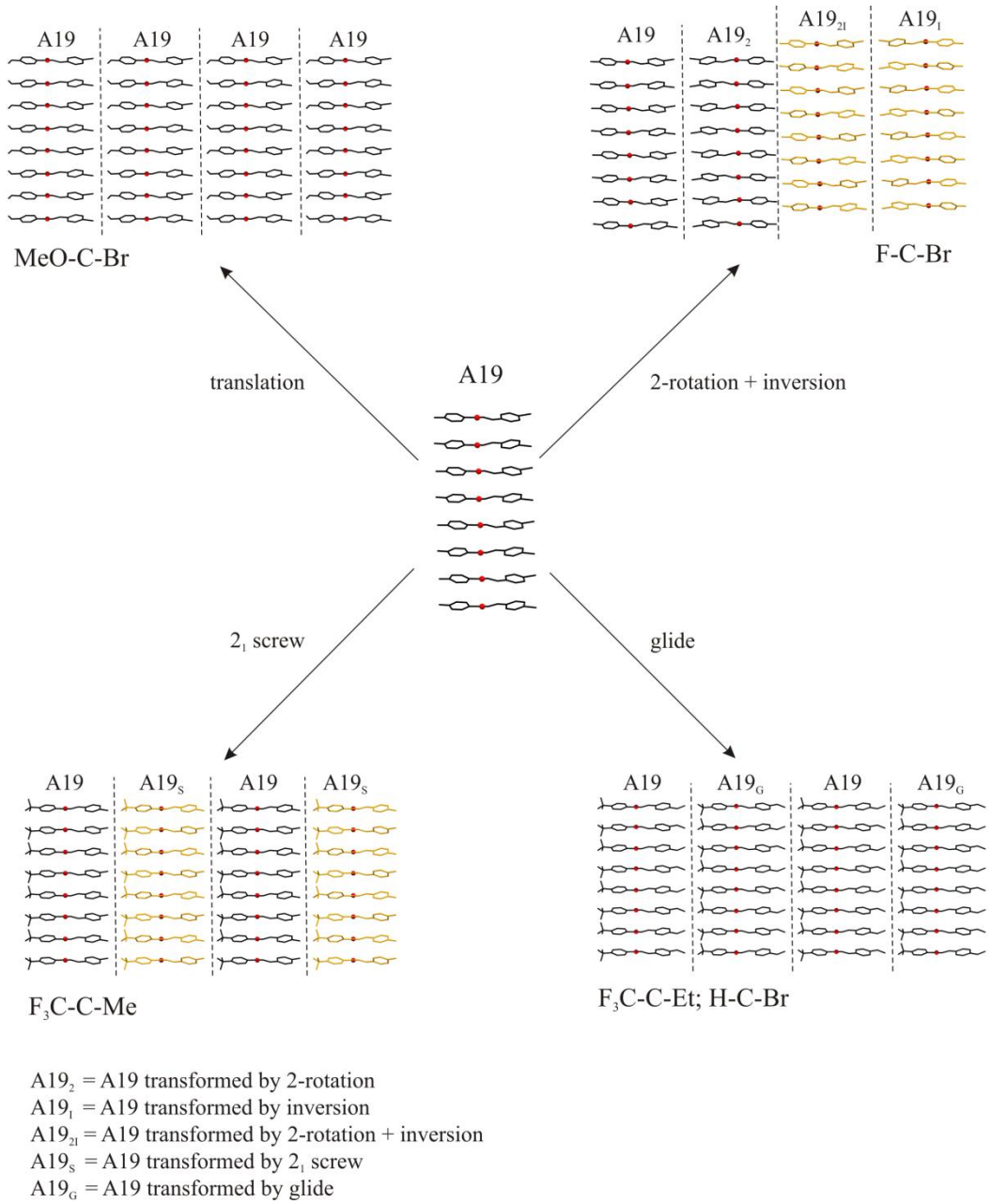

Figure 3-41: *Relationships between SC A19 and the structures displaying this SC.*

As mentioned earlier there are three structure types amongst the A group of chalcones which do not display any 2-D SCs, namely H-C-Me(1), MeO-C-Et and MeO-C-Me. However, the structure types of the two methoxy substituted chalcones uniquely display the 1-D SC A7 (see Figures 3-1 and 3-31). This SC is composed of two SC A rows of molecules linked across (pseudo-) inversion centres by non-classical hydrogen bonds between the methoxy substituents to form dimer rows and three layers of these dimer rows are then related by (pseudo-) glides. For the MeO-C-Me structure with Z'=3, most of the inversion centres and all the glide planes are non-crystallographic symmetry elements. In the MeO-C-Et structure, instances of SC A7 are related by translation along the direction of the long molecular axis and by a c glide in the direction of the short molecular axis, whereas instances of SC A7 are related by a 2_1 screw along the direction of the long molecular axis and a b glide along the direction of the short molecular axis in the MeO-C-Me structure, as illustrated in Figure 3-42 below.

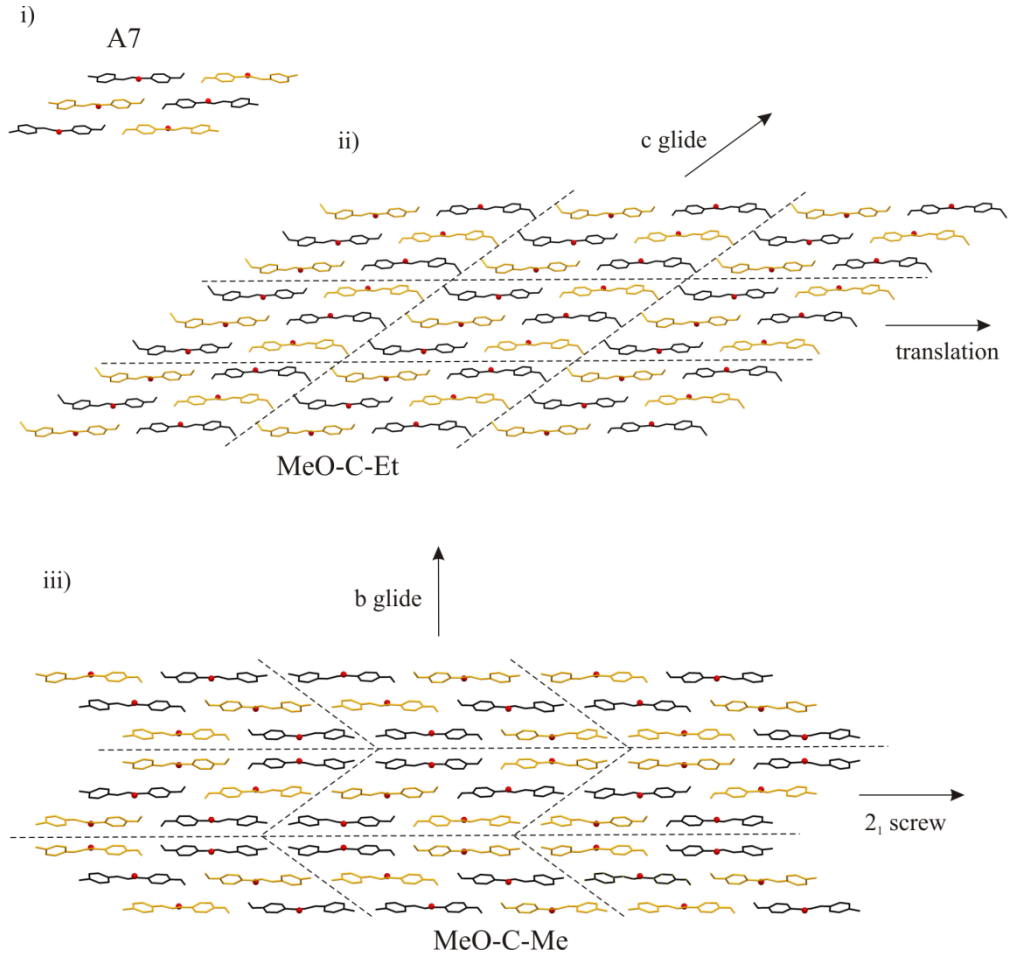

Figure 3-42: *SC A7 relationships; i) SC A7; ii) MeO-C-Et; iii) MeO-C-Me. For each structure an instance of SC A7along with eight neighbouring constructs along with the applicable symmetry operations to map to these neighbours.*

It can be seen that it is the interactions of the ethyl and methyl substituents of the molecules in MeO-C-Et and MeO-C-Me that dictate the packing of SC A7 in these structures. SC A7 packs in the MeO-C-Et structure more simply than in MeO-C-Me with instances related by the same c glide planes present in the SC in one dimension and simple translation in the second dimension, whereas in MeO-C-Me a variety of orientations of SC A7 are related by b glides and 2_1 screws. This may be attributed to the more limited ways available to efficiently pack the bulkier ethyl substituents of MeO-C-Et compared to the methyl substituents of MeO-C-Me. This is shown in figure 3-43, where it can be seen that the rows of ethyl substituents (shown in spacefill representation) of neighbouring molecules (colour coded red and green) in the MeO-C-Et structure form an interlocking arrangement resembling the teeth of a zip fastener. Conversely, the methyl groups of the molecules of the MeO-C-Me structure abut one another rather than interlocking and thus orientation is less important.

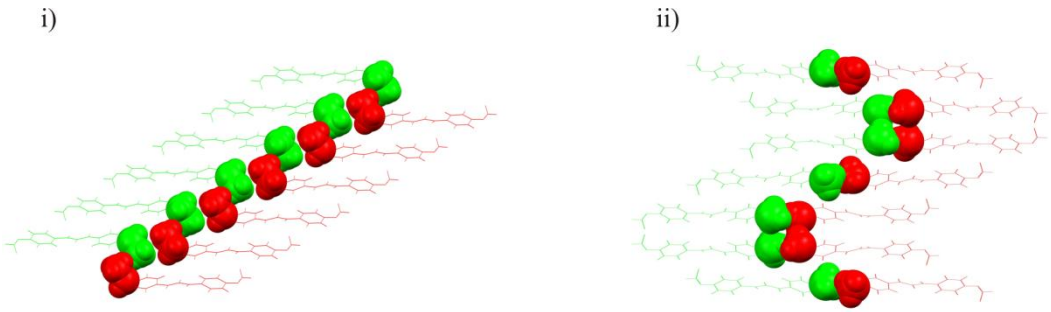

Figure 3-43: *Ethyl and methyl substituent packing in the i) MeO-C-Et and ii) MeO-C-Me structures respectively. The Et and Me substituents of each molecule are highlighted with spacefill representation whilst the remaining portion of the molecules is shown in wireframe; neighbouring molecules are colour coded red and green. The molecular structures are viewed parallel to the* ***t1****vector.*

The H-C-Me(1) structure is the only other structure of the A group that contains no 2-D SCs. The most complex SC displayed by this structure is the 1-D, SC A2 and it is unique amongst the A group of chalcone structures insofar as that in all the other structures, the constituent molecules are arranged in clearly defined sheet constructs with translation vectors aligned with the mid molecular axis and either the long, short, or both other molecular axes (N.B. these

arrangements may be unique to a structure and thus not necessarily defined as a SC). However, in the H-C-Me(1) structure, discrete instances of SC A2 double rows are arranged in an interlocking herringbone type arrangement (see Figure 3-32 above). Intriguingly, H-C-Me(1) is the most stable of the three para-methyl chalcone polymorphs, with the other metastable forms being regarded as 'disappearing polymorphs'[9]. However, it is these metastable forms that provide the more familiar structure types in terms of the SC A group.

As mentioned before, the primary SC A structure occurs in crystal structures as part of a more complex double-layer SC where instances of primary SC A are related by a glide (SC A1), an inversion (SC A2), a 2-fold axis (SC A3) or a 2_1 screw axis (SCs A4 and A5), the most common relationships being glides and inversions. In these double-layer SCs, the typical 'herringbone' edge-to-face packing of aromatic rings appears as the dominant packing motif with Ar C-H···centroid distances of 2.69-3.18Å across the range of structures exhibiting SCs A1 and A2. This packing is facilitated by the complementary shape of the chalcone in the short molecular axis as evidenced from the primary SC A tape.

All of the crystal structures of Br and Cl substituted chalcones, with the exceptions of Br-C-F, Cl-C-F and Cl-C-OMe(2) occur in the SC A group and it is amongst these structures where evidence of halogen···halogen interactions is likely to be found[15,16]. The halogen···halogen contacts found between Br and Cl substituted chalcones are given in table 3-4 below.

Structure	*Contact Atoms*	*θ_1 (°)*	*θ_2 (°)*	*Type*	*Distance (Å)*	*Distance- sum of VdW radii (Å)*
Br-C-Br	Br2…Br1	162.56	115.61	II	3.868	-0.01
Br-C-Cl	Cl1…Br1	161.07	114.37	II	3.7065	0.11
Br-C-H	Br1…Br11	139.46	134.94	I	3.8042	0.1
Cl-C-Br	Br1…Cl1	162.45	115.64	II	3.6227	0.02
Cl-C-Cl	Cl2…Cl1	161.49	114.53	II	3.6209	0.12
F-C-Br	Br11…Br1	163.06	96.52	II	3.8166	0.12
	Br11…Br1'	96.59	162.10	II	3.8519	0.15
	Br11…Br11	127.83	127.83	I	3.7746	0.07

Table 3-4: *Halogen···halogen contacts amongst the chalcones studied, θ_1 = C-contact atom 1···contact atom 2, θ_2 = C-contact atom 2···contact atom 1, Type = halogen interaction type, Distance = distance between contact atom centres.*

From the above results, it can be seen that there is only one halogen···halogen contact less than the sum of the VdW radii of the participating atoms and this occurs in the Br-C-Br structure and that none of the interactions is particularly strong, as evidenced by the atomic seperations. Br-C-Br, Br-C-Cl, Cl-C-Br and Cl-C-Cl are all members of the the isostructural '1+' group, which also includes F, Me, Et and OMe substituted chalcones providing further evidence for the lack of any strong structure-directing effect of these interactions. However, it is interesting to note that it is in the Br substituted chalcones where halogen···halogen interactions are expected to be strongest and as can be seen they occur in Br-C-H and F-C-Br in contrast to Cl-C-H and F-C-Cl, thus there is some indication that the stronger halogen···halogen interactions provide some structure-directing influence amongst this group of chalcones.

Further indirect evidence for halogen···halogen interactions may arise from investigation of chloro methyl exchange[17,18]. Thus in crystal structures where packing is dominated by dispersive and repulsive interactions, isostructural replacement of chloro by methyl groups may occur due to their similar molecular volumes (Cl -20Å^3, Me - 24 Å^3). Amongst the group of chalcones studied, nine chloro/methyl pairs of structures can be identified as shown in table 3-5 below.

Cl substituted chalcone	*Me substituted chalcone*	*Similarity*
Br-C-Cl	Br-C-Me	isostructural
Cl-C-Br	Me-C-Br	isostructural
Cl-C-Cl	Cl-C-Me	isostructural
H-C-Cl	H-C-Me (2)	SC A16
Cl-C-Me	Me-C-Me	SC A10
F-C-Cl	F-C-Me	SC A13
Cl-C-F	Me-C-F	none
Cl-C-OMe (1) & (2)	Me-C-OMe	none
Cl-C-H	Me-C-H	none

Table 3-5: *Similarity between chloro/methyl susbstituted chalcones; similarity is as defined by the XPac procedure and where an SC is given, this is the highest dimensionality SC common to both structures. H-C-Me(2) is the most similar of the H-C-Me polymorphs to H-C-Cl, both other H-C-Me polymorphs display primary SC A similarity with H-C-Cl.*

From the table above it can be seen that the pairs of structures split into three groups based on their similarity. The Br and Cl chloro substitiuted chalcones are isostructural with their methyl counterparts suggesting that the differing electronic properties of the Cl and Me substituents play no role in the formation of the crystal structures of these chalcones. Conversely, chloro methyl exchange in the alkene phenyl substituted F, OMe and H chalcones, leads to radically different crystal structures, suggesting alternative structure-forming interactions arising from the differences in the two substituents. Amongst the remaining structures, some common fragment is retained between the pairs. In all three cases these are 2D SCs involving Cl/Me substituents, thus whilst the different electronic properties of the chloro and methyl substituents are evidenced by the different crystal structures of the pairs, their effect appears less pervasive than amongst the alkene phenyl substituted F, OMe and H pairs of chalcones.

It is only amongst the SC A group of chalcones, where the few examples of halogen···O contacts occurring in the chalcones studied are found and these are shown in table 3-6 below.

Structure	*Contact Atoms*	*Distance (Å)*	*Distance- sum of VdW radii (Å)*
Br-C-OMe	Br1…O2	3.123	-0.25
	Br11…O102	3.116	-0.25
Cl-C-OMe(1)	Cl1…O2	3.084	-0.19
MeO-C-Br	Br1…O2	3.279	-0.09

Table 3-6: *Halogen···O contacts amongst the chalcones studied; Distance = distance between contact atom centres.*

In all three structures, halogen···O contacts occur between the halogen substituent and the etheric O of the methoxy substituent. As can be seen from the table above all of the contacts are less than the sum of the VdW radii of the participating atoms, suggesting relatively strong interactions. However, although the Br-C-OMe and MeO-C-Br structures are unique structures exhibited by these specific molecules, it is not clear that these differences can be directly attributed to the halogen···O interactions. Likewise, Cl-C-OMe(1) belongs to the isostructural 1+ group and the other 10 isostructures do not exhibit this interaction, suggesting it is of minor importance amongst the structure-forming interactions for this group of chalcones.

Overall, the primary SC A structure is clearly robust, being displayed across a large majority of the chalcone structures studied and it may be efficiently packed in a variety of ways as is also evidenced by the large number of secondary SCs based on this SC. Although there is some evidence for weak directional interactions, the results are not clear and it is the absence of strong directing interactions which means that dispersion and repulsion interactions dominate the drive for efficient packing in these structures.

Structures Containing SCs B and E

As can be seen from the chalcone structure relationship diagram (Figure 3-1), the SCs B and E are displayed by 6/50 chalcone crystal structures studied, including the three member isostructural group of '17+' (Et-C-F, Me-C-F, Me-C-OMe) along with three other distinct structures (Et-C-OMe, F-C-F and H-C-H(2)). This group of structures forms a separate, distinct group with no links to other structures or SCs and it encompasses three SCs: two primary SCs, B and E and a secondary SC, B1.

The primary SC B is the only 0-D SC found persistently amongst the chalcone structures studied. Although identified as a 'trimer', a more rigorous description of this SC is as a 'three-molecule fragment' insofar as although there are numerous short contacts amongst its components in most the structures in which it occurs, no common intermolecular bonding pattern is apparent. Also, although identified by the XPac procedure as 0-D because it is a discrete rather than continuous SC, in all of the structures that it is displayed, it occurs as a repeating motif along a single dimension. The component molecules of primary SC B are related by a (pseudo-) 2_1 screw, although in the F-C-F structure, the three components comprise two crystallographically independent molecules and a glide relates two of the components derived from one of these independent molecules, thus the 2_1 screw is approximate. This is the only SC displayed in the F-C-F structure and it is the common fragment of the 1-D SC B1 that occurs in this structure and links it to the structures displaying SC B1.

SC B1 is the only secondary SC of the B group; it is a 1-D 'corrugated' row of molecules related by a 2_1 screw axis parallel to the mid-molecular axis

and is displayed in four structures, Et-C-F, Me-C-F and Me-C-OMe of the isostructural '17+' group and H-C-H(2). In both of these structures SC B1 rows of molecules are related by glides to form 2-D layers which in turn are related by translation to form the '17+' structure type whereas in the H-C-H(2) structure, the layers are related by a glide. On first inspection, the 2-D layers within each structure type appear very similar however, close examination reveals subtle differences. When these layers are viewed parallel to the ***t6*** translation vector of SC B1 it can be seen that in the Me-C-F structure, the carbonyl groups of the molecules of a SC B1 row align with the phenyl rings at the carbonyl end of molecules of adjacent, inverted instances of SC B1, whilst in the H-C-H(2) structure they are aligned with the phenyl rings at the alkene end of the molecule. Thus, while SC B1 rows form 'skewed' (with respect to the short molecular axis) layers with aromatic C-H···O interactions between adjacent rows in both structure types, the interactions between the carbonyl oxygen atoms and the rings at the carbonyl end of the molecules in the '17+' structure type result in a layer with far more pronounced 'peaks' and 'troughs' when compared to the corresponding layer of the H-C-H(2) structure where the interactions are between the carbonyl oxygen atoms and rings at the alkene end of the molecules. These peaks and troughs of the layers allow efficient packing of the ring substituents of the '17+' group of structures, whereas this is not a consideration in the H-C-H(2) structure where no bulky substituents need to be accommodated. Figure 3-44 below illustrates these points.

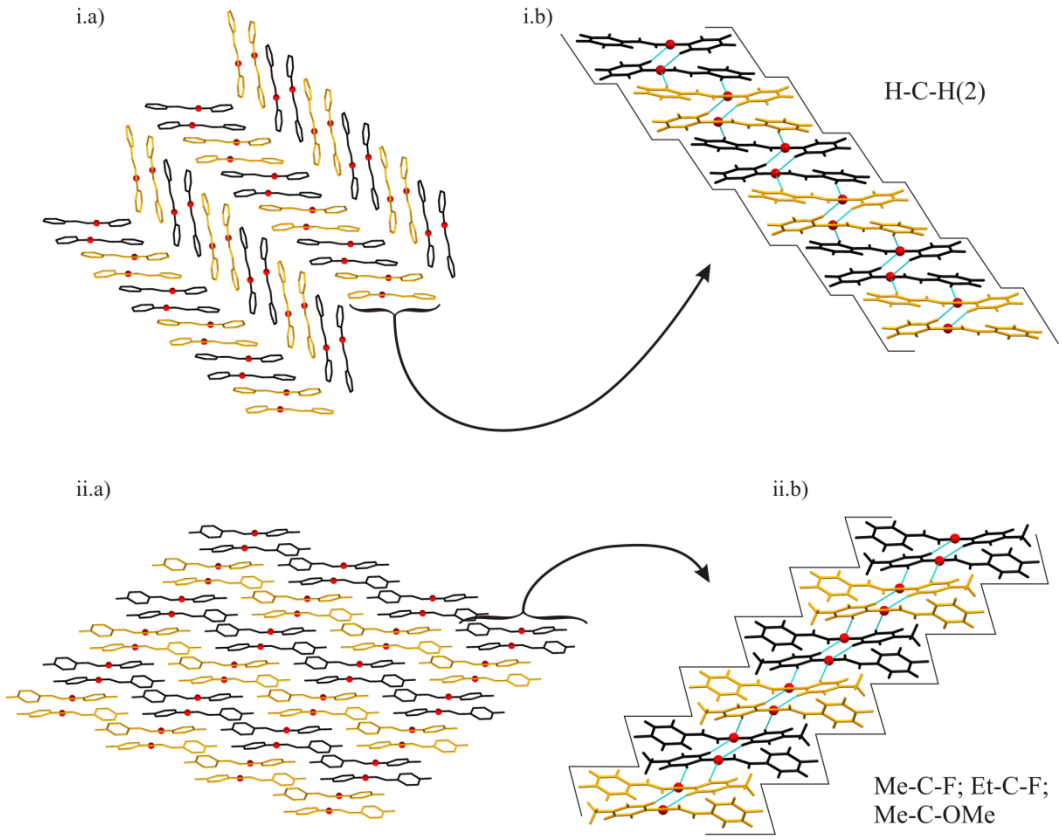

Structure	*Contact 1*	*Contact 2*	*Symmop 2*	*# contacts*	*length (Å)*	*length - VdW radii (Å)*
H-C-H(2)	O1	H2	1-x,1-y,-z	2	2.275	-0.445
	O1	H5	1/2+x,1/2-y,-z	1	2.596	-0.124
	H5	O1	-1/2+x,1/2-y,-z	1	2.596	-0.124
Me-C-F	O1	H9	-x,1-y,1-z	2	2.500	-0.220
	O1	H5	-x,1/2+y,-1/2-z	1	2.681	-0.039
	H5	O1	-x,-1/2+y,-1/2-z	1	2.681	-0.039
Et-C-F	O1	H9	1-x,-y,1-z	2	2.517	-0.203
	O1	H5	1/2-x,-1/2+y,1/2-z	1	2.611	-0.109
	H5	O1	1/2-x,1/2+y,1/2-z	1	2.611	-0.109
Me-C-OMe	O1	H9	-x,2-y,-z	2	2.525	-0.195
	O1	H5	-x,1/2+y,1/2-z	1	2.609	-0.111
	H5	O1	-x,-1/2+y,1/2-z	1	2.609	-0.111

N.B. Symmop 1 is x,y,z in all cases

Figure 3-44: *SC B1 relationships; the colour scheme is the same as used to illustrate the 'A' relationships; each pair of same-coloured molecules represents an instance of SC B1 viewed parallel to the* ***t6*** *vector. i.a) H-C-H(2) crystal structure, i.b) individual layer of H-C-H(2) structure, ii.a) '17+' isostructural group crystal structure (Me-C-F shown), ii.b) individual layer of '17+' isostructural group structure (Me-C-F). In both the layer diagrams H-atoms are shown and C-H…O contacts are shown in blue and also detailed in the table. The boundary lines to each layer highlight the shape differences between the two structure types.*

It can be clearly seen that the two different layer arrangements of these structures are each of two alternative arrangements that allow the aromatic C-H···O interactions present in SC B1 rows to be maintained between the pairs of SC B1, related by inversion, that make up the layer in each structure. Thus each of these different layers represents an alternative aromatic C-H···O network; in the '17+' isostructural group, only the ring proximal to the carbonyl group is involved in these interactions whereas, in the H-C-H(2) structure both rings of the chalcone molecules are involved in the aromatic C-H···O interactions. This is illustrated in Figure 3-45 below.

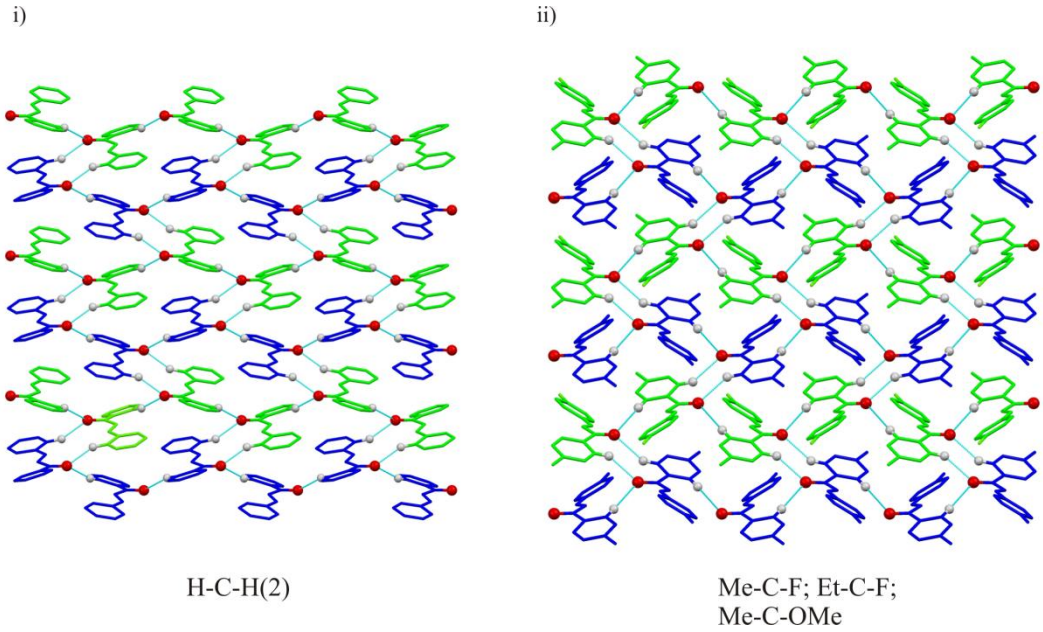

Figure 3-45: *Layer C-H···O networks of, i) H-C-H(2) structure, ii) '17+' isostructural group structure (Me-C-F shown). Both structures are viewed perpendicular to the* ***t6*** *vector of SC B1 (different instances of which are shown in blue and green), so as to provide the clearest view of the network in each structure. Hydrogen atoms except those involved in C-H···O interactions are omitted for clarity. All contact atoms are highlighted by ball and stick representation. In the H-C-H(2) structure both rings of the molecule are involved in the C-H···O interactions, whereas in the structures of the '17+' isostructural group it is only the rings adjacent to the carbonyl atoms that are involved.*

The SC E group comprises a single SC, primary SC E, which is displayed in two structure types, that of the isostructural group '17+' and the Et-C-OMe structure. Primary SC E is not related to any of B group SCs insofar as that it based on a translation vector aligned between the long and short molecular axis of the chalcone molecule, whilst that of SC B1 is aligned along the mid

molecular axis. However as the only other SC displayed by structures displaying SC E is SC B1, this is the most useful place to discuss this relationship.

Primary SC E is a 1-D close-packed row of molecules related by translation. In both the structure types in which it occurs, repeating instances of this SC, related by glides form close-packed layers within the structures. In the isostructural group '17+', these layers are perpendicular to the layers of SC B1 rows discussed above. The layers of both structure types appear very similar, although when viewed parallel to the glide planes relating the repeating instances of SC E the differences are apparent. The difference in position of instances of SC E with respect to the glide plane in the layer of the '17+' isostructural group compared with that of the Et-C-OMe structure results in a different layer structure in each of the structure types. These points are illustrated in Figure 3-46 below.

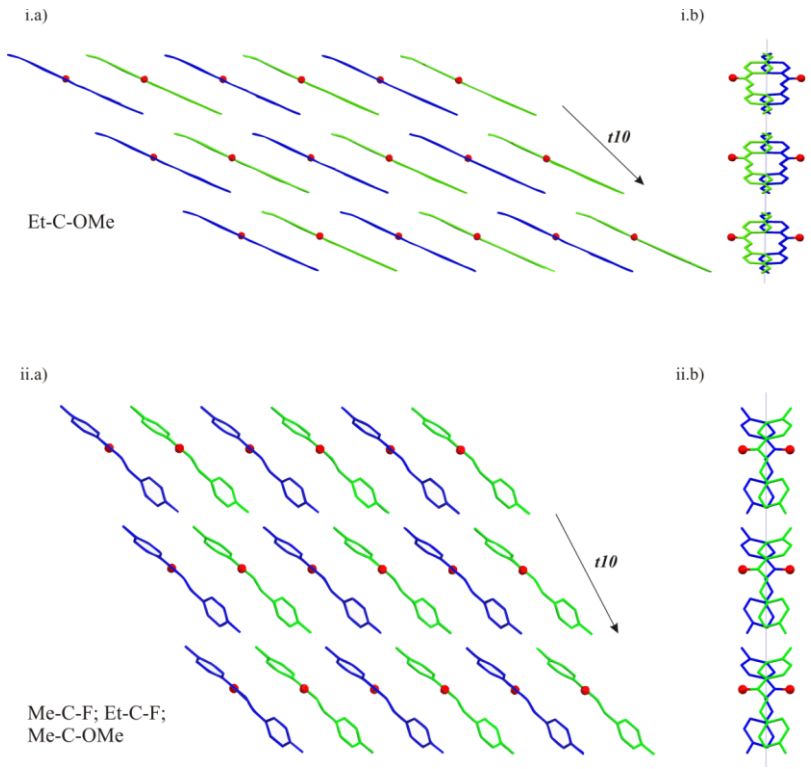

Figure 3-46: *SC E relationship; i.a) Et-C-OMe structure; ii.a) '17+' isostructural group structure (Me-C-F shown). Both structures are viewed perpendicular to the* ***t10*** *vector of SC E as shown and adjacent instances of SC E, related by glides in both structures, are shown coloured green and blue. i.b) Et-C-OMe structure; ii.b) '17+' isostructural group structure (Me-C-F shown); both structures are viewed along the horizontal rows in i.a) and ii.a) and the differences in position of SC E with respect to the glide plane (indicated by a light grey line in i.b) and ii.b)) in each structure can be clearly seen.*

Structures Containing SCs C and D

As can be seen from the chalcone structure relationship diagram (Figure 3-1), the SCs C and D are displayed by 7/50 chalcone crystal structures studied, including the two member isostructural group of '4+' (Br-C-F, Cl-C-F) along with five other distinct structures (Cl-C-OMe(2), F-C-OMe, H-C-OMe, Me-C-H and MeO-C-OMe). This group of structures forms a distinct group displaying no other primary SCs and it encompasses five SCs: two primary SCs, C and D and three secondary SCs, C/D1, D2 and D3. A further group of five structures, namely those displaying SC A19, also display primary SC D and these will also be discussed.

Primary SC C is a 1-D 'corrugated' row of molecules related by a 2_1 screw axis parallel to the mid-molecular axis. Although the molecular arrangement of this SC is similar to SC B1, the difference in position of the molecules with respect to the 2_1 screw axes in each of these SCs results in two distinct arrangements. Thus in SC B1 the carbonyl groups of the chalcone align and participate in C-H···O interactions with the rings of neighbouring molecules, whereas in primary SC C the molecules of the sub-layers are shifted with respect to each other such that the carbonyl groups are aligned with the ring substituents of neighbouring molecules within the crystal structure. It should also be noted that the carbonyl groups of molecules in SC B1 align parallel in each sub-layer of the SC with the ***t6*** translation vector of the SC whereas in SC C the carbonyl groups of the molecules are pointing away from the ***t7*** translation vector. Primary SC C is displayed in four structures: F-C-OMe, H-C-OMe, Me-C-H and MeO-C-OMe. Of these, the Me-C-H structure is the only one that displays solely this SC, whereas, notably, the structures of the methoxy substituted chalcones all display at least one other 2-D SC based on primary SCs C and D. Also, because these methoxy substituted chalcones all crystallise in chiral space groups, two forms of SC C are exhibited by this group of structures.

As is the case with the SC B1 structures, all of the SC C structures contain C-H···O short contact interactions and in each of these structures these interactions occur between neighbouring instances of the SC. In the Me-C-H structure, neighbouring instances of primary SC C, related by a 2 rotation, are involved in mutual aromatic C-H···O interactions between the carbonyl oxygen

atoms and rings at the alkene ends of the chalcone molecules to form stacked rows. In the Me-C-H structure the stacked rows close pack with neighbouring, inverted instances of themselves, between which there are no significant short contact atoms, to yield the crystal structure. The methoxy substituted chalcone structures exhibiting SC C also display a similar reciprocal C-H···O interaction arrangement as Me-C-H, although in the case of these structures the interaction occurs between the carbonyl oxygen atom and the methyl group of the methoxy substituent. This arrangement is common to all the methoxy substituted structures and is discussed more fully later. The preceding points are illustrated in Figure 3-47 below.

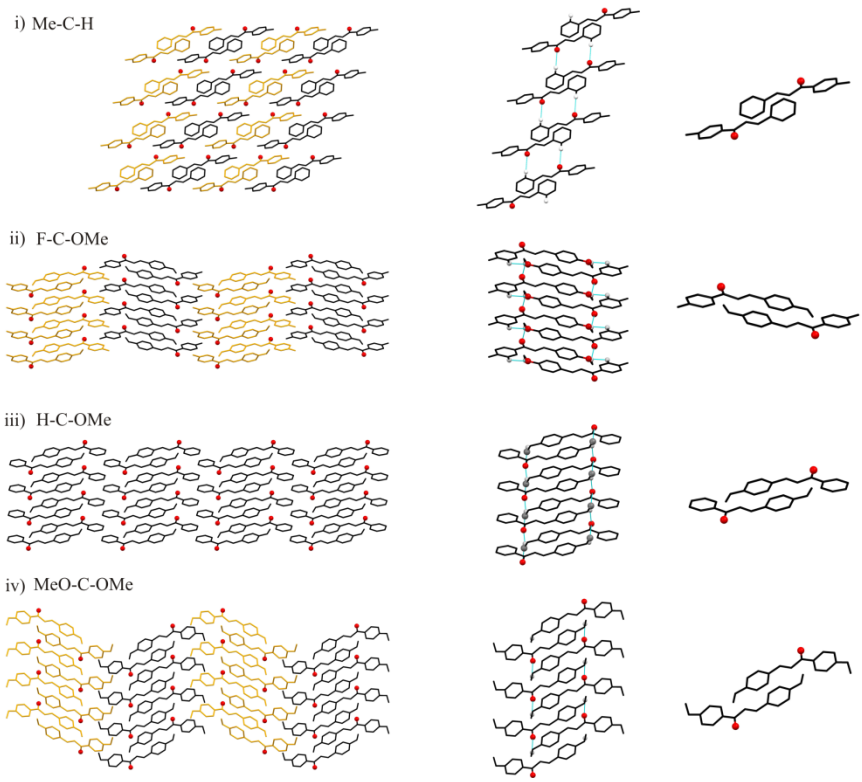

Structure	*Contact 1*	*Contact 2*	*Symmop 2*	*# contacts*	*length (Å)*	*length - VdW radii (Å)*
Me-C-H	O1	H11	1-x,y,3/2-z	2	2.483	-0.237
Me-C-F	O1	H16C	1-x,-1/2+y,-1/2-z	1	2.563	-0.157
	H16C	O1	1-x,1/2+y,-1/2-z	1	2.563	-0.157
	O2	H6	-x,-1/2+y,-1/2-z	1	2.655	-0.065
	H6	O1	-x,1/2+y,-1/2-z	1	2.655	-0.065
H-C-OMe	O1	H16A	1-x,-1/2+y,2-z	1	2.486	-0.234
	H16A	O1	1-x,1/2+y,2-z	1	2.486	-0.234
MeO-C-OMe	O1	H17A	-1-x,-1/2+y,1/2-z	1	2.556	-0.164
	H17A	O1	-1-x,1/2+y,1/2-z	1	2.556	-0.164

N.B. Symmop 1 is x,y,z in all cases

Figure 3-47: *Primary SC C structures. Three views are given for each structure, left is the crystal structure with differing orientations colour coded as previously, middle shows the C-H···O interactions between neighbouring instances of SC C , with contact atoms highlighted and these are detailed in the table below, right is SC C in each structure. All views are parallel to the* ***t7*** *translation vector of SC C so that each pair of molecules represents an instance of SC C. Note the opposite conformation of SC C and the resulting assembly of F-C-OMe and also that both conformations exist in Me-C-H. It can be seen that the three assemblies of the methoxy substituted structures are SC C1/D1 and are discussed more fully below.*

Primary SC D is a 1-D stack of molecules related by translation parallel to the short-molecular axis. It is displayed in six structures; the 2 member isostructural '4+' group (Br-C-F, Cl-C-F), Cl-C-OMe(2), F-C-OMe, H-C-OMe and MeO-C-OMe and in these structures the phenyl rings of the neighbouring

molecules within the SC align parallel to each other. The XPac procedure also identifies the five structures displaying SC A19 as displaying primary SC D, however in these structures the rings of the neighbouring chalcone molecules adopt a staggered conformation as shown in Figure 3-48 below. The difference in ring conformation between instances of primary SC D in the two groups of structures results in an elongation of the ***t8*** translation vector of SC D to accommodate this. Whilst no significant short contact interactions are observed between molecules of primary SC D in either of the groups of structures, the structures displaying secondary SCs based on primary SC D do exhibit short contact C-H···O interactions between instances of SC D whereas these are not present in the SC A19 group of structures. The geometry and molecular arrangement of SC A19 necessarily includes the SC D geometrical arrangement of molecules and from this and the previous points it is believed that the primary SC D arrangement arises independently in these two sets of structures and thus no significance should be attached to this result.

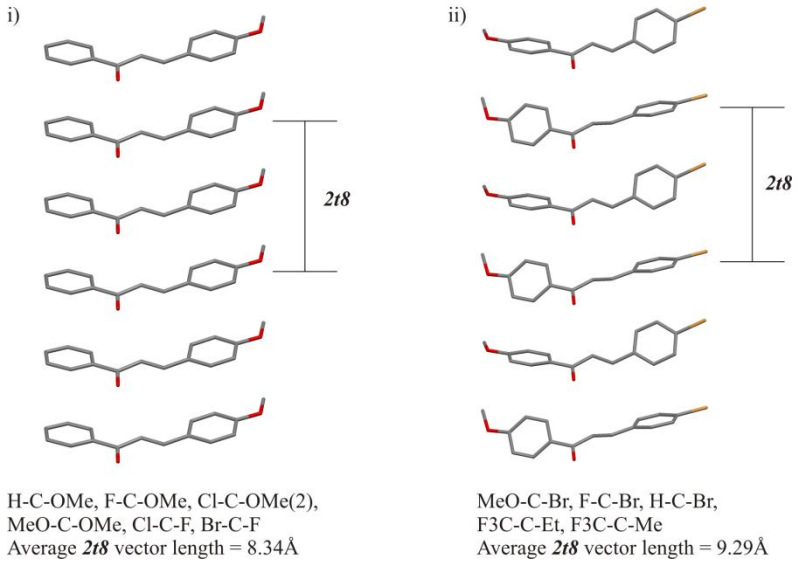

Figure 3-48: *Comparison of primary SC D between i) structures exhibiting secondary SCs based on primary SC D (H-C-OMe shown) and ii) structures exhibiting SC A19 (MeO-C-Br shown). The structures are viewed perpendicular to the* ***t8*** *translation vector and H atoms are omitted for clarity. The differing conformations of the molecules in each example of SC D can be clearly seen and the average* ***2t8*** *vector lengths are given for each of the structure types.*

As with primary SC A, there are no direct links between SC D and any crystal structures, all links are via secondary SCs. Aside from SC A19 which has

already been discussed, there are three secondary SCs based on Primary SC D as can be seen in the chalcone structure relationship diagram (Figure 3-1).

SC C1/D1 is a direct combination of primary SCs C and D with the translation vectors of each of the primary SCs, ***t7*** and ***t8*** respectively, running approximately perpendicular to each other in the structures in which this SC occurs. It is displayed in three structures, F-C-OMe, H-C-OMe, and MeO-COMe, all of which comprise chalcone molecules with methoxy substituted phenyl rings at the alkene end of the molecule. This SC is a 2-D sheet construct which may equally be viewed as stacked SC C rows as is shown in Figure 3-47 above or as rows of SC D stacks as shown in Figure 3-49 below. In the H-C-OMe structure instances of SC C1/D1 are related by translation whereas in the F-C-OMe and MeO-C-OMe structures they are related by 2_1 screw axes. It can be seen that aside from opposite molecular conformations, the F-C-OMe and MeO-C-OMe structures are very similar with both structures crystallising in $P2_12_12_1$, however the clearest differences between the two structures are revealed when viewed parallel to the ***t7*** vector as in Figure 3-47 where the different orientation of the molecules in each structure is apparent. As with primary SC C, none of the structures display significant short contact interactions between the constituent molecules of primary SC D, however all display C-H···O interactions between the carbonyl O atom and the methyl group of the methoxy substituents between neighbouring instances of primary SC D within SC C1/D1. Additionally, whilst no significant short contact interactions are observed between neighbouring instances of SC C1/D1 in the H-C-OMe structure, the substituents of F-C-OMe and MeO-C-OMe are involved in short contact interactions with molecules of neighbouring instances of SC C1/D1. Although these contacts, as with those of all the chalcones studied, are weak interactions and this along with the lack of a discernable similarity between them in each of the structures precludes these interactions from being 'structure directing' and it is assumed that they contribute towards the stabilizing interactions of each structure.

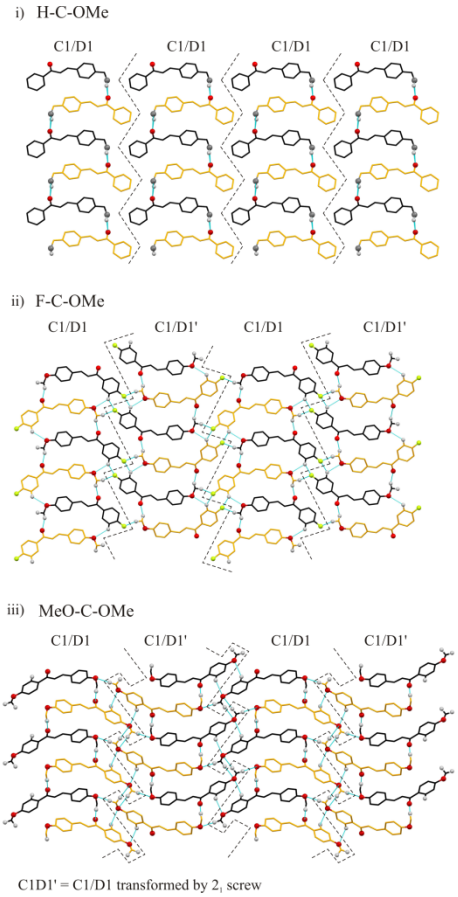

	Contact 1	*Contact 2*	*Symmop 2*	*# contacts*	*length (Å)*	*length - VdW radii (Å)*
H-C-OMe	O1	H16A	1-x,-1/2+y,2-z	1	2.486	-0.234
	H16A	O1	1-x,1/2+y,2-z	1	2.486	-0.234
F-C-OMe	O1	H16C	1-x,-1/2+y,-1/2-z	1	2.563	-0.157
	H16C	O1	1-x,1/2+y,-1/2-z	1	2.563	-0.157
	F1	H6	1/2+x,3/2-y,-z	1	2.553	-0.117
	H6	F1	-1/2+x,3/2-y,-z	1	2.553	-0.117
	F1	H16B	-1/2-x,1-y,1/2+z	1	2.576	-0.094
	H16B	F1	-1/2-x,1-y,-1/2+z	1	2.576	-0.094
	O2	H6	-x,-1/2+y,-1/2-z	1	2.655	-0.065
	H6	O2	-x,1/2+y,-1/2-z	1	2.655	-0.065
MeO-C-OMe	O1	H17A	-1-x,-1/2+y,1/2-z	1	2.556	-0.164
	H17A	O1	-1-x,1/2+y,1/2-z	1	2.556	-0.164
	O3	H16B	-1/2-x,2-y,-1/2+z	1	2.573	-0.147
	H16B	O3	-1/2-x,2-y,1/2+z	1	2.573	-0.147
	O2	H16C	-1/2+x, 5/2+x,1-z	1	2.678	-0.042
	H16C	O1	1/2+x, 5/2+x,1-z	1	2.678	-0.042
	O2	H9	1/2+x,3/2-y,1-z	1	2.708	-0.012
	H9	O2	-1/2+x,3/2-y,1-z	1	2.708	-0.012

N.B. Symmop 1 is x,y,z in all cases

Figure 3-49: *SC C1/D1structures, i) H-C-OMe, ii) F-C-OMe, iii) MeO-C-OMe. All views are parallel to the* ***t8*** *translation vector and each molecule represents a primary SC D stack. Different orientations of the carbonyl groups of SC D with respect to the plane of the page are indicated using the same colour scheme as previously and instances of SC C1/D1 are labelled and bounded with dashed lines. Short C-H···O and C-H···F interactions are indicated with blue lines and the contact atoms are highlighted in ball and stick representation and shown in standard element colours. Only H atoms involved in short contact interactions are shown. The interactions are detailed in the adjoining table.*

SCs D2 and D3 are related to one another such that SC D3 is a subset of SC D2 (D3 → D2). SC D2 is a 2-D single layer sheet structure comprising primary SC D stacks related by translation and is defined by translations vectors ***t8*** and ***t9***, whereas SC D3 is a 2-D double layer sheet defined by the same two translation vectors and comprising two SC D2 sheets related by a glide running parallel to the ***t9*** vector. Four structures display SC D2; H-C-OMe, Cl-C-OMe(2) and the isostructural group '4+' (Br-C-F, Cl-C-F) and of these, the isostructural '4+' group and Cl-C-OMe(2) also display SC D3. Comparing the SC D2 structure of H-C-OMe, with that of the other structures also displaying

this SC, it can be seen that there are no significant short contact interactions between neighbouring primary SC D stacks within SC D2 in the H-C-OMe structure. However, in the isostructural '4+' group and the Cl-C-OMe(2) structures, aromatic C-H···F and aromatic C-H···O interactions are displayed between the neighbouring constituent SC D stacks in SC D2 and as expected, the ***t9*** translation vector in these structures is significantly shorter (13.37-13.51 Å) than in the H-C-OMe structure (15.12 Å). In the H-C-OMe structure, neighbouring instances of SC D2 are related by a 2_1 screw to give SC C1/D1 rows and as discussed previously, C-H···O interactions occur between primary SC D stacks in this direction.

As mentioned above SC D3 is displayed by the isostructural '4+'pair and the Cl-C-OMe(2) structure. The isostructural '4+'pair of Br-C-F and Cl-C-F are noteworthy in that unlike previously discussed isostructural groups, these structures exhibit virtually identical C-H···Hal and C-H···O interactions, which result in 2-D network structures of 'corrugated' sheets which form close-packed layers to result in the crystal structures as shown in Figure 3-50 below.

Br-C-F Cl-C-F

	Contact 1	*Contact 2*	*Symmop 2*	*# contacts*	*length (Å)*	*length - VdW radii (Å)*
Br-C-F	O1	H11	-1-x,1-y,2-z	2	2.477	-0.243
	O1	H3	-1-x,1-y,2-z	2	2.651	-0.069
	F1	H8	1+x,y,1+z	1	2.607	-0.063
	H8	F1	-1+x,y,-1+z	1	2.607	-0.063
	Br1	H5	-1/2+x,1/2-y,-1/2+z	1	2.997	-0.053
	H5	Br1	1/2+x,1/2-y,1/2+z	1	2.997	-0.053
Cl-C-F	O1	H11	2-x,1-y,-z	2	2.467	-0.253
	F1	H8	-1+x,y,-1+z	1	2.602	-0.068
	H8	F1	1+x,y,1+z	1	2.602	-0.068
	O1	H3	2-x,1-y,-z	2	2.695	-0.025
	Cl1	H5	1/2+x,1/2-y,1/2+z	1	2.949	-0.001
	H5	Cl1	-1/2+x,1/2-y,-1/2+z	1	2.949	-0.001

Figure 3-50: *'4+' isostructural pair, Br-C-F and Cl-C-F, both viewed parallel to the -1 0 1 plane. C-H···O and C-H···Hal interactions are shown in blue and detailed in the table; it can be seen that these occur only between neighbouring molecules in a single layer, with no significant short contact interactions between layers.*

The common short contact C-H···Hal and C-H···O interactions between these two structures, suggests that although weak, these interactions may have some structure-directing role in these structures.

In the structures of the isostructural '4+' group, the two SC D2 layers comprising SC D3 exhibit C-H···Hal interactions between neighbouring molecules and adjacent instances of SC D3 are related by inversions with reciprocal bifurcated C-H···O interactions between the carbonyl O atoms and H atoms of the F substituted ring and the chalcone linker alkene of neighbouring molecules. As described, above these interactions form 2-D layers with no significant inter-sheet short contact interactions. On first inspection, when viewed parallel to the ***t8*** translation vector, as in Figure 3-51 below, the C-H···Cl and C-H···O short contact interactions between the constituent SC D2 layers of SC D3 of the Cl-C-OMe(2) structure appear very similar to those observed in the

isostructural '4+' group, with C-H···O interactions in the Cl-C-OMe(2) structure replacing C-H···F interactions in the isostructural '4+' group. However, whilst the C-H···Cl short contact interactions between neighbouring molecules lead to 2-D layers in both structures, the C-H···F interactions in the isostructural '4+' group occur between molecules of the same 2-D layer as those of C-H···Cl interactions, whilst the C-H···O interactions in the Cl-C-OMe(2) structure occur between the layers above and below. Thus, SC D3 in the Cl-C-OMe(2) structure displays a 3-D network of significant short contact interactions as opposed to the 2-D layer structure of the isostructural '4+' group, but despite these differences, the same SC occurs in both structures. In the Cl-C-OMe(2), neighbouring instances of SC D3 are related by 2_1 screw axes parallel to the ***t8*** translation vector and C-H···O short contact interactions are observed, leading to a helical network of interactions between neighbouring primary SC D stacks in adjacent SC D3 occurrences. The preceding points are illustrated in Figure 3-51 below.

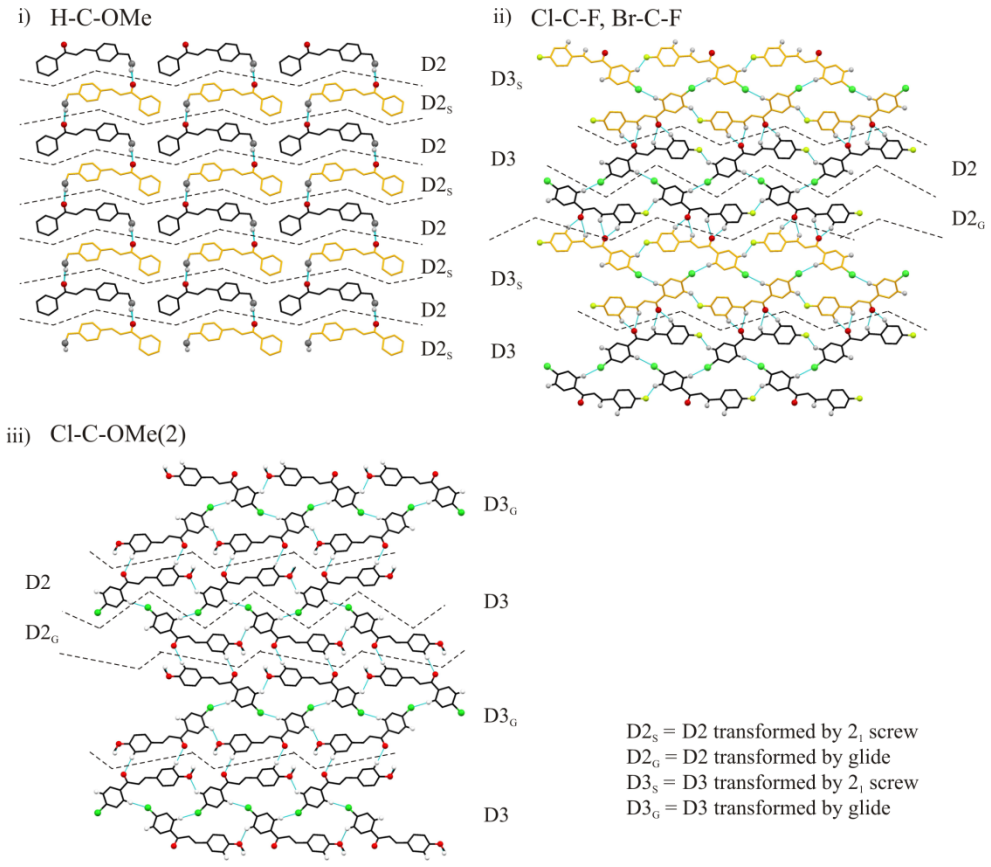

	Contact 1	*Contact 2*	*Symmop 2*	*# contacts*	*length (Å)*	*length - VdW radii (Å)*
Cl-C-OMe(2)	O1	H12	1-x,-y,1/2-z	1	2.536	-0.184
	H12	O1	1-x,-y,-1/2-z	1	2.536	-0.184
	Cl1	H5	-1/2+x,1/2-y,z	1	2.919	-0.031
	H5	Cl1	1/2+x,1/2-y,z	1	2.919	-0.031
	O2	H16B	x,y,1+z	1	2.706	-0.014
	H16B	O2	x,y,-1+z	1	2.706	-0.014
	O2	H8	1+x,y,-1+z	1	2.707	-0.013
	H8	O2	-1+x,y,-1+z	1	2.707	-0.013

Figure 3-51: *SC D2 and SC D3 structures of, i) H-C-OMe, ii)'4+' isostructural group (Cl-C-F shown) and iii) Cl-C-OMe(2). All views are parallel to the* ***t8*** *translation vector and each molecule represents a primary SC D stack. Different orientations of the carbonyl groups of SC D with respect to the plane of the page are indicated using the same colour scheme as previously and instances of SCs D2 and D3 are labelled and bounded with dashed lines. Short C-H···O and C-H···Hal interactions are indicated with blue lines and the contact atoms are highlighted in ball and stick representation and shown in standard element colours. Only H atoms involved in short contact interactions are shown. Cl-C_OMe(2) interactions are detailed in the table, values for H-C-OMe and the '4+' isostructural group are given previously in Figures 3-49 and 3-50 respectively.*

SCs and Chalcone Substitutions

Whilst no obvious correlation has emerged from this work with regards to SCs displayed by the structures of the differently substituted chalcones studied, some trends can be observed as can be seen from Figure 3-52 below. In this figure the headings of the rows are given by the substituted species on the phenyl ring at the carbonyl end, whilst the column headings are given by the substituted species on the phenyl ring at the alkene end as indicated. The substituents are ordered in decreasing electron-withdrawing power as recorded by the Hammett sigma value[19]. Each coloured circle represents a crystal structure and thus structures which gave more than one polymorphic form have more than one circle e.g. H-C-Me has three circles representing the three polymorphic forms of this structure studied. The circles are coloured as to which primary SC or combination of SCs are displayed by the structure as shown in the key. The numbers within the circles represent the 7 isostructural groups found amongst the chalcones studied numbered as in Figure 3-1. Combinations of substituents with no circles are the substituted chalcones for which no crystal structures were obtained.

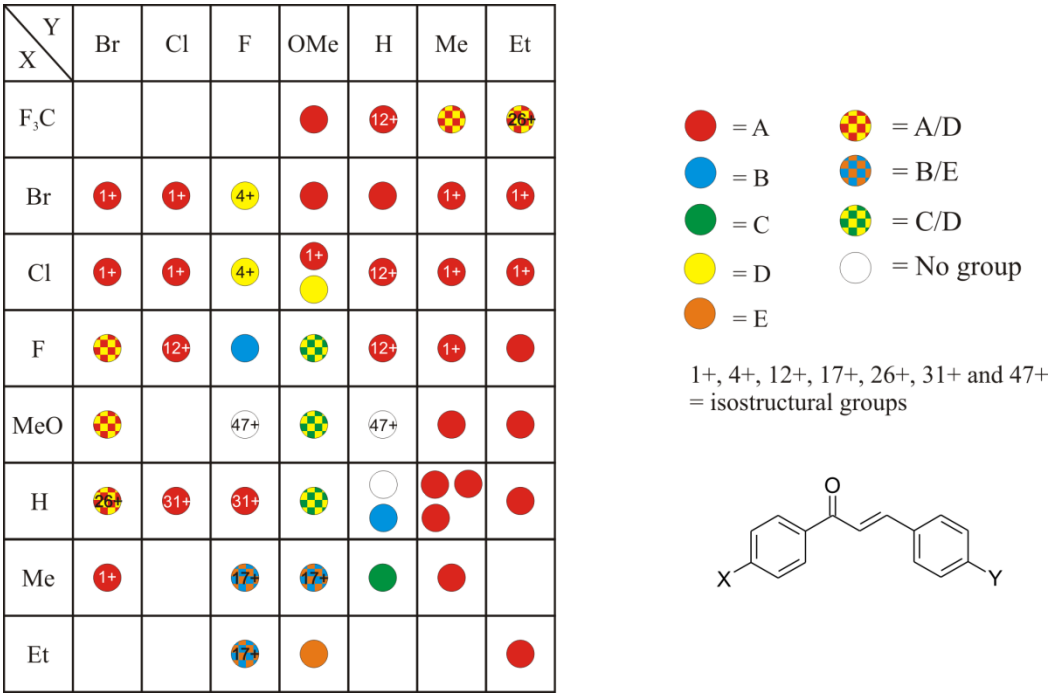

Figure 3-52: *Matrix showing primary SCs displayed by chalcones studied according to substituents.*

From the table above several results are evident. As is readily apparent from the chalcone structure relationship diagram (Figure 3-1), it can be seen that primary SC A is the most prevalent of the primary SCs amongst the chalcones. However more subtle trends are also in evidence. From the results above, it appears that the substitution of the phenyl ring at the alkene end of the chalcone molecule (Y substitution) is more influential in directing the crystal structure towards a particular SC than that of the ring at the carbonyl end (X substitution). Specifically all of the SCs derived from primary SCs B, C, D and E are displayed only in structures with Y = F, H and OMe (the occurrence of SC D with SC A has been discussed previously). Conversely, all the chalcone molecules studied with Y = Br, Cl, Me and Et display packing arrangements based on primary SC A. Whilst, gaps in the data from crystal structures that were unable to be obtained suggest caution in treating this result as more than a generalisation, it appears clear that the substitution of the phenyl ring at the alkene end of the chalcone molecule has a more profound effect on the crystal structure than that at the phenyl ring at the carbonyl end. The reasons as to why this is so are unclear and further work to investigate this effect is required.

Beyond what is mentioned above it is difficult to draw further generalisations between the substitution patterns and crystal structures of the chalcones. It can be seen that the majority of structures displaying SCs C and D have Y = OMe substitution, although Me-C-H and the isostructural '4+' pair of Br-C-F and Cl-C-F also display SCs C and D respectively. Likewise the isostructural '17+' group of Me-C-F, Me-C-OMe and Et-C-F along with Et-C-OMe display SC E although the '17+' group also display SC B along with H-C-H(2) and F-C-F.

Amongst the isostructural groups the trends are clearer but nonetheless exceptions occur. Thus the members of isostructural group '1+' are generally those chalcones with medium to large X and Y substituents, although F-C-Me is the exception. Also noteworthy amongst these structures is the number of X = Br and Cl substituted chalcones, which account for 9/11 species displaying this crystal structure. Many of the other isostructural groups consist of the crystal structures of species that share a common X or Y substituent and it is assumed that these are instrumental in the adoption of a common crystal structure within these groups. An exception to the above is isostructural group '26+' comprising

the H-C-Br and F_3C-C-Et structures and it suggests that for these structures, the substituent properties must play a minor role in the formation of the crystal structures.

[1]D. Rabinovich, G. M. J. Schmidt and Z. Shaked, *J. Chem. Soc., Perkin Trans.*, 1973, 2, 33-37. CSD Code BRCHAL

[2] F. Toda, K. Tanaka, M. Kato, *J. Chem. Soc., Perkin Trans.*, 1998, 1, 1315. CSD Codes PUQSOJ (Cl-C-H) and PUQSUP (Me-C-H)

[3] W. T. A. Harrison, H. S. Yathirajan, B. K. Sarojini, B. Narayana and J. Indira, *Acta Cryst*., 2006, **E62**, o1647-o1649. CSD Code MEGYON01

[4] Z. Li, F. Pa and G. Su, *Acta Cryst*., 1992, **C48**, 712-714. CSD Code TARCIY

[5] Z. Li and G. Su, *Acta Cryst*., 1994, **C50**, 126-127. CSD Code LEBGUU

[6] D. Rabinovich, *J. Chem. Soc. B*, 1970, 11-16. CSD Code BZYACO

[7] K. Ohkura, S. Kashino, M. Haisa, *Bull.Chem.Soc.Jpn*., 1973, **46**, 627. CSD Code BZYACO01

[8] E. M. Treadwell, *Acta Cryst*., 2006, **E62**, o5899-o5900. CSD Code CERYAA

[9] I. Barsky, J. Bernstein, P. W. Stephens, K. H. Stone, E. Cheung, M. B. Hickey and J.-O. Henck, *Cryst. Growth & Des*., 2008, **8**, 63-70. CSD Codes CERYAA03 (H-C-Me(2)) and CERYAA01 (H-C-Me(3))

[10] D. Rabinovich and Z. Shakked, *Acta Cryst*., 1974, **B30**, 2829. CSD Code DMCHAL

[11] Z. Li, L. Huang, G. Su, H. Wang, *Jiegou Huaxue (Chin.J.Struct.Chem.)*, 1992, **11**, 1. CSD Code KORROY

[12] Z. Li, L. Huang, G. Su, *Acta Cryst*., 1992, **C48**, 751. CSD Code KOTSER

[13] S. Skiena, "Hasse Diagrams" §5.4.2 in *Implementing Discrete Mathematics: Combinatorics and Graph Theory with Mathematica*, Addison-Wesley, Reading, MA, p. 163, 160-170 and 206-208, 1990.

[14] C. F. Macrae, P. R. Edgington, P. McCabe, E. Pidcock, G. P. Shields, R. Taylor, M. Towler and J. van de Streek, *J. Appl. Cryst.*, 2006, **39**, 453-457.

[15] G. R. Desiraju and R. Parthasarathy, *J. Am. Chem. Soc.*, 1989, **111**, 8725-8726.

[16] F. F. Awwadi, R. D. Willett, K. A. Peterson and B. Twamley, *Chem. Eur. J.* 2006, **12**, 8952-8960.

[17] G. R. Desiraju and J. A. R. P. Sarma, *Proc. Indian Acad. Sci.-Chem. Sci.*, 1986, **96**, 599–605.

[18] M. R. Edwards,W. Jones andW. D. S.Motherwell, *CrystEngComm*, 2006, **8**, 545–551.

[19] C. Hansch, A. Leo, R. W. Taft, *Chem. Rev.*, 1991, **91**, 165-195

Chapter 4 : Conclusions and Further Work

In this chapter the conclusions which may be drawn from this work are discussed, along with the further areas and directions in to which this project may be expanded.

Conclusions

This study involved the crystal structure characterisation of a specifically prepared family of 4,4' disubstituted chalcones by single crystal x-ray diffraction. These, along with other related crystal structures obtained from the CSD were systematically investigated with the XPac algorithm for identifying supramolecular constructs (SC's), which are substructures common to more than one crystal structure. The results of this were interpreted and collated to reveal the structural family relationships discussed in this work and several conclusions can be drawn from these.

This work has shown that the crystal structures of the vast majority of the family of chalcones studied may be described by combinations of five simple packing motifs, the primary SCs; A, B, C, D and E. Three of the primary SCs; A, B and C are 1-D substructures based on translational vectors that all run approximately parallel to the carbonyl bond of the chalcone molecule (primary SC B is in fact 0-D, but is a fragment of SC B1 which is 1-D). The three arrangements are thus mutually exclusive and no structures occur with combinations of these SCs. Accordingly, there are three distinct families of structures based around these primary SCs.

By far the largest and most complex of these are the structures based on primary SC A. This SC is exhibited by 34/50 chalcone crystal structures, and 19 secondary SCs based on primary SC A have been found. This group also displays the least evidence of any systematic directed intermolecular interactions and it can thus be concluded that the overarching factors dominating the crystal packing in this group of structures are molecular shape and thus shape of the chosen SCs. It can be seen that primary SC A is a simple 1-D close-packed, flat row of molecules, and so there are several possible ways that this SC may be close-packed. This is evidenced by the large number of secondary SCs found. It is interesting that primary SC A always occurs within structures as part of a more

complex secondary SC, which suggests it arises as the common fragment of several viable packing motifs within this group of structures. This makes it particularly robust as is shown by the large number of different crystal structures in which it is found. Within the SC A group 31/34 crystal structures display 2-D secondary SCs, each based on the primary SC A in one of four alternate basic arrangements. These are SC A10 and the secondary SCs derived from it, SC A11 and the secondary SCs derived from it, SC A18 and SC A19. Two of the arrangements, SCs A10 and A11, are based on vectors parallel to the long molecular axis and define two different layer relationships based on 'side-by-side' packing of instances of primary SC A related by translation or glides respectively and these are also mutually exclusive. Likewise, the other two arrangements, SCs A18 and A19, are based on vectors parallel to the short molecular axis and define two different stack relationships based on 'top-to-bottom' packing of pairs of primary SC A related by translation or inversion respectively and again these are mutually exclusive. It is also interesting to note that the three crystal structures that display none of these arrangements are structures where there is clear evidence of weak hydrogen bonding interactions.

The structures based on SCs B and E form the second group of chalcone structures. It comprises Y = F, H, OMe substituted chalcones and there is clear evidence of two alternative mutual C-H···O bonding patterns between instances of SC B1 leading to the different structures displaying this SC.

The structures based on SCs C and D form the third group of chalcone structures. It also comprises Y = F, H, OMe substituted chalcones, although the crystal structure of the Y = H substituted chalcone displays only SC C and the structures of the Y = F substituted chalcones display only SC D. Both of these primary SCs combine to form a 2-D SC and additionally SC D is displayed in different 2-D SCs suggesting that this SC is also particularly robust.

All of the Y = Br, Cl, Me, Et substituted chalcone structures belong to the A group of structures and this suggests that these structures are preferred by medium and large Y substituents. Different members of the Y = F, H, OMe substituted chalcone group of structures display all of the primary SCs and it is also these substitution patterns that yield the unique structures with no common SCs. It is unclear as to why the Y substituent appears to exert more influence over the crystal structure than the X substituent in this family of structures.

Only three of the chalcones in this study displayed polymorphic behaviour, Cl-C-OMe, H-C-H and H-C-Me. The Cl-C-OMe dimorphs gave structures displaying primary SC A and primary SC C, whilst the H-C-H dimorphs gave structures displaying primary SC B and a unique structure with no common SCs. The trimorphs of H-C-Me all give structures displaying SC A, although the 2-D packing modes of primary SC A are different in each structure. This suggests that the relative energy differences between substantially different structure types are small.

This study has shown that systematic investigation of similarity relationships amongst a related family of structures with only diffuse bonding interactions is a viable proposition. The concept of SCs and the XPac routine provided the most suitable tool for this task and useful structural information has been obtained that was not previously possible.

Further Work

The most useful immediate work would be to fill in the gaps in the data of the present family under study; this would give extra structures and possibly new structure types, which may provide links between the groups of structures based on the primary SCs and those with no SCs. Additionally the family of structures could be expanded by inclusion of chalcones with different substituents; I, NO_2 and SMe are suitable substituents with no strong H-bond donators. The family of structures could also be expanded with a systematic polymorph screen. This may involve cross-seeding experiments and alternative crystallization methods. However, the original difficulties with this project were obtaining suitable quality single crystals for study and these still remain, especially for any attempts to fill the gaps in the present family or for obtaining crystals from polymorph searching. During this project different crystal habits were observed for many of the chalcone species but most did not give useful diffraction data. Any new structures would allow a more complete picture of the relationships in the family of chalcone structures as a whole.

It would be useful to compare these results with those of similar families and to this end work has been undertaken comparing families of 4, 4' disubstituted N-pyridin-2-yl benzamides (I) and N-phenyl benzamides (II), both of which have a single hydrogen bond donor. In both of these families, particular

difficulties were met in obtaining useable crystals, and the family matrices are rather sparsely populated. On this basis, it was decided not to proceed with any detailed comparisons at this point. The structural data so far obtained are summarised in Figures 4-1 and 4-2 below. Full details of the structure determinations and results obtained are presented in the Appendix to this thesis, and will form a good foundation for any follow-on project.

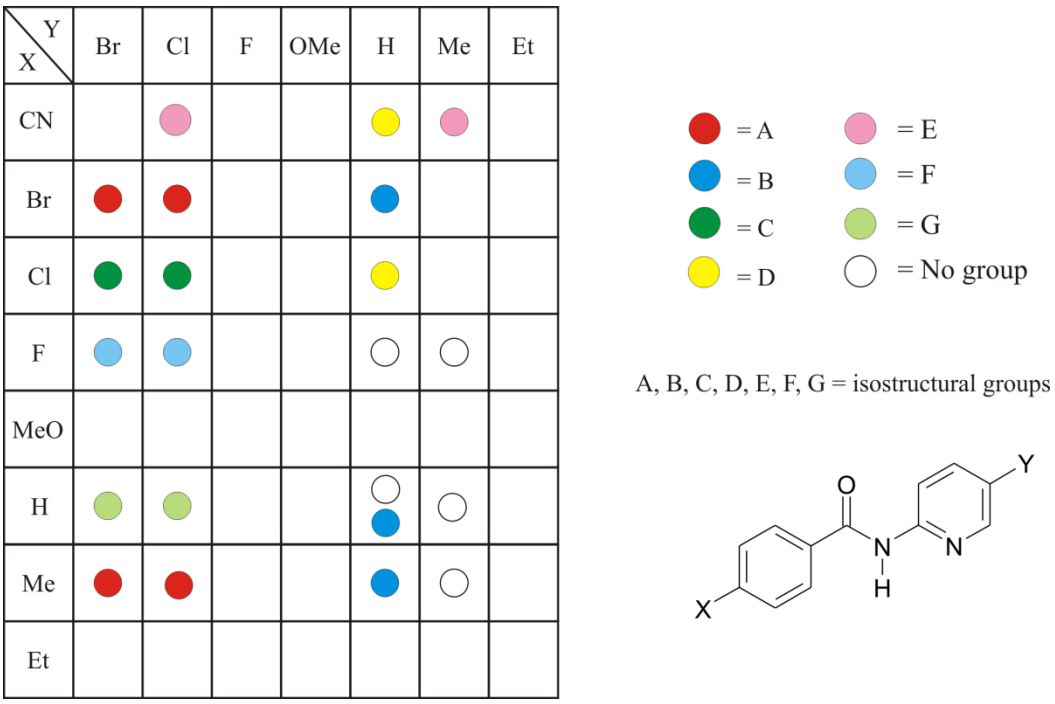

Figure 4-1: *Matrix showing the isostructural relationships amongst the 4, 4' disubstituted N-pyridin-2-yl benzamides*

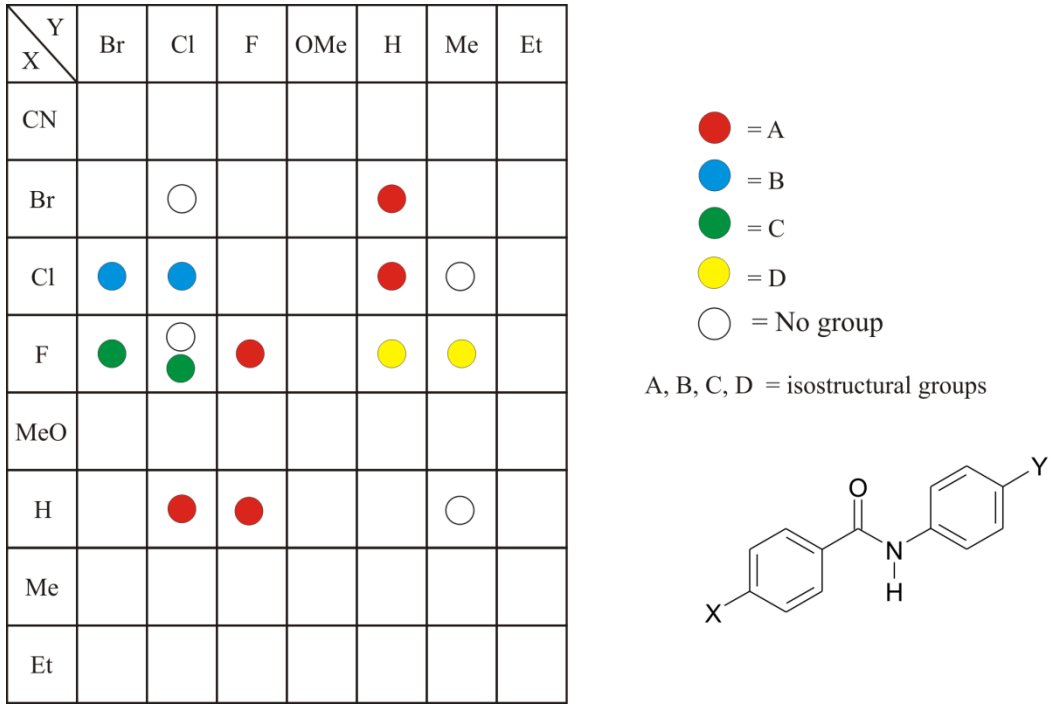

Figure 4-2: *Matrix showing the isostructural relationships amongst the 4, 4' disubstituted N-phenyl benzamides*